The Gradient Flow at Higher Orders in Perturbation Theory

Von der Fakultät für Mathematik und Naturwissenschaften der RWTH Aachen University zur Erlangung des akademischen Grades eines Doktors der Naturwissenschaften genehmigte Dissertation

vorgelegt von

Janosch Borgulat, M. Sc.

aus

Erkelenz

Berichter: Prof. Dr. rer. nat. Robert V. Harlander
Prof. Dr. rer. nat. Michał Czakon

Tag der mündlichen Prüfung: 10.03.2026

Diese Dissertation ist auf den Internetseiten der Universitätsbibliothek verfügbar

Abstract

The Gradient Flow formalism has proven to be a useful tool in both lattice gauge theory and perturbation theory since its introduction in its current form in 2010. Besides scale setting, which drove its prominence in lattice gauge theory, its smoothing properties and the connection to physical observables provided by the short flow-time expansion have made it a viable tool for lattice studies of various quantities, such as the energy-momentum tensor or four-quark operators describing B-meson mixing and lifetimes.

In this thesis, we apply the Gradient Flow to the quark chromomagnetic dipole operator as a first step towards a determination of the neutron electric dipole moment. This requires input from both lattice gauge theory and perturbation theory, since the matching coefficients relating the physical unflowed operators to flowed ones can be calculated perturbatively, while the hadronic matrix elements of such flowed operators are calculated on the lattice. We determine the matching coefficients through next-to-next-to-leading order, up to terms vanishing at zero flow-time. As a second application, we study the flowed topological charge density and the flowed singlet axial current, which appear in the Adler–Bell–Jackiw anomaly.

Finally, we extend the framework of flowed quantum chromodynamics to the unbroken phase of the Standard Model, excluding Yukawa interactions in this first approach. The flowed Standard Model offers an alternative method to infer the renormalization of Standard Model effective field theory operators to higher orders in perturbation theory. Such a calculation requires knowledge of the flowed field renormalization constants, which we determine, among other quantities, to next-to-next-to-leading order in the gauge couplings and the scalar coupling.

Zusammenfassung

Der Gradientenflussformalismus hat sich seit seiner Einführung in seiner gegenwärtigen Form im Jahr 2010 als hilfreiches Werkzeug sowohl in der Gittereichtheorie als auch in der Störungstheorie erwiesen. Neben der Skalenbestimmung, die ihn in der Gittereichtheorie bekannt gemacht hat, machen ihn seine Glättungseigenschaften und die durch die Entwicklung in kleinen Flusszeiten hergestellte Verbindung zu physikalischen Observablen zu einer wertvollen Methode, die unter anderem zur Implementierung des Energie-Impuls-Tensors auf dem Gitter und zur Untersuchung der Mischung und Lebensdauern von B-Mesonen zum Einsatz gekommen ist.

In dieser Dissertation wenden wir den bereits bekannten Gradientenfluss der Quantenchromodynamik als ersten Schritt zur Berechnung des elektrischen Dipolmoments des Neutrons auf den chromomagnetischen Dipoloperator an. Die Bestimmung des elektrischen Dipolmoments des Neutrons erfordert sowohl gittereichtheoretische als auch störungstheoretische Rechnungen, da zwar die Matching-Koeffizienten, die den Bezug zwischen Operatoren bei positiver Flusszeit und den physikalischen Operatoren bei verschwindender Flusszeit herstellen, perturbativ berechnet werden können, die Berechnung der hadronischen Matrixelemente dieser Operatoren allerdings auf dem Gitter erfolgen muss. Wir bestimmen das Matching der Operatoren bei positiver und verschwindender Flusszeit zu nächst-nächst-führender Ordnung unter Vernachlässigung von Termen, die im Limes verschwindender Flusszeit gegen null gehen. Eine weitere Anwendung, die wir betrachten, betrifft die Untersuchung der topologischen Ladungsdichte und des Singlet-Axialstroms, wie sie in der Adler–Bell–Jackiw-Anomalie auftreten, bei positiver Flusszeit.

Zuletzt erweitern wir den Gradientenflussformalismus der Quantenchromodynamik zum Standardmodell in ungebrochener Phase, wobei wir Yukawa-Wechselwirkungen zunächst vernachlässigen. Das bei positiver Flusszeit betrachtete Standardmodell bietet eine alternative Methode zur Bestimmung der Renormierung von Operatoren, die in der effektiven Feldtheorie des Standardmodells auftreten, zu höheren störungstheoretischen Ordnungen. Eine solche Bestimmung setzt allerdings die Kenntnis der Feldrenormierungen der Felder bei positiver Flusszeit voraus, die wir zu nächst-nächst-führender Ordnung in den Eichkopplungen und der Skalarkopplung bestimmen.

Eidesstattliche Erklärung

Ich, Janosch Borgulat, erkläre hiermit, dass diese Dissertation und die darin dargelegten Inhalte die eigenen sind und selbstständig, als Ergebnis der eigenen originären Forschung, generiert wurden.

Hiermit erkläre ich an Eides statt:

1. Diese Arbeit wurde vollständig oder größtenteils in der Phase als Doktorand dieser Fakultät und Universität angefertigt;
2. Sofern irgendein Bestandteil dieser Dissertation zuvor für einen akademischen Abschluss oder eine andere Qualifikation an dieser oder einer anderen Institution verwendet wurde, wurde dies klar angezeigt;
3. Wenn immer andere eigene- oder Veröffentlichungen Dritter herangezogen wurden, wurden diese klar benannt;
4. Wenn aus anderen eigenen- oder Veröffentlichungen Dritter zitiert wurde, wurde stets die Quelle hierfür angegeben. Diese Dissertation ist vollständig meine eigene Arbeit, mit der Ausnahme solcher Zitate;
5. Alle wesentlichen Quellen von Unterstützung wurden benannt;
6. Wenn immer ein Teil dieser Dissertation auf der Zusammenarbeit mit anderen basiert, wurde von mir klar gekennzeichnet, was von anderen und was von mir selbst erarbeitet wurde;
7. Teile dieser Arbeit wurden zuvor veröffentlicht und zwar in:

[JB1] R. Harlander et al. "Two-loop matching of the chromo-magnetic dipole operator with the gradient flow". In: *PoS* LATTICE2022 (2023), p. 313. DOI: 10.22323/1.430.0313. arXiv: 2212.09824 [hep-lat].

[JB2] J. Borgulat et al. "Short-flow-time expansion of quark bilinears through next-to-next-to-leading order QCD". In: *JHEP* 05 (2024), p. 179. DOI: 10.1007/JHEP05(2024)179. arXiv: 2311.16799 [hep-lat].

[JB3] J. Borgulat et al. "Two-loop gradient-flow renormalization of scalar QCD". In: *SciPost Phys. Core* 8 (2025), p. 032. DOI: 10.21468/SciPostPhysCore.8.1.032. arXiv: 2501.07150 [hep-ph].

Datum Unterschrift

List of publications

The research presented in this thesis was conducted at the Institute for Theoretical Particle Physics and Cosmology at RWTH Aachen University from May 2022 to October 2025. Parts of this thesis are based on, or were developed in close collaboration with, work previously published with other authors. Parts of the results presented in chapter 3 have already been published in Ref. [JB1]. Parts of the results of chapter 4 have already been obtained in Ref. [JB2] and chapter 5 is partially based on Ref. [JB3]. My contributions to these publications are specified in the corresponding chapters.

[JB1] R. Harlander et al. "Two-loop matching of the chromo-magnetic dipole operator with the gradient flow". In: *PoS* LATTICE2022 (2023), p. 313. DOI: 10.22323/1.430.0313. arXiv: 2212.09824 [hep-lat].

[JB2] J. Borgulat et al. "Short-flow-time expansion of quark bilinears through next-to-next-to-leading order QCD". In: *JHEP* 05 (2024), p. 179. DOI: 10.1007/JHEP05(2024)179. arXiv: 2311.16799 [hep-lat].

[JB3] J. Borgulat et al. "Two-loop gradient-flow renormalization of scalar QCD". In: *SciPost Phys. Core* 8 (2025), p. 032. DOI: 10.21468/SciPostPhysCore.8.1.032. arXiv: 2501.07150 [hep-ph].

Contents

Chapter 1

Introduction

The Yang-Mills Gradient Flow was first considered implicitly in 1982 by Atiyah and Bott [1] who studied classical Yang-Mills theory over a Riemann surface in the context of Morse theory to gain insight into the topological structure of the gauge connection configuration space. An explicit flow equation for the gauge connection was then later given in a paper by Donaldson [2] on a similar topic. Around the same time it has already been noted in lattice QCD that the extraction of non-perturbative effects in observables at small distances is hindered by high-momentum fluctuations and different methods had been used or suggested to circumvent this issue [3]. Among these was the idea to average the gauge fields over a small smearing region around every lattice site, which is described by a heat-equation like flow equation in the continuum [4], and leads to an exponential suppression of high-momentum contributions. A more rigorous treatment of the flow in continuum QCD was then done in 2006 by Narayanan and Neuberger [5], studying the large-N behavior of Wilson loops.

In 2009, Lüscher applied this technique to construct trivializing maps which map the gauge fields to their strong-coupling limit [6] with the original idea being to improve the efficiency of the lattice algorithms. In Ref. [7] he then analyzed the properties of the flows he used to generate the trivializing maps and laid the foundations of the technique commonly referred to now as the Gradient Flow formalism (GFF). Finding that the vacuum expectation value of the flowed gauge action density does not require renormalization through next-to-leading order (NLO) suggested that the GFF has some peculiar renormalization properties and a year later, Lüscher and Weisz proved that the flowed gauge field indeed does not require renormalization [8]. While this does not hold for flowed quarks [9], composite operators constructed from renormalized flowed fields do not require any additional renormalization beyond that of the fundamental parameters and the flowed fields and thus they do not mix under the renormalization group (RG) [8, 9].

The relation between the unphysical flowed composite operators and the physical observables is established by means of the short-flow-time expansion (SFTX) which expresses a flowed operator as a series of unflowed operators and flow-time dependent coefficients. Inverting this relation for a complete operator basis allows one to replace unflowed composite operators by flowed ones which are better behaved on the lattice due to their finiteness. The flow-time dependent coefficients can be calculated perturbatively and one can thus apply perturbative techniques developed for higher-order calculations in unflowed theories with only slight modifications. Since the ultraviolet (UV) properties of the theory are encoded in these coefficients, one can also use them to extract the anomalous dimensions of the unflowed operators. This motivates the investigation of using

the GFF to renormalize Standard Model effective field theory (SMEFT) operators. The flowed version of the Standard Model (SM) needed for this is formulated and investigated in chapter 5, where in this first approach we neglected the Yukawa couplings.

On the lattice side, the prominence of the GFF has been mainly driven by its use for scale setting [7, 10, 11], but its versatility has been proven by various other applications like the extraction of thermodynamical quantities from the flowed energy-momentum tensor [12–16], non-perturbative calculations of the beta function [17–19] and the mixing and life-times of B mesons [20, 21].

In chapter 2 we review the perturbative formulation of the GFF for a general SU(N) gauge theory including flowed quarks and discuss some of the main features and properties of the GFF. We introduce the SFTX which we make use of in all of the later chapters and briefly summarize some main properties of the renormalization of unflowed composite operators. A main difference to usual perturbative calculations is the appearance of new types of integrals in the GFF, the solution of which using analytical and numerical methods we discuss. We present the known two-loop master integrals and a selection of analytically known three-loop integrals.

In chapter 3 we apply the SFTX to the quark chromomagnetic dipole moment (CMDM) which contributes to rare kaon decays and the ϵ'/ϵ-ratio parameterizing direct CP-violation [22, 23]. We determine the SFTX coefficients through next-to-next-to-leading order (NNLO), improving on previous NLO results [24]. It also serves as a first step towards an analogous calculation for the quark chromoelectric dipole moment (CEDM) which contributes to the neutron electric dipole moment (nEDM) and the SFTX of which is currently known through NLO [24] . Since the upper bound on the experimental value of the nEDM is expected to be lowered by two orders of magnitude by new experiments in the near future [25–31] and the SM prediction is still many orders of magnitude smaller [32], the nEDM leaves a large window for possible beyond the Standard Model (BSM) effects which require an improvement of the current lattice results and thus improved matching with NNLO SFTX coefficients for lattice calculations using the GFF [33].

Another interesting quantity to study in the GFF is the topological charge density which appears in the chiral anomaly as a measure of the non-conservation of the axial vector current. In chapter 4 we calculate the SFTX for the operators appearing in the anomaly relation through NNLO, derive the corresponding flowed anomalous dimensions and discuss the relation of the GFF to the Nielsen-Ninomiya theorem (NNT).

As already mentioned, the finiteness of flowed operators allows us to extract the renormalization matrix of unflowed operators from the SFTX coefficients. The GFF thus offers a way to systematically calculate the renormalization of higher-dimensional operators. We have verified this approach already in chapter 3 where we could extract elements of the renormalization matrix for dimension five operators in quantum chromodynamics (QCD).

A natural application of this would be SMEFT for which the full renormalization is known through NLO, but only partial results are published for NNLO [34]. We thus adapt the GFF for the SM in the unbroken phase. We calculate all flowed field renormalizations and propose a new scheme independent renormalization of the fermion and scalar fields based on the finiteness of the Noether currents. The full treatment of Yukawa couplings is, however, delayed to future work and as a first step we only consider a fully flavor-conserving version of the SM.

Our results could also be used in future calculations in a lattice version of the SM

which has recently been proposed, although care must be taken when dealing with the continuum limit in theories that are not asymptotically free [35].

Altogether, in this thesis we consider several applications and an extension of the GFF. While we address specific aspects in each chapter, the overall aim is to provide a coherent perspective on its potential use in different contexts.

Chapter 2

The perturbative Gradient Flow in QCD

In this chapter we introduce the GFF for QCD, following Refs. [7–9]. From now on we work in Euclidean spacetime with $d = 4 - 2\epsilon$ dimensions, unless stated otherwise.

2.1 Flow equations and Lagrangian formulation

The Euclidean Lagrangian of an SU(N_c) Yang-Mills theory with n_f fermion fields ψ_i with bare mass m_B and the gauge boson field G^a_μ in R_ξ-gauge reads

$$\mathcal{L}_{\text{QCD}} = \frac{1}{4} G^a_{\mu\nu} G^a_{\mu\nu} + \overline{\psi} \left(\frac{1}{2} \overleftrightarrow{\not{D}} + m_B \right) \psi - \frac{1}{2\xi} \left(\partial_\mu G^a_\mu \right)^2 + \overline{c} \partial_\mu D^{ab}_\mu c^b \,, \tag{2.1.1}$$

where a summation over fundamental color and spinor indices is implied. The third term is the gauge-fixing term and the last term is the corresponding Faddeev–Popov ghost term. We will refer to this theory as QCD and to the gauge boson as the gluon for simplicity. The gluon field strength tensor is given by

$$G^a_{\mu\nu} = \partial_\mu G^a_\nu - \partial_\nu G^a_\mu + g_B f^{abc} G^b_\mu G^c_\nu \,, \tag{2.1.2}$$

and g_B is the bare strong coupling. The d-dimensional Euclidean spacetime indices are denoted by lower-case greek letters, while a, b and c are adjoint color indices and f^{abc} is the structure constant (cf. appendix A.1).

It is convenient for the calculations in the following chapters to parametrize the coupling through

$$a_s^B \equiv \frac{g_B^2}{4\pi^2} \,. \tag{2.1.3}$$

We used a form of the covariant derivative in the fundamental representation which is explicitly symmetric under integration by parts (IBP),

$$\overleftrightarrow{D}_\mu = D_\mu - \overleftarrow{D}_\mu \,, \qquad D_\mu = \partial_\mu + g_B G^a_\mu t^a \,, \qquad \overleftarrow{D}_\mu = \overleftarrow{\partial}_\mu - g_B G^a_\mu t^a \,. \tag{2.1.4}$$

In the adjoint representation, the covariant derivative reads

$$D^{ab}_\mu = \delta^{ab} \partial_\mu - g_B f^{abc} A^c_\mu \,. \tag{2.1.5}$$

The main idea of the GFF is to continue the spacetime dependence of the above fields to an additional dimension called the flow time t. At $t = 0$ the boundary conditions

ensure that usual QCD is recovered, while the evolution of the fields at $t > 0$ is fully determined by the dynamics at $t = 0$ and classical flow equations which evolve the fields from $t = 0$ to positive flow time. The flow equations are chosen in such a way that they are compatible with the symmetries of the theory and produce the heat equation at leading order in an expansion in the fields.

For QCD we choose the flow equations [8, 9]

$$0 = \partial_t \boldsymbol{G}^a_\mu - \boldsymbol{D}^{ab}_\nu \boldsymbol{G}^b_{\nu\mu} - \kappa \boldsymbol{D}^{ab}_\mu \partial_\nu \boldsymbol{G}^b_\nu \equiv \boldsymbol{F}^a_\mu \,, \tag{2.1.6}$$

$$0 = \left(\partial_t - \boldsymbol{D}^2\right)\boldsymbol{\psi} + \kappa \partial_\mu \boldsymbol{G}^a_\mu t^a \boldsymbol{\psi} \qquad \equiv \boldsymbol{F}_{\boldsymbol{\psi}} \,, \tag{2.1.7}$$

$$0 = \overline{\boldsymbol{\psi}}\left(\overleftarrow{\partial}_t + \overleftarrow{\boldsymbol{D}}^2\right) - \kappa \partial_\mu \boldsymbol{G}^a_\mu \overline{\boldsymbol{\psi}} t^a \qquad \equiv \bar{\boldsymbol{F}}_{\boldsymbol{\psi}} \,, \tag{2.1.8}$$

where $\boldsymbol{G}^a_\mu(t,x)$ is the flowed gluon field, $\boldsymbol{\psi}(t,x)$, $\overline{\boldsymbol{\psi}}(t,x)$ are the flowed quark and antiquark fields, respectively, and κ is an additional gauge fixing constant. The flowed field strength tensor $\boldsymbol{G}^a_{\mu\nu}(t,x)$ is defined analogously to the unflowed one, but with $\boldsymbol{G}^a_\mu$ instead of G^a_μ, as are the flowed covariant derivatives $\boldsymbol{D}_\mu$ and $\boldsymbol{D}^{ab}_\mu$. The initial conditions are

$$\boldsymbol{\psi}(0,x) = \psi(x)\,, \qquad \overline{\boldsymbol{\psi}}(0,x) = \overline{\psi}(x)\,, \qquad \boldsymbol{G}^a_\mu(0,x) = G^a_\mu(x)\,. \tag{2.1.9}$$

The new gauge fixing parameter κ arises due to the possibility of flow-time dependent gauge transformations. In fact, the solutions of the flow equations for $\kappa = 0$ are related to those with $\kappa \neq 0$ by [7]

$$\boldsymbol{G}_\mu|_{\kappa\neq 0} = \Lambda \boldsymbol{G}_\mu|_{\kappa=0}\Lambda^{-1} + \Lambda\partial_\mu\Lambda^{-1}\,, \tag{2.1.10}$$

where $\boldsymbol{G}_\mu = \boldsymbol{G}^a_\mu t^a$ and Λ is determined by

$$\partial_t \Lambda(t,x) = -\kappa\big(\partial_\mu \boldsymbol{G}_\mu(t,x)\big)\Lambda(t,x)\,. \tag{2.1.11}$$

The new gauge fixing term proportional to κ is required in order to dampen the gauge modes of the flowed gauge fields as we will explicitly see from the flowed gauge boson propagator later.

Note that only the gluon flow equation is actually a gradient-flow equation in the sense that it evolves the fields along the negative gradient of the unflowed action,

$$\partial_t \boldsymbol{G}^a_\mu(t,x) = -\frac{\delta S_{\mathrm{YM}}[G]}{\delta G^a_\mu(x)}\Big|_{G^a_\mu(x)\to \boldsymbol{G}^a_\mu(t,x)}\,, \tag{2.1.12}$$

driving them towards the classical solution. We have set $\kappa = 0$ here for brevity; other values can be obtained by a t-dependent gauge transformation. However, the action here is the pure Yang-Mills action without fermions. Fermionic terms arising in the gradient with respect to the gauge field are thus neglected in the minimal flow equation Eq. (2.1.6). The fermionic flow equations are not directly related to a gradient of the action. We will briefly consider modifications of the flow equations in section 2.3.

The flow equations can be solved iteratively as an expansion in g_{B}, expressing the flowed fields in terms of unflowed ones [8]. One can then insert the solution in a matrix element of a flowed operator and use standard techniques to calculate it to the desired perturbative order. This approach has been implemented through three-loop order in Ref. [17] for the determination of the flowed gluon action density.

Alternatively, one can formulate the GFF as a theory in $D+1$ dimensions and derive the corresponding Feynman rules [8, 36]. In this case, the flow equations can be implemented using Lagrange multiplier fields which appear only linearly in the action, thereby

ensuring that the flow equations hold exactly (without quantum corrections). Flowed QCD is thus described by the Lagrangian [8]

$$\mathcal{L}_{\text{fQCD}} = \mathcal{L}_{\text{QCD}} - 2\int_0^\infty \mathrm{d}s\, \boldsymbol{L}^a_\mu \boldsymbol{F}^a_\mu + \int_0^\infty \left(\bar{\boldsymbol{\eta}}\boldsymbol{F}_{\boldsymbol{\psi}} + \bar{\boldsymbol{F}}_{\boldsymbol{\psi}}\boldsymbol{\eta}\right) , \tag{2.1.13}$$

with the Lagrange multiplier fields $\boldsymbol{L}^a_\mu$, $\boldsymbol{\eta}$ and $\bar{\boldsymbol{\eta}}$, the equations of motion (EOM) of which are equivalent to the flow equations. The Feynman rules derived from this Lagrangian can be found in Ref. [36].

2.2 Perturbative solution of the flow equations

We now want to investigate some core properties of the GFF. For this, let us first consider flowed quarks. Their linearized flow equations both reduce to the heat equation,

$$(\partial_t - \partial^2)\boldsymbol{\psi} = 0\,, \tag{2.2.1}$$

which is solved by

$$\boldsymbol{\psi}(t,x) = \int_y K(t,x-y)\psi(y)\,, \qquad K(t,x-y) = \int_p e^{ip(x-y)}e^{-tp^2}\,. \tag{2.2.2}$$

Here we used the abbreviations

$$\int_x \equiv \int \mathrm{d}^d x\,, \qquad \int_p \equiv \int \frac{\mathrm{d}^d p}{(2\pi)^d}\,, \tag{2.2.3}$$

for spacetime and momentum integrals, respectively. We can now insert this solution into a two-point function of flowed quarks in momentum space,

$$\begin{aligned}\langle \overline{\boldsymbol{\psi}}_{i,\alpha}(t,p)\boldsymbol{\psi}_{j,\beta}(s,q)\rangle &= e^{-tp^2-sq^2}\langle \overline{\psi}_{i,\alpha}(p)\psi_{j,\beta}(q)\rangle \\ &= (2\pi)^d\delta^d(p+q)\delta_{ij}\frac{(-i\not{p}+m_{\text{B}})_{\alpha\beta}}{p^2+m_{\text{B}}^2}e^{-(t+s)p^2}\,,\end{aligned} \tag{2.2.4}$$

where we have made flavor and spinor indices explicit and used the result for the unflowed quark propagator,

$$\langle \overline{\psi}_{i,\alpha}(p)\psi_{j,\beta}(q)\rangle = (2\pi)^d\delta^d(p+q)\delta_{ij}\frac{(-i\not{p}+m_{\text{B}})_{\alpha\beta}}{p^2+m_{\text{B}}^2}\,. \tag{2.2.5}$$

We can thus identify the flowed quark propagator,

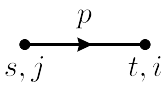

$$= \delta_{ij}\frac{-i\not{p}+m_{\text{B}}}{p^2+m_{\text{B}}^2}e^{-(t+s)p^2}\,, \tag{2.2.6}$$

where it is now apparent that the GFF suppresses high-momentum contributions, so t can be thought of as a cutoff scale which, however, preserves all relevant symmetries of the theory.

In order to derive the Feynman rule of the mixed propagator $\langle\bar{\eta}\boldsymbol{\psi}\rangle$, a so-called flow-line, we consider the generating functional of flowed QCD,

$$Z[J] \equiv \frac{1}{\mathcal{N}}\int \mathcal{D}\phi\, \exp\left[-\int_0^\infty \mathrm{d}t\int_x \mathcal{L}_{\text{fQCD}}(t,x) - \langle J,\phi\rangle\right], \tag{2.2.7}$$

where $\mathcal{N}$ is determined by $Z[0] = 1$. We denote the fields $\boldsymbol{G}$, $\overline{\boldsymbol{\psi}}$, $\boldsymbol{\psi}$, L, η and $\bar{\eta}$ collectively as ϕ and their corresponding sources as J and define the inner product of fields $\langle A, B\rangle = \int_0^\infty \mathrm{d}t \int_x A(t,x)B(t,x)$. The quark part of the exponent reads

$$-\langle \bar{\eta}, \mathcal{Q}\boldsymbol{\psi}\rangle + \langle J_{\boldsymbol{\psi}}, \boldsymbol{\psi}\rangle + \langle \bar{\eta}, J_{\bar{\eta}}\rangle + \mathcal{O}(\phi^3)\,, \tag{2.2.8}$$

where $\mathcal{Q}$ is the differential operator from the linearized flow equation acting on the flowed quark by

$$\mathcal{Q}\boldsymbol{\psi}(t,x) = \int_0^\infty \mathrm{d}s \int_y \delta^d(x-y)\delta(t-s)(\partial_s - \partial_y^2)\boldsymbol{\psi}(s,y)\,. \tag{2.2.9}$$

In order to complete the square, we have to find the Green's function $\mathcal{Q}^{-1}$ of $\mathcal{Q}$ which satisfies

$$\mathcal{Q}\mathcal{Q}^{-1}\boldsymbol{\psi}(t,x) = \boldsymbol{\psi}(t,x)\,. \tag{2.2.10}$$

As can be shown by a direct check of the above condition, it is given by

$$\mathcal{Q}^{-1}\boldsymbol{\psi}(t,x) = \int_0^\infty \mathrm{d}s \int_y \theta(t-s)K(t-s, x-y)\boldsymbol{\psi}(s,y)\,. \tag{2.2.11}$$

We can now complete the square by applying the shifts

$$\boldsymbol{\psi} \to \boldsymbol{\psi} + \mathcal{Q}^{-1}J_{\bar{\eta}}\,, \qquad \bar{\eta} \to \bar{\eta} + \mathcal{Q}^{-1}J_{\boldsymbol{\psi}}\,, \tag{2.2.12}$$

resulting in

$$-\langle \bar{\eta}, \mathcal{Q}\boldsymbol{\psi}\rangle + \langle J_{\boldsymbol{\psi}}, \boldsymbol{\psi}\rangle + \langle \bar{\eta}, J_{\bar{\eta}}\rangle \quad \longrightarrow \quad -\langle \bar{\eta}, \mathcal{Q}\boldsymbol{\psi}\rangle - \langle J_{\boldsymbol{\psi}}, \mathcal{Q}^{-1}J_{\bar{\eta}}\rangle \tag{2.2.13}$$

After performing the path integral and taking the functional derivatives of $Z[J]$ with respect to $J_{\boldsymbol{\psi}}$ and $J_{\bar{\eta}}$, one obtains the quark flow line

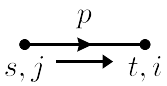

$$= \delta_{ij}\theta(t-s)e^{-(t-s)p^2}\,, \tag{2.2.14}$$

where the arrow denotes the direction of increasing flow-time. Since the linearized flow equation of the antiquark is the same as for the quark, the antiquark flow-line has the same Feynman rule. For the gluon, one obtains the flow-line [8]

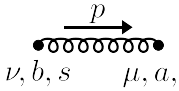

$$= \delta^{ab}\theta(t-s)\left[\left(\delta_{\mu\nu} - \frac{p_\mu p_\nu}{p^2}\right)e^{-(t-s)p^2} + \frac{p_\mu p_\nu}{p^2}e^{-\kappa(t-s)p^2}\right] \tag{2.2.15}$$

and the flowed propagator

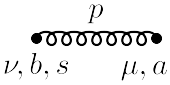

$$= \frac{\delta^{ab}}{p^2}\left[\left(\delta_{\mu\nu} - \frac{p_\mu p_\nu}{p^2}\right)e^{-(t+s)p^2} + \xi\frac{p_\mu p_\nu}{p^2}e^{-\kappa(t+s)p^2}\right] \tag{2.2.16}$$

by an analogous calculation. Note that the longitudinal part of the gluon flow-line is only exponentially suppressed if $\kappa > 0$ and the same holds true for the longitudinal term of the flowed gluon propagator (which only exists for $\xi \neq 0$).

The interaction terms in the flowed part of the Lagrangian give rise to flowed vertices at $t > 0$. We still write the Feynman rules in d-dimensional spacetime, so the flow time integrals $\int_0^\infty \mathrm{d}t$ are absorbed into the flowed vertices. Since a flowed vertex must always have exactly one outgoing flow-line, the domain of integration over t is always limited by the Heaviside step functions in the flow-lines. Examples for additional vertices at $t > 0$ are shown in Fig. 2.1. Note that in vertices like **(a)** involving quarks there cannot be an outgoing gluon flow-line since the gluon flow equation contains no quark terms and thus the action does not contain any products of quarks with the gluon multiplier field. As shown in vertex **(b)**, there are now interactions of flowed quarks with two gluons due to the quadratic covariant derivative in the quark flow equation. The Feynman rules for flowed vertices can be found in Refs. [36, 37].

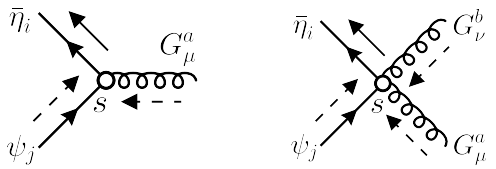

(a) **(b)**

Figure 2.1: Vertices at flow-time $s > 0$ introduced by the GFF. The dashed arrows represent lines which can be flowed propagators or incoming flow-lines. The field labels are as in Eq. (2.1.13), but all fields in the vertices can be at zero or positive flow time. The fermions here bear explicit fundamental color indices.

This also implies that closed loops composed entirely out of flow lines vanish since the flow-time integral domain is reduced to a point by the Heaviside step functions. Thus, a diagram in flowed QCD can always be decomposed into a tree of flow lines dressed with regular and flowed propagators. The tree structure of flow lines is a direct consequence of the fact that the flow equations hold exactly.

2.3 Alternative flow equations

We have seen in the previous sections how the flow equations lead to an exponential damping of the fields at $t > 0$, effectively providing a smooth gauge-invariant cut-off regularization. These features are a direct consequence of the two main properties imposed on the flow equations: They must be invariant under the same symmetries as the original theory and they have to reproduce the heat equation (or more generally a reaction-diffusion equation) at leading order. These conditions do not fix the form of the flow equations entirely and alternative forms of flow equations have been considered in the literature. In particular, a natural alternative to the minimal gluon flow equation Eqs. (2.1.6) is to derive it from the gradient of the full QCD action. Keeping $\kappa = 0$ for brevity, this results in

$$\partial_t \boldsymbol{G}^a_\mu(t,x) = -\frac{\delta S[\psi,\overline{\psi},G]}{\delta G^a_\mu}\bigg|_{(x)\to(t,x)} = D^{ab}_\nu \boldsymbol{G}^b_{\nu\mu} - g_{\mathrm{B}}\overline{\boldsymbol{\psi}}\gamma_\mu t^a \boldsymbol{\psi}\,, \tag{2.3.1}$$

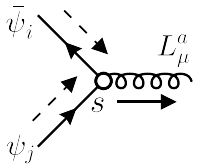

Figure 2.2: A vertex at flow-time $s > 0$ which is only present in non-minimal Gradient Flows when the gluon flow equation is modified by a quark term.

where $(x) \to (t, x)$ indicates that all fields should be replaced by flowed fields. For the fermions, one cannot simply use the gradient of the action since the fermion equation of motion is linear and thus one does not obtain the heat equation in first order in the fields. The gradient can, however, be multiplied by $\not{D}$, leading to

$$\partial_t \psi(t,x) = \not{D}^2 \psi(t,x)\,. \tag{2.3.2}$$

Mass terms could also potentially be included in the fermion flow equation, leading to a reaction-diffusion equation instead of a heat equation at leading order. Interestingly, due to the identity

$$\not{D}^2 = D^2 - \frac{\mathrm{i}}{2}\sigma_{\mu\nu} G^a_{\mu\nu} t^a\,, \tag{2.3.3}$$

the chromomagnetic dipole operator which we consider in section 3 appears as a term in the fermion flow equation in this case.

Another major difference with respect to the minimal flow equations are additional structures for flow-line trees emerging when fermions are included in the gauge boson flow equation. Other than in the minimal Gradient Flow, the extra quark term in the gluon flow equation can multiply the gluon multiplier field, giving rise to quark-gluon rules with an outgoing gluon flow-line like the one shown in Fig. 2.2. This can enhance the number of diagrams needed to calculate certain quantities. In the gluon action density, for example, only quarks at $t = 0$ have to be considered in the minimal Gradient Flow since flowed fermion vertices at $t > 0$ automatically lead to closed fermion flow-line loops. A similar simplification applies to the QCD static force as well [38]. This is no longer true if there are vertices like the one in Fig. 2.2 due to which the flow-lines can leave a fermion loop through a gluon.

In Ref. [39], the most general flow equations for the gauge and fermion fields have been derived and their effect on the gluon action density and the fermion field renormalization has been considered. The flowed ghosts are treated as in the minimal Gradient Flow, however. The general flow equations differ from the above ones only by arbitrary factors multiplying the additional terms (compared to the minimal flow equations). Apart from the chromomagnetic dipole operator in Eq. (2.3.2) and the non-singlet vector current in Eq. (2.3.1) no additional non-minimal terms can appear in the flow equations.

The gluon field does still not require additional renormalization in the non-minimal Gradient Flows. Regarding the renormalization of the flowed fermions, the two coefficients of the additional non-minimal terms can be chosen in such a way that they do not require renormalization through NLO [39], similar to the flowed scalar fields considered in section 5. While the non-minimal flows might thus offer some advantages, they lead to more complicated evolution equations and diagrammatic complexity. This becomes

particularly clear when a non-minimal evolution of a scalar field is considered. Let us assume a scalar version of QCD which we can view as the SU(2)-Higgs sector of the SM, a modification of which we consider in chapter 5. The flow equation is derived from the gradient of the action (which is possible since the equation of motion for scalars is elliptic, other than that for fermions), and reads [40]

$$\partial_t \boldsymbol{\phi} = -\frac{\delta S_{\text{sQCD}}}{\delta \phi^\dagger(x)}\bigg|_{(x)\to(t,x)} = (\boldsymbol{D}^2 + m_{\text{B}}^2)\boldsymbol{\phi} + \frac{\lambda_{\text{B}}}{2}\boldsymbol{\phi}|\boldsymbol{\phi}|^2 \,. \tag{2.3.4}$$

Thus, not only does this generate a flowed scalar self-interaction vertex, but the mass will occur in the exponential suppression factors in the scalar flowed propagators and flow-lines. This makes the calculation of higher terms in an expansion in the mass more computationally complex.

With the minimal flow equations (which we also choose for the scalar in section 5), these complications are avoided and we thus only consider minimal flow equations in the rest of this thesis.

2.4 BRST variation and flowed ghosts

The unflowed Lagrangian is symmetric under the Becchi-Rouet-Stora-Tyutin (BRST) transformation

$$\delta_{\text{BRST}} X = \theta s X \tag{2.4.1}$$

with a Graßmann constant θ and the operator s defined by [41]

$$\begin{aligned} sG_\mu^a &= D_\mu^{ab} c^b \,, & sB^a &= 0 \,, \\ sc_a &= -\frac{1}{2} g_0 f^{abc} c^b c^c \,, & s\psi &= -c^a T^a \psi \,, \\ s\overline{c}^a &= B^a \overset{\text{EOM}}{=} \frac{1}{\xi}\partial_\mu G_\mu^a \,, & s\overline{\psi} &= c^a \overline{\psi} T^a \,, \end{aligned} \tag{2.4.2}$$

where B^a is the Nakanishi-Lautrup field. This can be seen by considering the operator

$$\mathcal{O} = \overline{c}^a \left[\frac{1}{2}\xi - \partial_\mu A_\mu^a\right] \tag{2.4.3}$$

and its BRST variation

$$s\mathcal{O} = \frac{1}{2}\xi B^a B^a - B^a \partial_\mu G_\mu^a + \overline{c}^a \partial_\mu D_\mu^{ab} c^b \overset{\text{EOM}}{=} -\frac{1}{2\xi}(\partial_\mu G_\mu^a)^2 + \overline{c}^a \partial_\mu D_\mu^{ab} c^b \,, \tag{2.4.4}$$

where we have used the equation of motion of the Nakanishi-Lautrup field. This is the gauge fixing and ghost part of $\mathcal{L}_{\text{QCD}}$. Since the BRST transformation is nilpotent ($s^2 = 0$) and a gauge transformation for $\overline{\psi}$, ψ and G_μ^a, it follows that $s\mathcal{L}_{\text{QCD}} = 0$.

Since BRST symmetry restricts the possible counter terms, it is a vital tool in the proof of renormalizability [41] and an extension to flowed QCD has been found in Ref. [8].

Because of the initial conditions, we can simply replace the unflowed fields with flowed fields in the above unflowed BRST transformations. However, this is not a requirement for the flowed antighost since the antighost does not appear in the transformations of physical fields. Thus, it does not have to satisfy any particular boundary condition.

In fact, the flowed antighost $\bar{d}^a(t,x)$ is used as a multiplier field to implement the flow equation of the flowed ghost $d^a(t,x)$ via a term

$$\mathcal{L}_d = -\int_0^\infty dt\ \bar{d}^a(t,x)\left(\partial_t d^a(t,x) - \kappa \boldsymbol{D}_\mu^{ab}\partial_\mu d^b(t,x)\right)\,, \tag{2.4.5}$$

added to the Lagrangian, where $d^a(t,x)$ satisfies the boundary condition $d^a(0,x) = c^a(x)$. Note that the flow equation for the ghost reduces to $\partial_t d^a(t,x) = 0$ for $\kappa = 0$, so the flowed ghost is then independent of t. By requiring the BRST variation of the full flowed action to vanish, one obtains the transformations of the remaining fields [8, 39],

$$sL_\mu^a = f^{abc}L_\mu^b d^c\,, \tag{2.4.6}$$
$$s\eta = -d^a T^a \eta\,, \tag{2.4.7}$$
$$s\bar{\eta} = d^a\bar{\eta}T^a\,, \tag{2.4.8}$$
$$s\bar{d}^a = \bar{\eta}T^a\chi - \overline{\chi}T^a\eta - \boldsymbol{D}_\mu^{ab}L_\mu^b + f^{abc}\bar{d}^b d^c\,. \tag{2.4.9}$$

This treatment of the flowed antighost implies that we cannot define flowed versions of gauge variant operators which contain antighost fields. We can, however, still calculate matrix elements of flowed operators with unflowed ghosts as external states as might be useful in the context of the method of projectors discussed later.

Note that flowed ghosts do not contribute to matrix elements if there are no flowed ghosts in operator insertions or in the external states, since in this case the flowed ghosts necessarily form closed flow-line loops which vanish.

2.5 Properties of the Gradient Flow

In this section we give a brief summary of results obtained in Refs. [8, 9]. Among the most important properties of the GFF is the fact that composite operators at $t > 0$ do not require additional renormalization.

BRST symmetry furthermore prohibits the existence of counter-terms for the flowed gluon field on the boundary $t = 0$, too, so the flowed gluon does not require any field renormalization. However, this only holds as long as the convention of Ref. [8] (which is common in lattice gauge theory) is used where the explicit gauge coupling is removed from the covariant derivative by a rescaling of the gauge field. In the convention used in this thesis, the gauge field therefore requires a renormalization proportional to that of the gauge coupling.

For the flowed fermion the situation is different as it receives counter-terms from the terms

$$\int_x \left(\overline{\eta}(0,x)\,\psi(x) + \overline{\psi}(x)\,\eta(0,x)\right) \tag{2.5.1}$$

formed from fundamental fermions and Lagrange multiplier fields at $t = 0$ which are not excluded by BRST symmetry [9]. Their effect amounts to a field renormalization

$$\boldsymbol{\psi}_{\mathrm{R}}(t,x) = Z_{\boldsymbol{\psi}}^{1/2}\boldsymbol{\psi}_{\mathrm{B}}(t,x) \tag{2.5.2}$$

which we will consider in detail in section 2.11.

For Feynman diagrams in the GFF we have a number of rules:

1. Closed loops of flow lines vanish.

2. All flowed vertices have exactly one outgoing flow-line and can have none or multiple ingoing flow-lines.

3. As a consequence of the above, any diagram with an insertion of an operator at positive flow time contains a flow-line tree. The flow-lines start at the first flowed vertex and end at an insertion of an operator at $t > 0$.

4. In the minimal Gradient Flow, ghost and fermion flow-lines continue along the ghost or fermion line and cannot become gluon flow-lines.

5. As implied by the above properties, flowed ghosts do not appear in any diagram if only ghost-free flowed operators care considered.

6. Equally, flowed fermions do not appear in any diagram if only fermion-free operators are considered. This only holds if the minimal gluon flow equation is used, however.

We make use of these properties for example by setting diagrams with closed flow-line loops to zero using the Perl script `closedloops` [42] before any calculation is performed. In Tab. 3.1 we present and discuss the numbers of diagrams removed by this procedure for several calculations.

2.6 The short-flow-time expansion

Consider a set of composite operators $\mathcal{O}_i^{\mathrm{B}}$ in QCD and their flowed counterparts $\boldsymbol{\mathcal{O}}_i(t)$ which are constructed by replacing all fields in the $\mathcal{O}_i^{\mathrm{B}}$ by their flowed versions at $t > 0$.[1] One can then ask how the flowed operators are related to the unflowed ones in the limit $t \to 0$. The answer is provided by the so-called SFTX [8] which expresses the smeared (and in this sense non-local) operators $\boldsymbol{\mathcal{O}}_i(t)$ as a sum of unflowed local operators with flow-time dependent coefficients,

$$\boldsymbol{\mathcal{O}}_i(t,x) = \sum_j \zeta_{ij}^{\mathrm{B}}(t)\mathcal{O}_j^{\mathrm{B}}(x)\,. \tag{2.6.1}$$

We can split the operators into groups $\mathcal{O}_i^{n,\mathrm{B}}$ by their mass dimension n. Differences in mass dimension give rise to powers of t multiplying the matching coefficient, which we now assume does not contain any polynomial dependence on t,

$$\boldsymbol{\mathcal{O}}_i^n(t,x) = \sum_m t^{(m-n)/2} \sum_j \zeta_{nm|ij}^{\mathrm{B}}(t)\mathcal{O}_j^{m,\mathrm{B}}(x)\,, \tag{2.6.2}$$

implying that for $m > n$ the contributions on the right-hand side (RHS) are of order t and can be neglected in the SFTX if we are only interested in the $\mathcal{O}(t^0)$ behavior of the matching coefficients. We can then focus on the mixing with equal- or lower-dimensional operators.

If, however, we want to invert the matching matrix and there are inverse powers of t present due to mixing with lower-dimensional operators, the determinant of the matching

[1] In fact, this definition matches the one usually used in lattice calculations where the fields are evolved by solving the flow equations numerically. In principle, however, one could multiply flowed operators defined this way by a factor $f(m^2t)$ with an analytic function f such that $f(0) = 1$ and obtain equally valid flowed operators. Such non-trivial factors are neither required by our calculation nor considered in the literature, however, so we do not consider them any further.

matrix will involve products $t^{-n}t^n \sim 1$, so higher orders in t are required to obtain the determinant and thus the inverse to $\mathcal{O}(t^0)$. Let Δn be the maximal difference of mass dimensions of operators in a given complete basis. Then the matching matrix can have inverse powers of at most $t^{-\Delta n}$ and thus we need to take into account all matching matrix elements with at most a power $t^{+\Delta n}$, i.e., we need the full matching matrix and cannot neglect any of its elements due to the required order in t. In the problems considered in this thesis, this is only relevant in the case of the chromomagnetic dipole operator (see section 3.2).

A standard way of determining the mixing matrix elements ζ_{ij} is to perform a matching calculation, taking suitable matrix elements of both sides of Eq. (2.6.1). This comes with the disadvantage that on the RHS one ends up with regular Feynman integrals depending on m and external momenta and on the left-hand side (LHS) one has to compute Gradient-Flow integrals with t as an additional scale. This leads to cumbersome calculations which can be avoided using the so-called method of projectors [43–45].

This method has been developed in order to calculate Wilson coefficients in operator product expansions (OPE). Its main idea is that the separation scale of an operator product introduces a new scale and thus matrix elements of this product can be non-vanishing even if all the other scales are set to zero. In the expansion, however, the separation scale is only present in the Wilson coefficients and setting all other scales to zero leads to vanishing scaleless tadpole diagrams and only tree-level contributions remain which are trivial to calculate. Thus, by finding suitable matrix elements, one can define projectors which project out the desired Wilson coefficients.

We will now explain the application of the method of projectors in more detail in the context of the GFF where the separation scale is replaced by the flow time t.

The viability and usefulness of the method of projectors has already been verified in the context of the GFF in various cases. In Ref. [14] it has been used to determine the SFTX of the QCD energy-momentum tensor and in Ref. [46] it was applied to the SFTX of the dimension four QCD operators contributing to the hadronic vacuum polarization. In Ref. [47] it was used to determine the SFTX of fermionic bilinear operators in QCD.

To apply the method of projectors, we construct a projector P_i for each operator $\mathcal{O}_i$ such that $P_i[\mathcal{O}_j] = \delta_{ij}$ by taking an amputated Green's function which is one-particle irreducible with respect to all internal lines except for flow-lines and applying suitable derivatives with respect to external momenta and masses. Afterwards we set all scales except for the flow time to 0, arriving at scalar integrals with t as the only scale. The flow time naturally serves as the analogue of the separation scale in the context of OPEs here: It defines an effective smearing radius such that flowed fields depend on unflowed fields evaluated inside this radius. Since after the projection at $t = 0$ all integrals are scaleless, they vanish and we are only left with tree-level contributions on the RHS of Eq. (2.6.1). Higher perturbative orders only contribute to the LHS.

One may wonder if it is safe to set the external scales to zero. In fact, this is only possible since the diagrams generated by a projector must be one-particle irreducible with respect to propagators. This prevents terms of the form $\frac{1}{q^2+m^2}$ or $\frac{1}{q^2}$ with q being a combination of only external momenta. Such propagators would be undefined if the scales are set to zero. In one-particle irreducible diagrams, however, there is always a loop momentum flowing through every propagator which allows us to set the scales to zero in a well-defined way. The only lines with respect to which the diagrams are allowed to be reducible are the flow-lines which, however, have no denominator structure and are well-defined at vanishing momenta and masses.

Note that since the external legs connect to unflowed fields, their amputation just cancels the denominator, i.e., the unflowed propagator, leaving a remnant e^{-sp^2} term, where s is the flow time of the vertex connected to the external leg. In general, such exponentials arising from the external legs must be taken into account. In all cases considered in this thesis, however, they can be neglected due to the choice of projectors.

This is because no projectors used in the following chapters ever differentiate twice with respect to the same momentum. The differential operators D_P used in the projectors thus satisfy

$$D_P \prod_{i=1}^{n} e^{-s_i p_i^2}\Big|_{q_1,\dots,q_n,m=0} = 0\,, \tag{2.6.3}$$

so they can be safely commuted through the exponentials on the external legs which in the end reduce to 1 as all external momenta are set to 0.

If, however, we would have two derivatives with respect to the same momentum, we would obtain a non-vanishing contribution

$$\frac{\partial}{\partial q_\mu}\frac{\partial}{\partial q_\nu} e^{-tq^2}\Big|_{q=0} = -2t\delta_{\mu\nu} \tag{2.6.4}$$

from the external legs. This only vanishes if the projectors are defined to be traceless in the Lorentz indices.

Concerning the orthogonalization of the projectors, it is often more convenient to first choose a set of projectors which are only linearly independent and then orthogonalize the mixing matrix afterwards with its leading order (LO) part,

$$\zeta_{\text{orth.}}(t) = \zeta(t)\,\zeta_{\text{LO}}^{-1}(0)\,, \tag{2.6.5}$$

such that $\zeta_{\text{orth.}}^{\text{LO}}(0) = \mathbb{1}$. Here, taking $t = 0$ is understood as setting the flow-time to zero *before* taking the projectors, i.e., applying the projectors to the unflowed basis. Note that the LO matrix can only depend on t if there are loop diagrams at zeroth order in the couplings. This is only possible if the SFTX involves vacuum expectation values of operators which have a two-leg Feynman rule. Otherwise, ζ_{LO} is automatically t-independent, as we will see explicitly in chapter 3.

The method of projectors requires knowledge of the complete basis of operators up to the desired mass dimensions. Since the Green's functions appearing in the projectors are not physical, the projectors may yield non-vanishing results when applied to unphysical nuisance operators like EOM operators, total derivatives or BRST-exact operators which are the BRST variation of some other operator. Thus, such operators have to be considered in order to derive the correct orthonormalization of the projectors. Once the proper projectors are found, one can neglect the nuisance operators again as we will see in the next section.

With the method of projectors we obtain a bare SFTX matrix $\zeta^{\text{B}}(t)$. It is rendered finite by the renormalization of the flowed fields, masses and couplings as well as the renormalization matrix of the unflowed operators. Let us assume that in the flowed operators all fields and parameters are already renormalized. Then this implies that all UV divergences of the flowed operators are already removed. But then, we still have to renormalize the unflowed operators in order to obtain the finite $\zeta^{\text{R}}(t)$,

$$\boldsymbol{\mathcal{O}}(t,x) = \zeta^{\text{B}}(t)\mathcal{O}_{\text{B}}(x) = \zeta^{\text{B}}(t)Z^{-1}\mathcal{O}_{\text{R}}(x) = \zeta^{\text{R}}(t)\mathcal{O}_{\text{R}}(x)\,, \tag{2.6.6}$$

where Z is the renormalization matrix of the unflowed operators. Since $\zeta^{\mathrm{B}}(t)$ is calculated from matrix elements of renormalized flowed operators, this implies that Z^{-1} does not cancel UV but infrared (IR) divergences in $\zeta^{\mathrm{B}}(t)$. This can be understood by considering the effect of the Gradient Flow in an illustrative example calculation.

We consider a flowed complex scalar ϕ^4-theory (like the pure Higgs sector of the model considered in chapter 5) and the flowed operator $\boldsymbol{\phi}^\dagger(t,x)\boldsymbol{\phi}(t,x)$. We want to compute its matching coefficient with its unflowed version (which as a composite operator renormalizes like the scalar mass). At NLO the coefficient is determined by the diagram

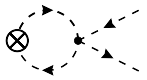

$$\sim \lambda_{\mathrm{B}} \int \frac{\mathrm{d}^{4+2\epsilon_{\mathrm{IR}}}p}{(2\pi)^{4+2\epsilon_{\mathrm{IR}}}} \frac{e^{-2tp^2}}{(p^2)^2} = \frac{\lambda}{\pi^2}\left(\frac{1}{\epsilon_{\mathrm{IR}}} + \text{fin.}\right) + \mathcal{O}(\lambda^2)\,, \tag{2.6.7}$$

where we have used $d = 4 + 2\epsilon_{\mathrm{IR}}$ since the diagram is UV finite, and λ is the scalar self-coupling. The crossed vertex represents the insertion of the flowed operator while the other vertex is a four-scalar interaction at $t = 0$ from which two flowed propagators connect to the operator vertex. Since we use minimal flow equations, this is the only NLO diagram (otherwise there may be outgoing flow-lines attached to the flowed version of the four-scalar vertex, for example). Considering the same diagram at $t = 0$ yields

$$\begin{aligned}
\lambda_{\mathrm{B}} \int_p \frac{1}{(p^2)^2} &= \lambda_{\mathrm{B}} \int_{|p|<\Lambda} \frac{\mathrm{d}^{4+2\epsilon_{\mathrm{IR}}}p}{(2\pi)^{4+2\epsilon_{\mathrm{IR}}}} \frac{1}{(p^2)^2} + \lambda_{\mathrm{B}} \int_{|p|>\Lambda} \frac{\mathrm{d}^{4-2\epsilon_{\mathrm{UV}}}p}{(2\pi)^{4-2\epsilon_{\mathrm{UV}}}} \frac{1}{(p^2)^2} \\
&= \frac{\lambda}{\pi^2}\left(\frac{\Lambda^{2\epsilon_{\mathrm{IR}}}}{\epsilon_{\mathrm{IR}}} + \frac{\Lambda^{-2\epsilon_{\mathrm{UV}}}}{\epsilon_{\mathrm{UV}}}\right) + \mathcal{O}(\lambda^2) \\
&= \frac{\lambda}{\pi^2}\left(\frac{1}{\epsilon_{\mathrm{IR}}} + \frac{1}{\epsilon_{\mathrm{UV}}} + \mathcal{O}(\epsilon_{\mathrm{IR}}) + \mathcal{O}(\epsilon_{\mathrm{UV}})\right) + \mathcal{O}(\lambda^2)\,,
\end{aligned} \tag{2.6.8}$$

where we have regulated the UV and IR divergences in their respective domain of convergence in the complex d plane. Setting $\epsilon_{\mathrm{IR}} = -\epsilon_{\mathrm{UV}}$, the integral vanishes as expected in dimensional regularization since it is a massless tadpole (like all diagrams beyond LO if a projector is applied to an unflowed operator). Comparing the divergences, we find that the IR divergence is the same, but the UV divergence is absent in the flowed result. Thus, we can infer the IR divergence from the flowed result and use the fact that IR and UV divergences cancel in massless tadpoles to infer the UV divergence caused by the respective unflowed composite operator. The IR divergences remaining in $\zeta^{\mathrm{B}}(t)$ after renormalizing the flowed fields and parameters are thus canceled by the unflowed operator renormalization. This fact had already been observed in the application of the method of projectors to unflowed operator product expansions in Ref. [44].

Note that the above matching coefficient can be extracted through NNLO from the matching coefficient of the Higgs field bilinear which we consider in section 5.9.

2.7 Gradient-Flow integrals

The integrals arising from the application of the method of projectors result in Gradient-Flow integrals which have t as the only scale. The main difference with respect to regular Feynman integrals is the presence of the exponential suppression factors and the additional integration over the flow-time variables. These are introduced through vertices at $t > 0$ and bounded from above by the flow time of the next vertex, i.e., the vertex the flow-line exiting the first vertex enters. Thus, the tree structure of flow lines gives rise to nested flow-time integrals in general.

The exponential suppression factors enter through the flow-lines and the flowed propagators. The exponentials of the external legs are already set to 1 after the method of projectors has been applied since they only depend on external momenta which are set to 0 after all derivatives with respect to momenta have been performed.

The general form of an L-loop Gradient-Flow integral obtained from the method of projectors is

$$I(t_1,...,t_F,T_1,...,T_N,b_1,...,b_N) \equiv \int_0^{t_1} \mathrm{d}s_1 \cdots \int_0^{t_F} \mathrm{d}s_F \int_{p_1,...,p_L} \frac{e^{-(T_1 P_1^2+\cdots+T_N P_N^2)}}{(P_1^2)^{b_1}\ldots(P_N^2)^{b_N}} \,. \tag{2.7.1}$$

Here, the upper bounds t_f of the flow-time integrals are in general functions of the flow-time variables associated with the outer integrations,

$$t_f : [0,\infty)^{f-1} \to [0,\infty), \quad (s_{f-1},...,s_1) \mapsto t_f(s_{f-1},...,s_1) \,. \tag{2.7.2}$$

The b_n are integers and the T_f are linear combinations of the flow-time integration variables s_f, arising from the product of the exponential factors, which are non-negative inside the flow-time integration domain.

The number of independent denominators N is given by $N = L(L+1)/2$ and the number of flow-time integrations F is limited by the number of vertices of a diagram.

The independent denominators P_i are linear combinations of loop momenta. Through three-loop order, there is only one topology from which all distributions of momenta in a diagram can be derived by pinching, i.e., contracting internal lines. We choose

$$\{P_i\}_{\text{1-loop}} = \{p_1\} \tag{2.7.3}$$
$$\{P_i\}_{\text{2-loop}} = \{p_1,\, p_2,\, p_1+p_2\} \tag{2.7.4}$$
$$\{P_i\}_{\text{3-loop}} = \{p_1,\, p_2,\, p_3,\, p_1-p_2,\, p_1-p_3,\, p_2-p_3\} \,. \tag{2.7.5}$$

Note that at four-loop and higher orders there are multiple topologies, so the integrals can in general not be described by a single set of denominators. These higher-order calculations are, however, beyond the scope of this thesis.

In order to simplify the integral structure, one can perform a linear substitution of the flow-time integral variables, normalizing them by their respective upper bounds,

$$s_f = u_f t_f \,. \tag{2.7.6}$$

This limits the range of the flow-time integrations to the interval $[0,1]$ and the integral now assumes the form [48]

$$I(\boldsymbol{c},\boldsymbol{a},\boldsymbol{b}) = \int_{[0,1]^F} \mathrm{d}\boldsymbol{u}\, \boldsymbol{u}^{\boldsymbol{c}} \int_{\boldsymbol{p}} \frac{\exp\{-t(a_1(\boldsymbol{u})P_1(\boldsymbol{p})^2 + \cdots + a_N(\boldsymbol{u})P_n(\boldsymbol{p})^2)\}}{(P_1(\boldsymbol{p})^2)^{b_1}\ldots(P_N(\boldsymbol{p})^2)^{b_N}} \,. \tag{2.7.7}$$

We also define normalized and dimensionless versions of the integrals,

$$\hat{I}(\boldsymbol{c},\boldsymbol{a},\boldsymbol{b}) = (4\pi t)^{Ld/2} t^{-b} I(\boldsymbol{c},\boldsymbol{a},\boldsymbol{b}) \,. \tag{2.7.8}$$

With $\boldsymbol{p} = (p_1,...,p_L)$ we abbreviate the L loop momenta, $\boldsymbol{c} = (c_1,...,c_F)$ are non-negative integers and we use multi-index notation, defining

$$\boldsymbol{u}^{\boldsymbol{c}} \equiv u_1^{c_1}\ldots u_F^{c_F} \,, \qquad b \equiv \sum_{i=1}^{N} b_i \,. \tag{2.7.9}$$

The functions $a_i(\boldsymbol{u})$ are polynomials in the flow-time integration variables which are again non-negative in the flow-time integration domain.

Since t is the only scale of the integrals calculated in this thesis, we can set $t = 1$ throughout the calculation and reconstruct the correct power of t from dimensional analysis. The polynomial t-dependence of the SFTX coefficients can be derived from the mass dimensions of the operators under consideration while their logarithmic t-dependence is determined by the $\log \mu^2$ terms which arise when the results are renormalized in the minimal subtraction (MS) scheme.

2.8 Integral reduction

Once a result is obtained in terms of scalar Gradient-Flow integrals, it is convenient to reduce the integrals to a set of master integrals before their evaluation since the number of integrals is usually drastically reduced by the reduction. The reduction of integrals relies on IBP relations and symmetries. The IBP relations are implied by translational invariance of the integrals in dimensional regularization. Since at this point all external momenta are set to 0, we can only take a total derivative with respect to a loop momentum,

$$\begin{aligned} 0 &= \int_{[0,1]^F} \mathrm{d}\boldsymbol{u}\, \boldsymbol{u}^{\boldsymbol{c}} \int_{\boldsymbol{p}} \frac{\partial}{\partial p_j^\mu} \left(p_i^\mu \frac{e^{-t(a_1 P_1^2 + \cdots + a_N P_n^2)}}{(P_1^2)^{b_1} \dots (P_N^2)^{b_N}} \right) \\ &= \delta_{ij} dI(\boldsymbol{c}, \boldsymbol{a}, \boldsymbol{b}) - \int_{[0,1]^F} \mathrm{d}\boldsymbol{u}\, \boldsymbol{u}^{\boldsymbol{c}} \int_{\boldsymbol{p}} \frac{e^{-t(a_1 P_1^2 + \cdots + a_N P_n^2)}}{(P_1^2)^{b_1} \dots (P_N^2)^{b_N}} \sum_{n=1}^{N} \left(t a_n + \frac{b_n}{P_n} \right) p_i^\mu \frac{\partial P_n}{\partial p_j^\mu} \,. \end{aligned} \tag{2.8.1}$$

The scalar products of loop momenta arising from $\partial P_n / \partial p_j^\mu$ can be rewritten in terms of the P_i again. Thus, the IBP identities arising from insertion of derivatives with respect to loop momenta relate integrals with shifted indices c_f and b_n.

For the specific case of Gradient-Flow integrals, we can also insert derivatives with respect to the flow time,

$$\int_0^{t_f} \mathrm{d}s_f \, \frac{\partial}{\partial s_f} f(s_f, \dots) = f(t_f, \dots) - f(0, \dots) \,, \tag{2.8.2}$$

which thus relates integrals with one flow-time integration less. When the flow-time integration variables are substituted to the u_i, there is an analogous relation. An algorithm for the automatic generation of both kinds of IBP relations for Gradient-Flow integrals has been developed in Ref. [49] and implemented in `Mathematica` [50]. An alternative implementation in `Python` has been developed in Ref. [51].

These identities can be used to reduce the integrals to a smaller set of master integrals using the Laporta Algorithm [52]: For the indices $\boldsymbol{b}$, integer values are inserted, leading to a set of *seed integrals*. These are chosen in such a way that their complexity is the same as the complexity of the integrals one wants to reduce. The complexity is encoded by a lexicographical ordering of the integrals with respect to an integral identification number which can be defined in different ways, leading to different bases of master integrals. From the seed integrals, IBP relations are generated which then relate the seed integrals to the integrals one wants to calculate. The resulting system is then reduced with a Gauß-type elimination algorithm. The details of this procedure in the context of the GFF are explained in detail in Ref. [37].

Several programs have implemented the Laporta algorithm. In our calculations, we use `Kira` [53–55] and `FireFly` [56, 57] together with custom `Mathematica` [50] scripts.

2.9 Master integrals and integral evaluation

At one-loop order, all occurring integrals can be reduced to a single master integral,

$$\hat{I}(0,2,0) = (4\pi t)^{d/2} \int_p e^{-2tp^2} = \frac{1}{4} + \epsilon \frac{1}{4} \log 2 + \epsilon^2 \frac{1}{8} \log^2 2 + \epsilon^3 \frac{1}{24} \log^3 2 + \dots . \tag{2.9.1}$$

At two-loop order, there are six master integrals,

$$M_1^{(2)} = \hat{I}(\{0\},\{1,1,1\},\{1,1,0\}), \qquad M_2^{(2)} = \hat{I}(\{0\},\{2,0,0\},\{0,1,1\}), \tag{2.9.2}$$

$$M_3^{(2)} = \hat{I}(\{0\},\{2,2,0\},\{0,0,0\}), \qquad M_4^{(2)} = \hat{I}(\{0\},\{2-u_1,u_1,u_1\},\{0,0,0\}), \tag{2.9.3}$$

$$M_5^{(2)} = \hat{I}(\{0\},\{1,1,1\},\{0,0,0\}), \qquad M_6^{(2)} = \hat{I}(\{0\},\{1-u_1,1+u_1,1+u_1\},\{0,0,0\}). \tag{2.9.4}$$

They have all been evaluated in closed analytical form in Ref. [14] using Schwinger parametrization and consequent direct integration with `Mathematica` [50]. They are then expanded in ϵ through $\mathcal{O}(\epsilon^6)$ using the `Mathematica` package `HypExp` [58, 59]. The closed form and the first terms in the expansion are given by

$$M_1^{(2)} = \frac{1}{d-2}\left(\frac{3^{2-\frac{d}{2}}\,{}_2F_1\left(1,1;3-\frac{d}{2};\frac{3}{4}\right)}{d-4} - 2\pi \csc\left(\frac{\pi d}{2}\right)\right) \tag{2.9.5}$$

$$= \log\left(\frac{4}{3}\right) + \epsilon\left(\mathrm{Li}_2(1/4) + 2\log^2(2) - \frac{\log^2(3)}{2} + \log\left(\frac{4}{3}\right)\right) + \dots , \tag{2.9.6}$$

$$M_2^{(2)} = -\frac{1}{d-2} 2^{3-d} \pi \csc\left(\frac{\pi d}{2}\right) \tag{2.9.7}$$

$$= \frac{1}{4\epsilon} + \frac{1}{4} + \frac{\log(2)}{2} + \epsilon\left(\frac{\zeta_2}{4} + \frac{1}{4} + \frac{\log^2 2}{2} + \frac{\log 2}{2}\right) + \dots , \tag{2.9.8}$$

$$M_3^{(2)} = 2^{-d} = \frac{1}{16}\left(1 + 2\log(2)\epsilon + \dots\right), \tag{2.9.9}$$

$$M_4^{(2)} = 2^{2-2d} B_{\frac{1}{4}}\left(1-\frac{d}{2},1-\frac{d}{2}\right) = \frac{1}{32\epsilon} - \frac{7}{96} + \frac{\log 2}{8} - \frac{\log 3}{32}$$
$$+ \epsilon\left(-\frac{7}{96} - \frac{\log 2}{8} + \frac{\log^2 2}{8} - \frac{\log 3}{96} - \frac{\log^2 3}{64} - \frac{\mathrm{Li}_2(1/4)}{16}\right) + \dots , \tag{2.9.10}$$

$$M_5^{(2)} = 3^{-d/2} = \frac{1}{9}\left(1 + \log(3)\epsilon + \dots\right) \tag{2.9.11}$$

$$M_6^{(2)} = 2^{2-2d}\left(B_{\frac{3}{4}}\left(1-\frac{d}{2},1-\frac{d}{2}\right) - B_{\frac{1}{2}}\left(1-\frac{d}{2},1-\frac{d}{2}\right)\right) = \frac{1}{24} + \frac{\log 3}{32}$$
$$+ \epsilon\left(\frac{\mathrm{Li}_2(1/4)}{16} - \frac{\zeta_2}{32} + \frac{1}{24} + \frac{\log^2 3}{64} + \frac{\log^2 2}{8} + \frac{\log 3}{96}\right) + \dots , \tag{2.9.12}$$

where the dots indicate that the expansion in ϵ has been performed through $\mathcal{O}(\epsilon^6)$. The special functions appearing in these integrals are the incomplete Euler beta function $\mathrm{B}_x(z_1,z_2)$, the hypergeometric function ${}_2F_1(a,b;c;z)$ and the dilogarithm function $\mathrm{Li}_2(z)$ for which there is a reflection identity,

$$\mathrm{Li}_2(1-z) = -\mathrm{Li}_2(z) + \zeta_2 - \log(z)\log(1-z). \tag{2.9.13}$$

Making use of the reflection identity for the case $z = 1/4$ allows us to express all special values of the dilogarithm function appearing in our results in terms of $\mathrm{Li}_2(1/4)$.

While no new one- or two-loop master integrals have been found since the finding of the first six ones despite greatly expanding the scope of two-loop calculations, at three-loop order the basis of master integrals is usually very sensitive to the specific problem under consideration and new problems frequently require new master integrals.

This may hint at the basis of master integrals not being finite at three-loop order. In fact, the proofs provided in Refs. [60–62] for finiteness of the master integral basis only apply to standard Feynman integrals and not to Gradient-Flow integrals (or not in a straightforward way, at least) because of significant differences like the presence of flow-time integrals which do not map to usual Schwinger parameter integrals (see below) due to the different domain of integration.

Since the three-loop master integrals are usually only known numerically and depend on the specific problem, and because the reduction does not provide a significant speed-up for the cases considered in this thesis, we evaluate the three-loop integrals directly by numerical integration, without performing a prior reduction.

For the numerical evaluation of the three-loop integrals we use the program `ftint` [48, 63]. It rewrites the Gradient-Flow integrals in Schwinger parametrization, where negative denominator powers are accounted for by derivatives with respect to (generalized) Schwinger parameters,

$$\begin{aligned} I(\boldsymbol{c},\boldsymbol{a},\boldsymbol{b}) &= \int_{[0,1]^F} \mathrm{d}\boldsymbol{u}\, \boldsymbol{u}^{\boldsymbol{c}} \int_{\boldsymbol{p}} \frac{\exp\left\{-t\sum_{n=1}^{N} a_n P_n^2\right\}}{\prod_{n=1}^{N} (P_n^2)^{b_n}} \\ &= \prod_{b_i<0} (-t)^{b_i} \frac{\partial^{b_i}}{\partial x_i^{b_i}} \prod_{b_j>0} \frac{(-t)^{b_j}}{(b_j-1)!} \int_0^\infty \mathrm{d}x_j\, x_j^{b_j-1} \\ &\qquad \times \int_{[0,1]^F} \mathrm{d}\boldsymbol{u}\, \boldsymbol{u}^{\boldsymbol{c}} \int_{\boldsymbol{p}} \exp\left\{-t\left(\sum_{n=1}^{N} a_n P_n^2 + \sum_{b_i\neq 0} x_i P_i^2\right)\right\}. \end{aligned} \tag{2.9.14}$$

The loop integral now is a multivariate Gaußian integral and can be evaluated analytically. The result is then handed over to `pySecDec` [63–65] which performs the remaining integrations numerically using the sector decomposition algorithm [66–68]. `ftint` also allows us to reduce the number of integrals by symmetry relations before numerical integration.

Through two-loop order, we have compiled a comprehensive list of integrals and their reductions to master integrals. This list currently contains 55 one-loop integrals and 17,200 two-loop integrals.

At three-loop order, we have compiled a list of symmetry relations currently counting 1115 integrals. Numerical values have been obtained for 6247 three-loop integrals.

Note that not all of the integrals in the above lists are directly related to results presented in this thesis since these lists also include integrals from test calculations, for example.

Since some quantities at three-loop order require a rather small amount of master integrals, we have tried to obtain some three-loop results analytically. By direct calculation, this was only possible for integrals with at most two propagators since after Schwinger parametrization the dimensionality of the domain of integration complicates the analytic integration otherwise. However, none of the three-loop quantities considered in this paper exclusively depends on these analytically known integrals and thus no three-loop result in this thesis is given in analytical form. This might be possible, however, if more sophisticated methods like integrand expansion [69] are applied to the remaining master

integrals, as has been proved useful in determining other three-loop results in analytical form [36]. Therefore, we still give the analytical results for the three-loop master integrals here. For compactness of notation we will write the integrals as

$$\hat{I}(\boldsymbol{c},\boldsymbol{a},\boldsymbol{b}) = \hat{I}(\boldsymbol{c})^{\boldsymbol{a}}_{\boldsymbol{b}}\,. \tag{2.9.15}$$

The analytical results are

$$\hat{I}(0)^{1,1,0,1,0,0}_{0,0,1,0,1,0} = -\frac{\pi}{d-2}2^{\frac{d}{2}-1}3^{2-d}\csc\left(\frac{\pi d}{2}\right)\,, \tag{2.9.16}$$

$$\hat{I}(0)^{0,1,1,1,1,0}_{0,0,0,0,0,0} = 2^{-D}\,, \tag{2.9.17}$$

$$\hat{I}(0)^{0,1,1,1,1,0}_{0,0,1,1,0,0} = \frac{1}{d-2}\left(\frac{2^{6-d}\,{}_2F_1\left(1,1;3-\frac{d}{2};\frac{8}{9}\right)}{9(d-4)} - \pi 2^{\frac{d}{2}-1}\csc\left(\frac{\pi d}{2}\right)\right)\,, \tag{2.9.18}$$

$$\hat{I}(0)^{0,1,1,1,1,0}_{0,1,1,0,0,0} = \hat{I}(0)^{0,1,1,1,1,0}_{0,0,1,1,0,0}\,, \tag{2.9.19}$$

$$\hat{I}(0)^{0,1,1,1,1,0}_{1,1,0,0,0,0} = \frac{2^{1-d}}{d-2}\left(\frac{8\,{}_2F_1\left(1,1;3-\frac{d}{2};\frac{2}{3}\right)}{3(d-4)} - \pi 2^{d/2}\csc\left(\frac{\pi d}{2}\right)\right)\,, \tag{2.9.20}$$

$$\hat{I}(0)^{1,1,2,1,0,0}_{0,0,0,0,0,0} = 6^{-d/2}\,, \tag{2.9.21}$$

$$\hat{I}(0)^{1,1,2,1,0,0}_{1,1,0,0,0,0} = \frac{6^{-d/2}}{(d-4)(d-2)}\left(9\,{}_2F_1\left(1,1;3-\frac{d}{2};\frac{3}{4}\right) - 2\pi 3^{d/2}(d-4)\csc\left(\frac{\pi d}{2}\right)\right)\,, \tag{2.9.22}$$

$$\hat{I}(0)^{1,1,2,1,0,0}_{1,0,0,1,0,0} = \hat{I}(0)^{1,1,2,1,0,0}_{1,1,0,0,0,0}\,, \tag{2.9.23}$$

$$\tag{2.9.24}$$

$$\hat{I}(0)^{1,1-\mathrm{u}1,\mathrm{u}1,\mathrm{u}1+1,\mathrm{u}1,0}_{0,0,0,0,0,0} = -\frac{2^{1-d/2}3^{-d/2}}{d-2}F_1\left(1-\frac{d}{2};\frac{d}{2},\frac{d}{2};2-\frac{d}{2};-\frac{2}{-1+\sqrt{13}},\frac{2}{1+\sqrt{13}}\right)\,, \tag{2.9.25}$$

where the Appell hypergeometric function of the first kind F_1 appears as a new special function. The above results have all been checked to agree with the corresponding numerical results by evaluating them numerically at small finite values of ϵ.

2.10 Renormalization of composite operators

Composite operators appear in many highly relevant contexts in quantum field theory. Apart from the Lagrangian density itself, they are required for the formulation of Ward identities and constitute such important physical observables like the energy-momentum tensor. At higher mass dimensions, non-renormalizable composite operators appearing in effective field theories like SMEFT are used to parametrize BSM effects in a model-independent way.

Taking the limit of a product of fields at different spacetime points where the distance between the points goes to zero usually leads to additional UV divergencies. Using an operator product expansion, the UV or small-distance effects can be absorbed into Wilson coefficients multiplying composite operators which are compatible with the symmetries of the theory.

The fact that composite operators constructed from flowed fields are free of exactly these kinds of extra divergencies and their matrix elements are renormalized by multiplicative renormalization of the fundamental parameters and fields makes the Gradient Flow a

valuable tool in the study of composite operators. The renormalization pattern of composite operators is restricted by a number of conditions. In dimensional regularization, for example, where the regulator is dimensionless, composite operators of different mass dimension do not mix under renormalization (at least if we count operators multiplied by different powers of a mass factor as distinct operators) [70].

A second condition which we will make use of in the following chapters is a theorem due to Joglekar and Lee [71–73]: We abbreviate gauge-invariant physical operators by $\mathcal{G}$, operators vanishing due to EOM by $\mathcal{E}$, and BRST-exact ones by $\mathcal{V}$. With this classification, the renormalization matrix and its inverse are triangular,

$$\begin{pmatrix} \mathcal{G} \\ \mathcal{V} \\ \mathcal{E} \end{pmatrix}_B = \begin{pmatrix} Z^{-1}_{GG} & Z^{-1}_{GV} & Z^{-1}_{GE} \\ 0 & Z^{-1}_{VV} & Z^{-1}_{VE} \\ 0 & 0 & Z^{-1}_{EE} \end{pmatrix} \begin{pmatrix} \mathcal{G} \\ \mathcal{V} \\ \mathcal{E} \end{pmatrix}_R , \tag{2.10.1}$$

Applying this to the bare SFTX, we obtain

$$\boldsymbol{\mathcal{O}} = \zeta^B_G \mathcal{G}^B + \zeta^B_V \mathcal{V}^B + \zeta^B_E \mathcal{E}^B \tag{2.10.2}$$

$$= \zeta^B_G Z^{-1}_{GG} \mathcal{G}^R + \left(\zeta^B_G Z^{-1}_{GV} + \zeta^B_V Z^{-1}_{VV}\right)\mathcal{V}^R + \left(\zeta^B_G Z^{-1}_{GE} + \zeta^B_V Z^{-1}_{VE} + \zeta^B_E Z^{-1}_{EE}\right)\mathcal{E}^R . \tag{2.10.3}$$

Note that ζ^{B}_G only renormalizes through Z^{-1}_{GG}. Thus, if we have made sure that the projectors are orthogonal over the full basis (including EOM and BRST-exact operators), the renormalization of the physical part ζ^{B}_G of the mixing matrix can be performed, neglecting nuisance operators. If, however, the projectors are not orthogonal with respect to nuisance operators, the SFTX mixes operators of the different classes $\mathcal{G}$, $\mathcal{E}$ and $\mathcal{V}$, rendering the seemingly physical sub-matrix non-renormalizable if counter-terms provided by unphysical operators are not taken into account.

2.11 Renormalization Group in the Gradient Flow

In this section we consider the new renormalization constants needed in flowed QCD. Most of the results of this section can be generalized to the modified version of the SM considered in section 5 in a straightforward way.

In our convention, the flowed gauge boson requires a field renormalization $Z_{\boldsymbol{G}}$,

$$\boldsymbol{G}_{\mathrm{R}} = Z^{1/2}_{\boldsymbol{G}} \boldsymbol{G}_{\mathrm{B}} , \tag{2.11.1}$$

where $Z_{\boldsymbol{G}} = Z_s$, i.e., the flowed gauge boson renormalizes in the same way as the coupling (cf. section 2.5 and appendix B), while the flowed fermion is renormalized in the MS scheme by multiplication with the renormalization constant $Z_{\boldsymbol{\psi}}$,

$$\boldsymbol{\psi}_{\mathrm{R}} = Z^{1/2}_{\boldsymbol{\psi}} \boldsymbol{\psi}_{\mathrm{B}} . \tag{2.11.2}$$

The requirement of a flowed fermion renormalization leads to problems when combining lattice and perturbative results since the field is renormalized in different schemes on the lattice and in perturbation theory, respectively. This problem can be solved by introducing a finite renormalization for the flowed fermion which cancels its anomalous dimension, called the ringed scheme. We define

$$\mathring{\boldsymbol{\psi}} = \left(\mathring{Z}_{\boldsymbol{\psi}}\right)^{1/2} \boldsymbol{\psi}_{\mathrm{B}} , \qquad \text{with} \quad \mathring{Z}_{\boldsymbol{\psi}} = \zeta_{\boldsymbol{\psi}} Z_{\boldsymbol{\psi}} , \tag{2.11.3}$$

where $\zeta_{\boldsymbol{\psi}}$ is determined by requiring the all-order identity

$$\left\langle \overset{\circ}{\overline{\boldsymbol{\psi}}}(t,x) \overleftrightarrow{\not{\boldsymbol{D}}} \overset{\circ}{\boldsymbol{\psi}}(t,x) \right\rangle_{m=0} \equiv -\frac{2N_c n_f}{(4\pi t)^2} \tag{2.11.4}$$

for the vacuum expectation value (VEV) of the flowed so-called fermion kinetic operator. The finite renormalization $\zeta_{\boldsymbol{\psi}}$ is known through NNLO [36] and the RHS of Eq. (2.11.4) is chosen such that $\zeta_\psi = 1 + \mathcal{O}(a_s)$.

Note that this is not the only way to remove the anomalous dimension of the flowed fermion. In general, any SFTX coefficient matching a fermionic flowed operator to a finite unflowed operator offers a possibility to define a similar scheme since requiring the matching coefficient to equal its LO value makes the RHS of the SFTX RG-invariant in such a case. For the ringed scheme, we use the matching of the fermion kinetic operator to the unit operator (which is trivially finite). Another possibility which we explore in section 5.5, although in a different model, is to choose the matching of the flowed non-singlet vector current to the unflowed non-singlet vector current (which is finite due to Ward identities). For QCD, the required matching coefficient has been obtained in Ref. [47] through NNLO.

The flowed fermion renormalization has been obtained for the first time in Ref. [9] through NLO. In Ref. [14] the finiteness of the energy-momentum tensor has been used in order to obtain it through NNLO analytically. In the MS scheme it is given by

$$Z_{\boldsymbol{\psi}} = 1 - a_s \frac{\gamma_{\boldsymbol{\psi},0}}{\epsilon} + a_s^2 \left[\frac{\gamma_{\boldsymbol{\psi},0}}{2\epsilon^2} (\gamma_{\boldsymbol{\psi},0} + \beta_0) - \frac{\gamma_{\boldsymbol{\psi},1}}{2\epsilon} \right] + \mathcal{O}(a_s^3) \,, \tag{2.11.5}$$

where

$$\gamma_{\boldsymbol{\psi}} = \sum_{n=0}^{\infty} a_s^{n+1} \gamma_{\boldsymbol{\psi},n} = a_s \beta \frac{\mathrm{d}}{\mathrm{d}a_s} \log Z_{\boldsymbol{\psi}} \,, \tag{2.11.6}$$

with the coefficients of the anomalous dimension through NNLO given by

$$\gamma_{\boldsymbol{\psi},0} = -\frac{3}{4} C_\mathrm{F} \,, \qquad \gamma_{\boldsymbol{\psi},1} = \left(\frac{1}{2} \log 2 - \frac{223}{96} \right) C_\mathrm{A} C_\mathrm{F} + \left(\frac{3}{32} + \frac{1}{2} \log 2 \right) C_\mathrm{F}^2 + \frac{11}{24} C_\mathrm{F} T_\mathrm{R} n_\mathrm{f} \,. \tag{2.11.7}$$

The conversion factor to the ringed scheme has first been defined and calculated through NLO in Ref. [74].[2] The NNLO contribution has been calculated in Ref. [36]. In total, we have

$$\begin{aligned} \zeta_{\boldsymbol{\psi}} = 1 &- a_s \left(\gamma_{\boldsymbol{\psi},0} L_{\mu t} + \frac{3}{4} C_\mathrm{F} \log 3 + C_\mathrm{F} \log 2 \right) \\ &+ a_s^2 \left(\frac{\gamma_{\boldsymbol{\psi},0}}{2} (\gamma_{\boldsymbol{\psi},0} - \beta_0) L_{\mu t}^2 + \left[\gamma_{\boldsymbol{\psi},0} (\beta_0 - \gamma_{\boldsymbol{\psi},0}) \log 3 \right. \right. \\ &\left. \left. + \frac{4}{3} \gamma_{\boldsymbol{\psi},0} (\beta_0 - \gamma_{\boldsymbol{\psi},0}) \log 2 - \gamma_{\boldsymbol{\psi},1} \right] L_{\mu t} + \frac{c_\chi^{(2)}}{16} \right) + \mathcal{O}(a_s^3) \,, \end{aligned} \tag{2.11.8}$$

where the flow-time dependence enters through the logarithm

$$L_{\mu t} = \log\left(8\pi\mu^2 t\right) \tag{2.11.9}$$

[2] In fact, there a normalization by the scalar fermion bilinear instead of the fermion kinetic operator had been considered as an option but this has been rejected. As opposed to the vector current, this operator has an anomalous dimension at $t = 0$ which needs to be accounted for, and its VEV vanishes at vanishing fermion mass.

and we have collected the non-logarithmic NNLO contributions in the coefficient

$$c_\chi^{(2)} = C_\mathrm{A} C_\mathrm{F} c_{\chi,\mathrm{A}} + C_\mathrm{F}^2 c_{\chi,\mathrm{F}} + C_\mathrm{F} T_\mathrm{R} n_\mathrm{f} c_{\chi,\mathrm{R}} \tag{2.11.10}$$

with

$$\begin{aligned} &C_\mathrm{A} C_\mathrm{F} c_{\chi,\mathrm{A}} = -23.7947\,, \qquad C_\mathrm{A} C_\mathrm{F} c_{\chi,\mathrm{F}} = 30.3914\,, \\ &C_\mathrm{A} C_\mathrm{F} c_{\chi,\mathrm{R}} = -\frac{131}{18} + \frac{46}{3}\zeta_2 + \frac{944}{9}\log 2 + \frac{160}{3}\log^2 2 - \frac{172}{3}\log 3 + \frac{104}{3}\log 2 \log 3 \\ &\qquad - \frac{178}{3}\log^2 3 + \frac{8}{3}\mathrm{Li}_2(1/9) - \frac{400}{3}\mathrm{Li}_2(1/3) + \frac{112}{3}\mathrm{Li}_2(3/4) = -3.92255\ldots\,. \end{aligned} \tag{2.11.11}$$

Note that the digits in the above numerical coefficients are not affected by numerical uncertainty.

Let us now consider a set of operators $\mathcal{O}_\mathrm{B}(x)$ and their respective flowed versions $\boldsymbol{\mathcal{O}}_\mathrm{B}(t,x)$. They are all expressed in terms of the bare flowed fields $(\boldsymbol{G}_\mu^a)_\mathrm{B}$ and $\boldsymbol{\psi}_\mathrm{B}$ which are independent of the renormalization scale μ. In order to obtain renormalized results, the operators need to be multiplied by some powers of $Z_{\boldsymbol{\psi}}$ and $Z_{\boldsymbol{G}}$ (and possibly other renormalization constants like Z_m^{-1} if they depend linearly on the bare mass, for example). Note that we do not fix any scheme for the renormalization constants here, i.e., we allow for additional finite renormalizations. All these renormalization constants are then collected in a diagonal matrix $F(t)$ such that in the product

$$\boldsymbol{\mathcal{O}}_\mathrm{R}(t,x) \equiv F(t)\boldsymbol{\mathcal{O}}_\mathrm{B}(t,x) \tag{2.11.12}$$

all fields and parameters are properly renormalized. Note that F depends on t if we use a non-minimal subtraction scheme like the ringed scheme.

From our setup, which operates with the bare flowed and unflowed fields, we obtain an SFTX of the form

$$\boldsymbol{\mathcal{O}}_\mathrm{B}(t,x) = \zeta_\mathrm{B}(t)\mathcal{O}_\mathrm{B}(x)\,. \tag{2.11.13}$$

As discussed, the unflowed operators require non-multiplicative renormalization in general,

$$\mathcal{O}_\mathrm{B} = Z^{-1}\mathcal{O}_\mathrm{R}\,, \tag{2.11.14}$$

where Z is a renormalization matrix which only depends on a_s and μ. With this, We obtain the renormalized SFTX

$$\boldsymbol{\mathcal{O}}_\mathrm{R}(t,x) = F(t)\boldsymbol{\mathcal{O}}_B(t,x) = F(t)\zeta_\mathrm{B}(t)Z^{-1}\mathcal{O}_\mathrm{R}\,, \tag{2.11.15}$$

which allows us to define the renormalized mixing matrix by

$$\zeta(t) \equiv F(t)\zeta_\mathrm{B}(t)Z^{-1}\,. \tag{2.11.16}$$

The unflowed operators have an anomalous dimension γ defined by

$$\mu^2\frac{\mathrm{d}}{\mathrm{d}\mu^2}\mathcal{O}_\mathrm{R}(x) \equiv \gamma\mathcal{O}_\mathrm{R}(x) \tag{2.11.17}$$

which we can obtain from the renormalization matrix (which itself can be obtained from the bare mixing matrix ζ_B) by

$$\gamma = \left[\left(a_s\beta\frac{\partial}{\partial a_s} + \mu^2\frac{\partial}{\partial\mu^2}\right)Z\right]Z^{-1} \equiv \sum_{n\geq 0} a_s^n\gamma_n\,. \tag{2.11.18}$$

The partial derivative with respect to μ is necessary if the renormalization matrix has an explicit μ dependence as is the case for bases which include operators differing by non-integer mass dimension.

We can now make use of the RG invariance of the bare mixing matrix and operators in order to derive the relation

$$\gamma = -\zeta^{-1}(t)\left(a_s\beta\frac{\partial}{\partial a_s} + \frac{\partial}{\partial L_{\mu t}}\right)\zeta(t) + \zeta^{-1}(t)\left[\left(a_s\beta\frac{\partial}{\partial a_s} + \frac{\partial}{\partial L_{\mu t}}\right)F(t)\right]F^{-1}(t)\zeta(t)\,, \tag{2.11.19}$$

where $L_{\mu t}$ is defined in Eq. (2.11.9). This provides a check of the calculation of the mixing matrix since the LHS is independent of t, such that the nontrivial t-dependence of the RHS must cancel. Requiring this cancellation also allows us to express the logarithmic t-dependent terms in terms of the anomalous dimensions.

If there are only fermionic operators which are renormalized in the ringed scheme, the second term in Eq. (2.11.19) vanishes since the ringed flowed fields have a vanishing anomalous dimension.

Our definition of the anomalous dimension of the flowed gluon is

$$\gamma_{\boldsymbol{G}}\boldsymbol{G}_{\mathrm{R}} = -2\mu^2\frac{\mathrm{d}}{\mathrm{d}\mu^2}\boldsymbol{G}_{\mathrm{R}} \quad \Rightarrow \quad \gamma_{\boldsymbol{G}} = -\mu^2\frac{\mathrm{d}}{\mathrm{d}\mu^2}\log Z_{\boldsymbol{G}} = +\beta|_{\epsilon=0} \tag{2.11.20}$$

where we have used $Z_{\boldsymbol{G}} = Z_s$. Note that this anomalous dimension can be canceled by rescaling the gluon with the gauge coupling as is done in the lattice convention where the coupling only appears as a factor multiplying the gluon action density in the Lagrangian. However, this convention has the disadvantage that the coupling now appears in the gluon propagators, which is why we stick to the convention in which the flowed gluon requires a field renormalization.

The flowed fermion has an anomalous dimension defined by

$$\gamma_{\boldsymbol{\psi}}^{\mathrm{MS}}\boldsymbol{\psi}_{\mathrm{R}} \equiv -2\mu^2\frac{\mathrm{d}}{\mathrm{d}\mu^2}\boldsymbol{\psi}_{\mathrm{R}} \quad \Rightarrow \quad \gamma_{\boldsymbol{\psi}}^{\mathrm{MS}} = -\mu^2\frac{\mathrm{d}}{\mathrm{d}\mu^2}\log Z_{\boldsymbol{\psi}}\,. \tag{2.11.21}$$

This implies that for operators which are renormalized by the flowed gluon field renormalization Z_s alone, the second term on the RHS of Eq. (2.11.19) reduces to $-\beta$ while for flowed operators which are rendered finite by the flowed fermion renormalization $Z_{\boldsymbol{\psi}}$ alone, it reduces to $-\gamma_{\boldsymbol{\psi}}$.

With the fermions being renormalized in the ringed scheme, the only remaining object directly related to the MS scheme is the gauge coupling.[3] A GFF scheme for the coupling has been proposed and calculated through NLO in Ref. [7] and the results have been extended to NNLO in Ref. [17]. The flowed gauge coupling is defined as

$$a_s^{\mathrm{GF}} \equiv a_s\frac{32\pi^2t^2}{3N_{\mathrm{A}}}\langle\boldsymbol{G}^a_{\mu\nu}\boldsymbol{G}^a_{\mu\nu}\rangle\,, \tag{2.11.22}$$

where the prefactor normalizes the RHS such that we have $a_s^{\mathrm{GF}} = a_s + \mathcal{O}(a_s^2)$. Since a_s^{GF} is independent of μ (see section 5.4 where we discuss the corresponding quantities in the SM), one can choose μ always in such a way that the $L_{\mu t}$ terms vanish and a_s^{GF} only depends on the flow-time.

[3] Anomalous dimensions of composite operators can be translated into a GFF scheme, too, see section 3.4.

The results of this chapter can be generalized to theories with multiple couplings in a straightforward way. Note that in chapter 5, where we discuss a modified version of the SM, the beta functions are defined in a different way, however (cf. Eqs. (C.1.4) and (C.1.13)).

2.12 Automation

The calculation of SFTX coefficients is automated using a tool chain developed in Refs. [36, 49, 75]. It is based on an automatic generation of the diagrams using `QGRAF` [76, 77]. We then use `tapir` [78] for the insertion of the Feynman rules and `exp` [79, 80] for the identification of topologies. As a result, we obtain an expression for each diagram which is readable by `FORM` [81, 82] and simplified until it is expressed in terms of scalar integrals. Integrals which vanish due to closed flow-line loops are identified using `closedloops` [42] and directly set to 0. Two-loop integrals are then reduced to a set of master integrals using `Kira` [53–55] and `FireFly` [56, 57] together with custom `Mathematica` [50] scripts. At three loops, we compute the integrals numerically using `ftint` [48, 63]. The configuration of these tools and the preparation of the input files, including the definition of projectors and the derivation of Feynman rules, is performed using `prepsetup` [83] and `frules` [84].

Chapter 3

The chromomagnetic dipole operator

One of the most profound open questions in modern physics is the origin of the matter-antimatter asymmetry in the universe. The Sakharov conditions [85] require any interaction responsible for the baryon asymmetry to violate CP-symmetry. However, the amount of CP-violation predicted by the SM is insufficient to explain the observed baryon asymmetry [86]. This discrepancy strongly motivates the search for new sources of CP-violation beyond the SM, which could manifest at energy scales not directly accessible to current experiments.

The nEDM provides an observable sensitive to BSM CP-violating effects which is free of backgrounds for many orders of magnitude (see Ref. [87] for a review). The experimental upper bound on the nEDM has been determined most precisely using ultra-cold neutrons [88, 89], the latest experiments [90, 91] reaching an upper bound of order $10^{-26}\,e\,\mathrm{cm}$, while the SM prediction (due to the CP-violating phase of the CKM matrix) is of order $10^{-32}\,e\,\mathrm{cm}$ [32], leaving a large window of possible BSM effects to be discovered in future experiments [25–31] which aim at reducing the upper bound by up to two orders of magnitude.

The BSM contributions to the nEDM can be systematically modeled by an effective field theory approach, where BSM effects are captured in the Wilson coefficients multiplying higher-dimensional operators which are renormalizable up to higher orders in the inverse BSM scale. At hadronic scales the dynamics is governed by QCD. At mass dimension five, the only CP-violating operator is the CEDM operator

$$\mathcal{O}_{\mathrm{CE}} = g_{\mathrm{B}}\epsilon_{\mu\nu\rho\sigma}\overline{\psi}\sigma_{\mu\nu}G_{\mu\nu}\psi\,, \tag{3.0.1}$$

while at dimension six the four-fermion operators and a purely gluonic operator are expected to give the dominant contributions to the nEDM [92]. In this chapter, we only consider dimension five operators, though.

Note that even at dimension four there is a possible CP-violation due to the topological charge density

$$\mathcal{L} \ni \frac{\theta g_s^2}{64\pi^2}\epsilon_{\mu\nu\rho\sigma}G_{\mu\nu}G_{\rho\sigma} \tag{3.0.2}$$

or complex quark masses that can appear in the Lagrangian. The two contributions are, however, not independent due to chiral rotations, and one commonly chooses to move all the CP-violating effects into the topological charge density. In this case, the nEDM

offers a valuable restriction since the current experimental upper bound on the nEDM requires the value [93]

$$\theta \lesssim 10^{-10}\,, \tag{3.0.3}$$

the unnatural smallness of which is known as the strong CP-problem. We will study the topological charge density in the GFF in a different context in chapter 4.

The nEDM d_{N} can be determined from Wilson coefficients C_i and hadronic matrix elements M by [87]

$$d_{\mathrm{N}} = M_\theta \theta + \left(\frac{v}{\Lambda_{\mathrm{BSM}}}\right) \sum_i M_i C_i\,, \tag{3.0.4}$$

where v is the Higgs field expectation value and Λ_{BSM} is the BSM scale. While the Wilson coefficients multiplying the effective CP-violating operators in an effective field theory can be calculated perturbatively (as they capture the small-distance physics) [94], the hadronic matrix elements required to determine the nEDM are inaccessible to perturbative calculations due to confinement and one has to resort to non-perturbative techniques like lattice QCD. However, the renormalization of the CEDM operator is complicated on the lattice and requires matching with the MS scheme used for the perturbative evaluation of the Wilson coefficients.

The GFF provides a method to circumvent these issues as it renders composite operators finite. Thus, flowed operators can be evaluated on the lattice and by an SFTX they can be matched to physical operators perturbatively, allowing a definition of flowed Wilson coefficients. This approach circumvents both matching of regularization schemes and the renormalization of lattice matrix elements. Lattice calculations involving the CEDM have been performed in Refs. [33, 95, 96] and NLO matching required for the flowed Wilson coefficients has been investigated in [24, 97].

In this chapter, we calculate the NNLO matching of the CMDM operator as a first step towards the NNLO matching of the CEDM operator, avoiding in a first approach nuisances caused by the implementation of γ_5 in d-dimensional space-time. The CMDM is, however, also an interesting quantity on its own as it contributes to the $K^0 - \bar{K}^0$ oscillation caused by indirect CP violation and rare kaon decays leading to direct CP violation parameterized by the ϵ'/ϵ ratio [22, 23].

Also note that in the massless case [24], the CMDM results also apply to the CEDM since in this case there appear no singlet-like diagrams requiring a special treatment of γ_5. We have already published our NNLO results for the massless case in Ref. [98].

3.1 Operator basis and construction of projectors

We work in QCD with n_f fermions of mass m. Since the chromomagnetic dipole operator has mass dimension five, the SFTX includes operators of dimensions one, three and five. Higher-dimensional operators only contribute terms which vanish in the limit $t \to 0$. At dimension one, there is only an operator proportional to unity,

$$\mathcal{O}_1^{\mathrm{B}} = m_{\mathrm{B}} \mathbb{1}\,, \tag{3.1.1}$$

while at dimension three there are the two operators

$$\mathcal{O}_2^{\mathrm{B}} = m_{\mathrm{B}}^3 \mathbb{1}\,, \qquad \mathcal{O}_3 = \overline{\psi}\psi\,. \tag{3.1.2}$$

At dimension five, there are three operators which vanish in the limit of massless quarks,

$$\mathcal{O}_4^{\mathrm{B}} = m_{\mathrm{B}}^5 \mathbb{1}\,, \qquad \mathcal{O}_5^{\mathrm{B}} = m_{\mathrm{B}} \overline{\psi} \overleftrightarrow{\not{D}} \psi\,, \qquad \mathcal{O}_6^{\mathrm{B}} = m_{\mathrm{B}} G^a_{\mu\nu} G^a_{\mu\nu}\,, \tag{3.1.3}$$

and the chromomagnetic dipole operator

$$\mathcal{O}_7^{\mathrm{B}} = \mathrm{i}g_{\mathrm{B}}\overline{\psi}\sigma_{\mu\nu}G^a_{\mu\nu}t^a\psi\,, \tag{3.1.4}$$

with $\sigma_{\mu\nu} \equiv \frac{\mathrm{i}}{2}[\gamma_\mu, \gamma_\nu]$. The factor $\mathrm{i}g_{\mathrm{B}}$ here serves to make the perturbative order in the coupling match the loop-order and ensures that the operator is hermitian and the matching coefficients are real.

Since the flow time has mass dimension -2, the mass dimensions of operators in the SFTX can only differ by even integers. Consequently, no operators of dimension zero, two, or four appear in our basis. This does not, however, reduce the complexity of the calculation, as dimension-five operators can always be constructed from dimension-four ones by multiplying with a mass factor.

In addition to the physical operators above, there are five nuisance operators (four at dimension five and one dimension-four operator multiplied by a mass factor) [99],

$$\mathcal{N}_1 = \partial^2(\overline{\psi}\psi)\,, \qquad \mathcal{N}_2 = m_{\mathrm{B}}\overline{\psi}\left(\overleftrightarrow{\not{D}} + 2m_{\mathrm{B}}\right)\psi\,, \tag{3.1.5}$$

$$\mathcal{N}_3 = \overline{\psi}\left(\not{D}^2 + \overleftarrow{\not{D}}^2 - 2m_{\mathrm{B}}^2\right)\psi\,, \qquad \mathcal{N}_4 = \overline{\psi}\left(\overleftarrow{\not{D}}\,\not{D} + m_{\mathrm{B}}^2\right)\psi\,, \tag{3.1.6}$$

$$\mathcal{N}_5 = g_{\mathrm{B}}\overline{\psi}\left(\not{A}\not{D} - \overleftarrow{\not{D}}\,\not{A} + 2m_{\mathrm{B}}\not{A}\right)\psi\,. \tag{3.1.7}$$

$\mathcal{N}_1$ is a total derivative while $\mathcal{N}_2$, $\mathcal{N}_3$ and $\mathcal{N}_4$ vanish by EOM. $\mathcal{N}_5$ is a BRST-exact operator. One might also think of the total derivative operator $\partial_\mu(\overline{\psi}\sigma_{\mu\nu}D_\nu)\psi$ which, however, is not linearly independent of the set of operators listed above, since

$$2\mathrm{i}\partial_\mu\left(\overline{\psi}\sigma_{\mu\nu}D_\nu\psi\right) + \mathcal{N}_3 + 2\mathcal{N}_4 - \mathcal{N}_1 = 0 \tag{3.1.8}$$

holds without use of EOM or IBP relations as follows from

$$\overline{\psi}\left(\not{D}\,\overleftarrow{\not{D}} - \overleftarrow{\not{D}}\,\not{D}\right)\psi = 2\mathrm{i}\partial_\mu\left(\overline{\psi}\sigma_{\mu\nu}D_\nu\psi\right)\,, \quad \text{and} \quad \partial^2(\overline{\psi}\psi) = \overline{\psi}\left(\not{D} + \overleftarrow{\not{D}}\right)^2\psi\,. \tag{3.1.9}$$

As discussed in section 2.10, these nuisance operators are required to obtain renormalizable and gauge-invariant results: While they themselves vanish in physical matrix elements, they do contribute to projections (as projectors are usually not defined using physical matrix elements or respecting momentum conservation). Thus, neglecting the nuisance operators leads to non-orthogonal projectors and thus gauge-variant and non-renormalizable terms are projected out of the flowed operators. For this reason we must keep track of the nuisance operators until we have arrived at an orthonormal set of projectors.

Expressing $\mathcal{O}_7$ in terms of flowed operators requires knowledge of the inverse SFTX matrix of the flowed versions of the above physical operators. We thus define flowed versions for each of the operators by

$$\boldsymbol{\mathcal{O}}_1(t,x) = Z_m^{-1}m_{\mathrm{B}}\mathbb{1}\,, \tag{3.1.10}$$

$$\boldsymbol{\mathcal{O}}_2(t,x) = Z_m^{-3}m_{\mathrm{B}}^3\mathbb{1}\,, \tag{3.1.11}$$

$$\boldsymbol{\mathcal{O}}_3(t,x) = \overset{\circ}{Z}_{\boldsymbol{\psi}}\overline{\boldsymbol{\psi}}_{\mathrm{B}}(t,x)\boldsymbol{\psi}_{\mathrm{B}}(t,x)\,, \tag{3.1.12}$$

$$\boldsymbol{\mathcal{O}}_4(t,x) = Z_m^{-5}m_{\mathrm{B}}^5\mathbb{1}\,, \tag{3.1.13}$$

$$\boldsymbol{\mathcal{O}}_5(t,x) = \overset{\circ}{Z}_{\boldsymbol{\psi}}Z_m^{-1}m_{\mathrm{B}}\overline{\boldsymbol{\psi}}_{\mathrm{B}}(t,x)\,\overleftrightarrow{\boldsymbol{D}}_{\mathrm{B}}\,\boldsymbol{\psi}_{\mathrm{B}}(t,x)\,, \tag{3.1.14}$$

$$\boldsymbol{\mathcal{O}}_6(t,x) = Z_sZ_m^{-1}m_{\mathrm{B}}\boldsymbol{G}^a_{\mathrm{B},\mu\nu}(t,x)\boldsymbol{G}^a_{\mathrm{B},\mu\nu}(t,x)\,, \tag{3.1.15}$$

$$\boldsymbol{\mathcal{O}}_7(t,x) = \overset{\circ}{Z}_{\boldsymbol{\psi}}\overline{\boldsymbol{\psi}}_{\mathrm{B}}(t,x)\sigma_{\mu\nu}\boldsymbol{G}^a_{\mathrm{B},\mu\nu}(t,x)t^a\boldsymbol{\psi}_{\mathrm{B}}(t,x)\,. \tag{3.1.16}$$

We determine the coefficients in the SFTX of $\mathcal{O}_7(t,x)$ using the method of projectors (the rest of the matching matrix being already known [46]). Since the corresponding operators are proportional to unity times a power of the mass, the projectors P_1, P_2 and P_4 are trivial, only taking mass derivatives of a VEV,

$$P_i[X] = \frac{1}{n_i!}\frac{\partial^{n_i}}{\partial m_{\mathrm{B}}^{n_i}}\langle 0|X|0\rangle^{\mathrm{1PI}}_{m_{\mathrm{B}}=0}\,, \tag{3.1.17}$$

where $i \in \{1,2,4\}$ and $n_1 = 1$, $n_2 = 3$ and $n_4 = 5$. The superscript on the matrix element indicates that it is one-particle irreducible in all internal lines except for flow-lines. Note that the above projectors are precisely of the form which allows for non-vanishing 1-loop contributions to the LO matrix as explained in section 2.6. Since they have no external legs, inserting an operator with a two-leg rule, such as the fermion bilinear $\overline{\psi}\psi$, would give rise to a non-vanishing one-loop diagram at zeroth order in the coupling. However, the chromomagnetic operator considered here has rules with at least three legs, so no such contributions appear in its SFTX.

The projector onto the fermion bilinear is given by

$$P_3[X] = -\frac{1}{4N_{\mathrm{c}}}\langle\overline{\psi}_i(q_1)\psi_i(q_2)|X|0\rangle^{\mathrm{1PI,\,amp}}_{q_1,q_2,m_{\mathrm{B}}=0}\,, \tag{3.1.18}$$

where the fermion in the projector has a fixed flavor, so no normalization factor $1/n_f$ is required, and the unflowed parts of the external propagators are amputated (the exponentials generated by the external legs are not relevant here, either, see section 2.6). So far, all projectors are already orthonormal. For the rest of the physical dimension-five projectors, we first define normalized linearly independent projectors,

$$P'_7[X] = -\frac{\mathrm{i}}{8D(D-1)g_{\mathrm{B}}}\frac{1}{N_{\mathrm{A}}T_{\mathrm{R}}}\frac{\partial}{\partial q_3^\nu}\langle\overline{\psi}_i(q_1)\psi_i(q_2)G^a_\mu(q_3)|\sigma_{\mu\nu}t^a_{ij}X|0\rangle^{\mathrm{1PI,\,amp}}_{q_1,q_2,q_3,m_{\mathrm{B}}=0}\,, \tag{3.1.19}$$

$$P'_6[X] = -\frac{1}{4D(D-1)N_{\mathrm{A}}}\frac{\partial}{\partial m_{\mathrm{B}}}\frac{\partial}{\partial q_1^\rho}\frac{\partial}{\partial q_2^\rho}\langle G^a_\mu(q_1)G^a_\mu(q_2)|X|0\rangle^{\mathrm{1PI,\,amp}}_{q_1,q_2,m_{\mathrm{B}}=0}\,, \tag{3.1.20}$$

$$P'_5[X] = -\frac{\mathrm{i}}{4DN_{\mathrm{c}}}\frac{\partial}{\partial m_{\mathrm{B}}}\frac{\partial}{\partial q_2^\mu}\langle\overline{\psi}_i(q_1)\psi_i(q_2)|\gamma^\mu X|0\rangle^{\mathrm{1PI,\,amp}}_{q_1,q_2,m_{\mathrm{B}}=0}\,. \tag{3.1.21}$$

For the orthogonalization of the above projectors, we further need projectors onto the nuisance operators which we again require to be linearly independent and normalized,

$$P'_{\mathcal{N}1}[X] = \frac{1}{8DN_{\mathrm{c}}}\frac{\partial}{\partial q_1^\mu}\frac{\partial}{\partial q_2^\mu}\langle\overline{\psi}_i(q_1)\psi_i(q_2)|X|0\rangle^{\mathrm{1PI,\,amp}}_{q_1,q_2,m_{\mathrm{B}}=0}\,, \tag{3.1.22}$$

$$P'_{\mathcal{N}2}[X] = -\frac{1}{16N_{\mathrm{c}}}\frac{\partial}{\partial m_{\mathrm{B}}^2}\langle\overline{\psi}_i(q_1)\psi_i(q_2)|X|0\rangle^{\mathrm{1PI,\,amp}}_{q_1,q_2,m_{\mathrm{B}}=0}\,, \tag{3.1.23}$$

$$P'_{\mathcal{N}3}[X] = \frac{1}{16Dg_{\mathrm{B}}^2N_{\mathrm{A}}T_{\mathrm{R}}}\langle G^a_\mu(q_1)G^a_\mu(q_2)\overline{\psi}_i(q_3)\psi_i(q_4)|X|0\rangle^{\mathrm{1PI,\,amp}}_{q_1,q_2,q_3,q_4,m_{\mathrm{B}}=0}\,, \tag{3.1.24}$$

$$P'_{\mathcal{N}4}[X] = \frac{\mathrm{i}}{4D(D-1)N_{\mathrm{c}}}\frac{\partial}{\partial q_1^\mu}\frac{\partial}{\partial q_2^\nu}\langle\overline{\psi}_i(q_1)\psi_i(q_2)|\sigma_{\mu\nu}X|0\rangle^{\mathrm{1PI,\,amp}}_{q_1,q_2,m_{\mathrm{B}}=0}\,. \tag{3.1.25}$$

$$P'_{\mathcal{N}5}[X] = \frac{\mathrm{i}}{4Dg_{\mathrm{B}}N_{\mathrm{A}}T_{\mathrm{R}}}\frac{\partial}{\partial q_1^\mu}\langle G^a_\mu(q_1)\overline{\psi}_j(q_2)\psi_i(q_3)|t^a_{ij}X|0\rangle^{\mathrm{1PI,\,amp}}_{q_1,q_2,q_3,m_{\mathrm{B}}=0}\,. \tag{3.1.26}$$

Note that none of these projectors take derivatives with respect to the same momentum more than once. Thus, there are no contributions from exponentials in the external legs and we can safely set these to 1.

Calculating and inverting the LO mixing matrix, we see that the orthogonalization of the physical projectors is given by

$$P_7 = P'_7 - P'_{\mathcal{N}3} + \frac{1}{2}P'_{\mathcal{N}4} + P'_{\mathcal{N}5}\,, \tag{3.1.27}$$

$$P_6 = P'_6\,, \tag{3.1.28}$$

$$P_5 = P'_5 - P'_{\mathcal{N}2} + P'_{\mathcal{N}3} - P'_{\mathcal{N}5}\,. \tag{3.1.29}$$

Note that in the orthogonalization of the physical operators, there is no contribution from $P'_{\mathcal{N}1}$, so we can drop the total derivative operator $\mathcal{N}_1$ from the basis.

3.2 Renormalization

Since the projectors as defined above project onto the bare operators, the SFTX needs to be renormalized. We define renormalized operators by

$$\mathcal{O}_i = \sum_j Z_{ij}\mathcal{O}_j^{\mathrm{B}}\,. \tag{3.2.1}$$

Since in dimensional regularization, operators of different mass dimension do not mix under renormalization, the renormalization matrix is split into blocks according to the mass dimensions of the operators. The sub-matrix renormalizing the subset $\{\mathcal{O}_4^{\mathrm{B}}, \mathcal{O}_5^{\mathrm{B}}, \mathcal{O}_6^{\mathrm{B}}\}$ can be expressed in terms of the anomalous dimensions of QCD since these operators appear in the QCD Lagrangian [100, 101]. It is given by [46]

$$Z_{3\mathrm{x}3} = Z_m^{-1}\begin{pmatrix} Z_m^{-4} & 0 & 0 \\ 8\mu^{-2\epsilon}Z_m^{-4}Z_0 & 1 & 0 \\ 4\mu^{-2\epsilon}Z_m^{-4}a_s\frac{\partial Z_0}{\partial a_s} & -2\frac{\gamma_m}{\beta} & -\frac{\epsilon}{\beta} \end{pmatrix}, \tag{3.2.2}$$

where Z_m, γ_m and β are defined in appendix B. Z_0 is the renormalization constant of the QCD vacuum energy [101–103]. It appears due to the presence of operators proportional to the identity in the basis and leads to mixing of other elements of the SFTX matrix into VEVs due to renormalization. The anomalous dimension of the vacuum energy is given by

$$\gamma_0 = (4\gamma_m - \epsilon) + \beta a_s\frac{\partial Z_0}{\partial a_s} \equiv -\frac{N_{\mathrm{c}}n_{\mathrm{f}}}{(4\pi)^2}\sum_{n=0}^{\infty}a_s^n\gamma_{0,n}\,, \tag{3.2.3}$$

with

$$\begin{aligned}&\gamma_{0,0} = 1\,, \quad \gamma_{0,1} = C_{\mathrm{F}}\,,\\ &\gamma_{0,2} = -C_{\mathrm{F}}^2\left(\frac{131}{32} - 3\zeta_3\right) - C_{\mathrm{F}}C_{\mathrm{A}}\left(-\frac{109}{32} + \frac{3}{2}\zeta_3\right) - \frac{29}{8}C_{\mathrm{F}}T_{\mathrm{R}}n_{\mathrm{f}}\,,\end{aligned} \tag{3.2.4}$$

where $\zeta_3 = \zeta(3) = 1.202...$ is the the Riemann zeta function evaluated at 3. Z_0 is then given by

$$\begin{aligned}Z_0 = \frac{N_{\mathrm{c}}n_{\mathrm{f}}}{(4\pi)^2\epsilon}\Bigg[1 + a_s\left(\frac{\gamma_{0,1}}{2} - \frac{2\gamma_{m,0}}{\epsilon}\right) + a_s^2\Bigg(\frac{2}{3\epsilon^2}(\beta_0\gamma_{m,0} + 4\gamma_{m,0}^2)\\ - \frac{1}{6\epsilon}(\beta_0\gamma_{0,1} + 4\gamma_{0,1}\gamma_{m,0} + 8\gamma_{m,1}) + \frac{1}{3}\gamma_{0,2}\Bigg)\Bigg] + \mathcal{O}(a_s^3)\,.\end{aligned} \tag{3.2.5}$$

In the renormalization matrix, the explicit μ-dependence due to the factor $\mu^{-2\epsilon}$ is required since the operators $\mathcal{O}_2^{\mathrm{B}}$ and $\mathcal{O}_3^{\mathrm{B}}$ have mass dimension $d = 4 - 2\epsilon$ while $\mathcal{O}_4^{\mathrm{B}}$ has mass dimension 4.

Similarly, the renormalization of the dimension three operators $\{\mathcal{O}_2^{\mathrm{B}}, \mathcal{O}_3^{\mathrm{B}}\}$ can be derived from the renormalization of the dimension four operators $m_{\mathrm{B}}\overline{\psi}\psi$ and m_{B}^4 which also appear in the Lagrangian. It is given by

$$Z_{2\mathrm{x}2} = \begin{pmatrix} Z_m^{-3} & 0 \\ -4\mu^{-2\epsilon} Z_m^{-3} Z_0 & Z_m \end{pmatrix}, \tag{3.2.6}$$

where again the factor $\mu^{-2\epsilon}$ accounts for the difference in the mass dimensions. We can now write the renormalization of the full basis

$$\mathcal{O} = \{\mathcal{O}_1, \mathcal{O}_2, \mathcal{O}_3, \mathcal{O}_4, \mathcal{O}_5, \mathcal{O}_6, \mathcal{O}_7\} \tag{3.2.7}$$

of physical operators as

$$\mathcal{O} = Z\mathcal{O}^{\mathrm{B}}, \qquad Z = \begin{pmatrix} Z_m^{-1} & & & \\ & Z_{2\mathrm{x}2} & & \\ & & Z_{3\mathrm{x}3} & \\ & & \vec{Z}_{\mathrm{CM}}^T & Z_{\mathrm{CM}} \end{pmatrix}, \tag{3.2.8}$$

where the empty entries of Z are understood to vanish. The block-diagonal form of the renormalization matrix arises due to non-mixing of operators of different mass dimension in dimensional regularization. The coefficient Z_{CM} can be extracted from [104], while the mixing coefficients $\vec{Z}_{\mathrm{CM}}^T$ have not been calculated yet to our knowledge.[1]

The anomalous dimension matrix can be obtained from Z by Eq. (2.11.18) and assumes the form

$$\gamma = \begin{pmatrix} \gamma_m & & & \\ & \gamma_{2\mathrm{x}2} & & \\ & & \gamma_{3\mathrm{x}3} & \\ & & \vec{\gamma}_{\mathrm{CM}}^T & \gamma_{\mathrm{CM}} \end{pmatrix}. \tag{3.2.9}$$

Due to the complicated relation of the renormalization matrix elements to the anomalous dimensions (caused by the presence of a VEV leading to poles already at $\mathcal{O}(a_s^0)$) we only give the final results for $\vec{Z}_{\mathrm{CM}}$ for convenience, without formally expressing it in terms of the anomalous dimensions using the renormalization group equation (RGE) Eq. (2.11.18). We use the RGE, however, to express the higher-order poles in terms of lower-order coefficients which allows us to give analytical results for these in the case of

[1] It might be possible to extract them from the results of Ref. [105].

$Z_{\rm CM,1}$. We obtain

$$Z_{\rm CM,1} = \mu^{-2\epsilon}\frac{a_s C_{\rm F} N_{\rm c} n_{\rm f}}{4\pi^2\epsilon}\Bigg\{1 + \frac{3}{2\epsilon} + a_s\Bigg(0.33333\,C_{\rm A} + 0.74999\,C_{\rm F} + 3.0833\,n_{\rm f}T_{\rm R} + \frac{1}{\epsilon}\left[\frac{47}{24}C_{\rm A} + \frac{31}{12}C_{\rm F} - \frac{7}{2}n_{\rm f}T_{\rm R}\right] + \frac{1}{\epsilon^2}\left[-\frac{17}{24}C_{\rm A} + \frac{23}{8}C_{\rm F} + \frac{2}{3}n_{\rm f}T_{\rm R}\right]\Bigg)\Bigg\} + \mathcal{O}(a_s^3)\,, \tag{3.2.10}$$

$$Z_{\rm CM,2} = \frac{3a_s C_{\rm F}}{\epsilon} + a_s^2 C_{\rm F}\Bigg(\frac{1}{\epsilon}\left[\frac{175}{48}C_{\rm A} - \frac{5}{4}C_{\rm F} - \frac{31}{6}n_{\rm f}T_{\rm R}\right] + \frac{1}{\epsilon^2}\left[-\frac{17}{8}C_{\rm A} + 3C_{\rm F} + 2n_{\rm f}T_{\rm R}\right]\Bigg) + \mathcal{O}(a_s^3)\,, \tag{3.2.11}$$

$$Z_{\rm CM,3} = -\frac{a_s n_{\rm f}T_{\rm R}}{\epsilon} + a_s^2 n_{\rm f}T_{\rm R}\Bigg(\frac{1}{\epsilon}\left[-\frac{5}{8}C_{\rm A} - \frac{3}{4}C_{\rm F}\right] + \frac{1}{\epsilon^2}\left[\frac{7}{6}C_{\rm A} - C_{\rm F} - \frac{1}{3}n_{\rm f}T_{\rm R}\right]\Bigg) + \mathcal{O}(a_s^3)\,, \tag{3.2.12}$$

where the factor $\mu^{-2\epsilon}$ is required again due to the difference in the mass dimensions of the operators, cf. $Z_{3\times3}$ in Eq. (3.2.2).

We can estimate the uncertainty of the numerical results for the $1/\epsilon$ poles of $Z_{\rm CM,1}$ by considering the cancellation of poles in the anomalous dimension matrix. The remaining poles are all smaller that $\mathcal{O}\left(10^{-10}\right)$. Thus, the results and the numerical precision suggest that the exact result is given by

$$0.33333\,C_{\rm A} + 0.74999\,C_{\rm F} + 3.0833\,n_{\rm f}T_{\rm R} \approx \frac{1}{3}C_{\rm A} + \frac{3}{4}C_{\rm F} + \frac{37}{12}n_{\rm f}T_{\rm R}\,, \tag{3.2.13}$$

the difference of the LHS and the RHS being $\mathcal{O}\left(10^{-7}\right)$ (note that we only display the first 5 significant digits in the numerical result and we use the full result to calculate the above difference).

The diagonal element $Z_{\rm CM}$ can be expressed in terms of the anomalous dimensions in a straightforward way,

$$Z_{\rm CM} = 1 - a_s\frac{\gamma_{\rm CM}^{(1)}}{\epsilon} + a_s^2\left[-\frac{\gamma_{\rm CM}^{(2)}}{2\epsilon} + \frac{1}{2\epsilon^2}\left(\gamma_{\rm CM}^{(1)}\beta_0 + \left(\gamma_{\rm CM}^{(1)}\right)^2\right)\right], \tag{3.2.14}$$

with

$$\gamma_{\rm CM}^{(1)} = \frac{1}{2}C_{\rm A} - \frac{5}{4}C_{\rm F}\,, \tag{3.2.15}$$

$$\gamma_{\rm CM}^{(2)} = \frac{11}{9}C_{\rm A}^2 - \frac{1057}{288}C_{\rm A}C_{\rm F} + \frac{51}{32}C_{\rm F}^2 + n_{\rm f}T_{\rm R}\left(\frac{41}{72}C_{\rm F} - \frac{43}{144}C_{\rm A}\right) \tag{3.2.16}$$

being the coefficients of the anomalous dimension matrix element

$$\gamma_{\rm CM} = \sum_{n=1}^{\infty}\gamma_{\rm CM}^{(n)}a_s^n\,. \tag{3.2.17}$$

We write the SFTX as in Eq. (2.11.15) with

$$F(t) = {\rm diag}(Z_m^{-1},\ Z_m^{-3},\ \mathring{Z}_\psi(t),\ Z_m^{-5},\ \mathring{Z}_\psi(t)Z_m^{-1},\ Z_s Z_m^{-1},\ \mathring{Z}_\psi(t))\,, \tag{3.2.18}$$

where we have made the t-dependence of the flowed fermion renormalization constant in the ringed scheme explicit. The renormalized mixing matrix is then given by

$$\overset{\circ}{\zeta}(t) = F(t)\zeta^{\mathrm{B}}(t)Z^{-1}\,. \tag{3.2.19}$$

As a check we calculate the regular anomalous dimension matrix using Eq. (2.11.19) and Eq. (2.11.18) and find that both calculations agree with each other and with the literature in the cases where the results are already known.

In order to write the physical CMDM operator in terms of flowed operators, the full matching matrix $\zeta(t)$ is needed since it must be inverted,

$$\mathcal{O}_7(x) = \sum_{j=1}^{7} (\zeta^{-1})_{7j}(t)\boldsymbol{\mathcal{O}}_j(t,x)\,, \tag{3.2.20}$$

where the sum runs over the set of physical operators defined in Eq. (3.2.7). For the entries $\zeta_{7j}(t)$ corresponding to the SFTX of the chromomagnetic operator only NLO results are known [24] while the rest of the matrix has already been calculated through NNLO, neglecting terms of $\mathcal{O}(t)$ [36, 46].

In this thesis, we generally neglect contributions of $\mathcal{O}(t)$. While this truncation prevents us from obtaining the exact inverse matrix, the results remain directly relevant for the subtraction of power divergences in t on the lattice [24]. The missing $\mathcal{O}(t)$ contributions are confined to four additional non-vanishing elements, $\zeta_{34}(t)$, $\zeta_{35}(t)$, $\zeta_{36}(t)$, and $\zeta_{37}(t)$.

3.3 Results

In the following, we present the results for the SFTX coefficients of $\boldsymbol{\mathcal{O}}_7$ through NNLO in the ringed scheme. We give the coefficients mutliplying the flow-time dependent logarithms $L_{\mu t}$ defined in Eq. (2.11.9) explicitly although they can be inferred from the renormalization group. We obtain

$$\begin{aligned}\overset{\circ}{\zeta}_{71} = \frac{3a_s C_{\mathrm{F}} N_{\mathrm{c}} n_{\mathrm{f}}}{8\pi^2 t^2}\Bigg\{ &\log\left(\frac{4}{3}\right) + a_s\Bigg(0.5207\,C_{\mathrm{A}} + 0.2679\,C_{\mathrm{F}} - 0.08789\,T_{\mathrm{R}} n_{\mathrm{f}} \\ &+ L_{\mu t}\Big[0.2637\,C_{\mathrm{A}} + 0.2157\,C_{\mathrm{F}} - 0.09589\,T_{\mathrm{R}} n_{\mathrm{f}}\Big]\Bigg)\Bigg\}\,,\end{aligned} \tag{3.3.1}$$

$$\begin{aligned}\overset{\circ}{\zeta}_{72} = \frac{9a_s C_{\mathrm{F}} N_{\mathrm{c}} n_{\mathrm{f}}}{8\pi^2 t}\Bigg\{ &\log\left(\frac{4}{3}\right) + \frac{1}{3}L_{\mu t} + a_s\Bigg(0.6464\,C_{\mathrm{A}} - 0.4491\,C_{\mathrm{F}} + 0.2853\,T_{\mathrm{R}} n_{\mathrm{f}} \\ &+ L_{\mu t}\Big[1.057\,C_{\mathrm{A}} + 0.03075\,C_{\mathrm{F}} - 0.2810\,T_{\mathrm{R}} n_{\mathrm{f}}\Big] \\ &+ L_{\mu t}^2\Big[0.3055\,C_{\mathrm{A}} + 0.25\,C_{\mathrm{F}} - 0.1111\,T_{\mathrm{R}} n_{\mathrm{f}}\Big]\Bigg)\Bigg\}\,,\end{aligned} \tag{3.3.2}$$

$$\begin{aligned}\overset{\circ}{\zeta}_{73} = -\frac{C_{\mathrm{F}}}{t}\Bigg\{ &\frac{3}{2}a_s + a_s^2\Bigg(-\frac{5}{6}T_{\mathrm{R}} n_{\mathrm{f}} + C_{\mathrm{F}}\Big(-\frac{3}{4} - 14\log 2 + \frac{45}{8}\log 3\Big) \\ &+ C_{\mathrm{A}}\Big(\frac{91}{24} + \frac{13}{4}\log 2 - \frac{9}{4}\log 3\Big) + L_{\mu t}\Big[\frac{11}{8}C_{\mathrm{A}} - \frac{9}{8}C_{\mathrm{F}} - \frac{1}{2}T_{\mathrm{R}} n_{\mathrm{f}}\Big]\Bigg)\Bigg\}\,,\end{aligned} \tag{3.3.3}$$

$$\overset{\circ}{\zeta}_{74} = -\frac{21 a_s C_{\rm F} N_{\rm c} n_{\rm f}}{64\pi^2}\Bigg\{1 - 12\log 2 + 6\log 3 - \frac{8}{7}{\rm Li}_2(1/4) - \frac{30}{7}L_{\mu t} - \frac{8}{7}L_{\mu t}^2 + a_s\Bigg(1.917\,C_{\rm A} - 5.501\,C_{\rm F} - 1.860\,T_{\rm R} n_{\rm f} + L_{\mu t}\Big[-5.479\,C_{\rm A} - 4.108\,C_{\rm F} + 5.113\,T_{\rm R} n_{\rm f}\Big] + L_{\mu t}^2\Big[-5.055\,C_{\rm A} - 8.051\,C_{\rm F} + 4.349\,T_{\rm R} n_{\rm f}\Big] - L_{\mu t}^3\Big[0.5079\,C_{\rm A} + 2.190\,C_{\rm F} + 0.1269\,T_{\rm R} n_{\rm f}\Big]\Bigg)\Bigg\}, \tag{3.3.4}$$

$$\overset{\circ}{\zeta}_{75} = C_{\rm F}\Bigg\{a_s\Bigg(\frac{29}{8} + 3L_{\mu t}\Bigg) + a_s^2\Bigg(C_{\rm A}\Bigg(\frac{6049}{480} - \frac{7}{16}\zeta_2 + \frac{4343}{240}\log 2 - \frac{333}{20}\log 3 - \frac{11}{16}{\rm Li}_2(1/4)\Bigg) + C_{\rm F}\Bigg(\frac{2441}{480} + \frac{9}{8}\zeta_2 - \frac{5123}{240}\log 2 + \frac{477}{80}\log 3 - \frac{7}{4}{\rm Li}_2(1/4)\Bigg) + T_{\rm R} n_{\rm f}\Bigg(-\frac{23}{2} - \frac{1}{2}\zeta_2 - 18\log 2 + 9\log 3 + \frac{3}{2}{\rm Li}_2(1/4)\Bigg) + L_{\mu t}\Bigg[\frac{875}{96}C_{\rm A} - \frac{205}{24}T_{\rm R} n_{\rm f} - C_{\rm F}\Big(\frac{29}{32} + 3\log 2 + \frac{9}{4}\log 3\Big)\Bigg] + L_{\mu t}^2\Bigg[\frac{5}{8}C_{\rm A} + 3C_{\rm F} + T_{\rm R} n_{\rm f}\Bigg]\Bigg)\Bigg\}, \tag{3.3.5}$$

$$\overset{\circ}{\zeta}_{76} = -n_{\rm f} T_{\rm R}\Bigg\{a_s\,(1 + L_{\mu t}) + a_s^2\Bigg(C_{\rm A}\Bigg(\frac{35}{48} + \frac{1}{8}\zeta_2 + 6\log 2 - \frac{13}{4}\log 3 + {\rm Li}_2(1/4)\Bigg) + C_{\rm F}\Bigg(\frac{101}{24} + \frac{9}{4}\log 2 - \frac{39}{8}\log 3 - \frac{9}{4}{\rm Li}_2(1/4)\Bigg) + L_{\mu t}\Bigg[\frac{3}{4}C_{\rm A} + C_{\rm F}\Bigg(\frac{15}{8} - \log 2 - \frac{3}{4}\log 3\Bigg)\Bigg] + L_{\mu t}^2\Big[C_{\rm F} - \frac{1}{4}C_{\rm A}\Big]\Bigg)\Bigg\}, \tag{3.3.6}$$

$$\overset{\circ}{\zeta}_{77} = 1 - a_s\Bigg\{\frac{1}{2}C_{\rm A} + C_{\rm F}\Bigg(\frac{3}{8} + \log 2 + \frac{3}{4}\log 3\Bigg) - \frac{1}{4}(5C_{\rm F} - 2C_{\rm A})L_{\mu t}\Bigg\} + a_s^2\Bigg\{C_{\rm A}^2\Bigg(-\frac{311}{108} - \frac{5}{24}\zeta_2 - \frac{251}{48}\log 2 + \frac{129}{32}\log 3 + \frac{7}{32}{\rm Li}_2(1/4)\Bigg) + C_{\rm A}C_{\rm F}\Bigg(\frac{1601}{1728} + \frac{5}{16}\zeta_2 + \frac{425}{72}\log 2 + \frac{1}{4}\log^2 2 - \frac{61}{32}\log 3 - \frac{9}{16}{\rm Li}_2(1/4)\Bigg) + C_{\rm F}^2\Bigg(\frac{10}{9} - \frac{5}{12}\zeta_2 + \frac{265}{144}\log 2 + \frac{1}{4}\log^2 2 - \frac{13}{4}\log 3 + \frac{19}{12}{\rm Li}_2(1/4)\Bigg) + C_{\rm F}T_{\rm R} n_{\rm f}\Bigg(\frac{7}{54} - \frac{1}{12}\zeta_2\Bigg) + C_{\rm A}T_{\rm R} n_{\rm f}\Bigg(\frac{1021}{1728} + \frac{1}{12}\zeta_2\Bigg) + L_{\mu t}\Bigg[-\frac{103}{72}C_{\rm A}^2 + \frac{67}{144}C_{\rm A}T_{\rm R} n_{\rm f} + C_{\rm F}^2\Big(-\frac{33}{16} - \frac{5}{4}\log 2 - \frac{15}{16}\log 3\Big) + C_{\rm A}C_{\rm F}\Big(\frac{26}{9} - \frac{5}{12}\log 2 - \frac{5}{16}\log 3\Big) + C_{\rm F}T_{\rm R} n_{\rm f}\Big(-\frac{4}{9} + \frac{1}{3}\log 2 + \frac{1}{4}\log 3\Big)\Bigg] + L_{\mu t}^2\Bigg[-\frac{5}{48}C_{\rm A}^2 - \frac{5}{96}C_{\rm A}C_{\rm F} + \frac{25}{32}C_{\rm F}^2 + \frac{1}{12}C_{\rm A}T_{\rm R} n_{\rm f} - \frac{5}{24}C_{\rm F}T_{\rm R} n_{\rm f}\Bigg] + \frac{c_\chi^{(2)}}{16}\Bigg\}. \tag{3.3.7}$$

The coefficient $c_\chi^{(2)}$ is defined in Eq. (2.11.10). Note that we have already presented the coefficients $\mathring{\zeta}_{73}$ and $\mathring{\zeta}_{77}$ in Ref. [98].

We can estimate the uncertainty of the numerical results in $\mathring{\zeta}_{71}$, $\mathring{\zeta}_{72}$ and $\mathring{\zeta}_{74}$ from the ϵ poles remaining after renormalization. These are at most of order $\mathcal{O}(10^{-9})$ (keeping the color factors as algebraic variables). We only give four significant digits for the numerical results, however.

Through NLO, our results for the above SFTX coefficients of $\boldsymbol{\mathcal{O}}_7$ agree with Ref. [24]. We also calculated the rest of the matching matrix as a check and find agreement with Ref. [46] through NNLO. Furthermore, we performed all calculations for the above results in general R_ξ gauge and found them to be independent of the gauge parameter.

The gauge dependence only cancels after the proper orthogonalization of the projectors. In particular, neglecting the contribution of the gauge variant operator leads to a gauge dependent result for ζ_{57} at NNLO. This shows that a proper treatment of the nuisance operators is crucial in order to obtain the correct results and gauge variant operators have to be taken into account when setting up the basis of operators.

Sample diagrams contributing to the projections are shown in Fig. 3.1. In Tab. 3.1 we show the numbers of diagrams generated for the naive projections of the CMDM grouped by the external legs appearing in the projectors.

External legs	**Projectors**	**Diagrams**	**Closed flow-line loops**
none	P_1, P_2, P_4	157	24
$\overline{\psi}$, ψ	P_3 , P_5', $P_{\mathcal{N}1}'$, $P_{\mathcal{N}2}'$, $P_{\mathcal{N}4}'$	222	30
G, G	P_6'	497	0
$\overline{\psi}$, ψ, G	$P_{\mathcal{N}5}'$	3089	468
$\overline{\psi}$, ψ, G, G	$P_{\mathcal{N}3}'$	49866	8280

Table 3.1: Numbers of NNLO diagrams generated for the naive projections of the CMDM (third column) and the number of diagrams vanishing due to the presence of closed flow-line loops (fourth column). The numbers only depend on the external legs defined in the projectors. For the projectors P_1, P_2 and P_4 the NNLO diagrams are of 3-loop order, while they are of 2-loop order for the other projectors.

3.4 Flowed anomalous dimensions

The flow-time dependence of the flowed operators is governed by an equation resembling the RGE [46],

$$t\frac{\mathrm{d}}{\mathrm{d}t}\boldsymbol{\mathcal{O}} = \boldsymbol{\gamma}\boldsymbol{\mathcal{O}}\,, \tag{3.4.1}$$

where $\boldsymbol{\gamma}$ is the flowed anomalous dimension matrix. Noting that the fundamental operators are independent of t and the mixing matrix only depends on t through

$$L_{\mu t} = \log\bigl(8\pi\mu^2 t\bigr)\,, \tag{3.4.2}$$

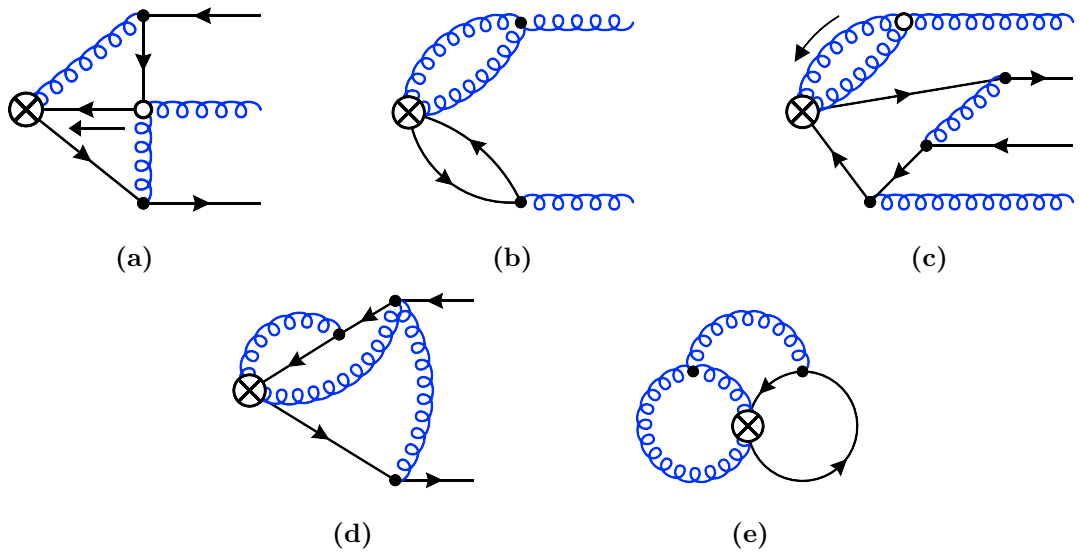

Figure 3.1: Sample diagrams for the four combinations of external legs appearing in the projectors. Diagram (a) contributes to ζ_{77} and ζ_{75}, (b) to ζ_{76}, (c) to ζ_{77} and ζ_{75}, (d) contributes to ζ_{73} and (e) to ζ_{71}, ζ_{72} and ζ_{74}.

the flowed anomalous dimension can be obtained by

$$\gamma = \left(t\frac{\mathrm{d}}{\mathrm{d}t}\zeta(t)\right)\zeta^{-1}(t) = \left(\frac{\partial}{\partial L_{\mu t}}\zeta(t)\right)\zeta^{-1}(t)\,. \tag{3.4.3}$$

Note, however, that this only holds for the full matching matrix since it involves the inverse of $\zeta(t)$ which, as discussed before, cannot be obtained if $\mathcal{O}(t)$ contributions are neglected in $\zeta(t)$.

3.5 Outlook on the chromoelectric operator

In this chapter we considered the SFTX of the quark chromomagnetic operator. The chromoelectric operator

$$\mathcal{O}_{\mathrm{CE}} = \epsilon_{\mu\nu\rho\sigma}\overline{\psi}\sigma_{\mu\nu}G_{\rho\sigma}\psi \tag{3.5.1}$$

on the other hand is an interesting object as it directly contributes to the CP violation leading to the nEDM. The operator basis mostly generalizes from the CP even case, replacing the CP even operators by CP odd ones by inserting a γ_5 (if the operators are bilinear in the quark fields) or replacing the field strength tensor by its Hodge dual in the case of the action density (resulting in the topological charge density operator). In one case, however, there is an ambiguity: The chromoelectric operator can be defined as above or as

$$\mathcal{O}'_{\mathrm{CE}} = \frac{1}{2\mathrm{i}}\overline{\psi}\{\sigma_{\mu\nu},\gamma_5\}G_{\mu\nu}\psi\,, \tag{3.5.2}$$

where $\{\cdot,\cdot\}$ is the anticommutator which makes sure that the operator is hermitian even in schemes in which γ_5 does not anticommute with the other Dirac matrices (see section 4.1 for a detailed treatment of this issue). These two operators are only linearly

dependent in four dimensions, but independent in $D = 4 - 2\epsilon$ dimensions [106], because of the strictly four-dimensional identity

$$\epsilon_{\mu\nu\rho\sigma}\sigma^{\rho\sigma} \overset{D=4}{=} 2\mathrm{i}\sigma^{\mu\nu}\gamma_5 \,. \tag{3.5.3}$$

The operator $\mathcal{E} \equiv \mathcal{O}_{\mathrm{CE}} - \mathcal{O}'_{\mathrm{CE}}$ therefore vanishes in four dimensions, but not in dimensional regularization. Such operators are known as evanescent operators and they must be taken into account since they can provide counter-terms to the physical operators [106] and the projectors have to be orthogonalized with respect to the evanescent operators as well.

3.6 Conclusion

We have presented the NNLO contributions to the SFTX coefficients of the flowed CMDM in QCD with massive quarks, neglecting $\mathcal{O}(t)$ coefficients, thereby extending and improving upon the previously known NLO results [24] and the NNLO results for the massless case [98]. As a by-product, we have also obtained three new entries of the renormalization matrix of QCD dimension-five operators. In deriving these results, we confirmed that a consistent treatment requires the inclusion of several nuisance operators, including gauge-variant ones, in accordance with the general structure of the renormalization matrix found by Joglekar and Lee (see section 2.10).

Beyond their intrinsic technical interest, these results strengthen the theoretical foundation for GFF techniques applied to higher-dimensional operators. In particular, they provide the first step towards a full determination of the SFTX of the CEDM, a quantity of direct phenomenological relevance for studies of CP violation. We have shown that, in general, gauge-variant nuisance operators have to be considered in the construction of the operator basis required for a proper definition of projectors. This offers a blueprint for future analyses of other higher-dimensional operators within flowed QCD and its extension to the SM which we will discuss in chapter 5.

Chapter 4

The chiral anomaly

The chiral anomaly plays a crucial role in perturbative and lattice QCD. While the continuum action is invariant under chiral transformations classically, this symmetry is broken by quantization since the measure of the fermionic path integral breaks chiral symmetry. [107]. This breaking leads to the anomaly and has important physical consequences, such as allowing pseudoscalar bosons coupled to axial currents to decay into two gauge bosons at one loop via the famous triangle diagram—the most prominent example being the $\pi^0 \to \gamma\gamma$ decay [108, 109].

The anomalous Slavnov–Taylor identity corresponding to chiral symmetry transformations relates the divergence of the singlet axial current to the topological charge density. Remarkably, the coefficient of this relation is already exact at one loop; higher-order corrections vanish due to the Adler–Bardeen theorem [110], a property referred to as one-loop exactness of the anomaly.

Higher-order calculations generally require a regularization scheme in order to control divergences. It is well-known that dimensional regularization breaks crucial properties of γ_5, leading to a breaking of global invariance under chiral transformations or a wrong anomaly relation, depending on the implementation of γ_5. These issues are reflections of the NNT which is a no-go theorem concerning the regularization of chiral fermions.

A lattice version of the NNT was first stated in Refs. [111, 112]. It implies that under a natural set of assumptions, there must necessarily be an equal number of left- and right-handed fermions, leading to the problem of fermion doubling on the lattice. Subsequently, a version accounting for general regularization methods has been developed in Ref. [113].

Since the topological charge plays a central role in lattice QCD and exhibits special properties under the Gradient Flow, it is natural to ask how the anomaly is realized within a GFF-based regularization. A first step in this direction was made in Ref. [114], where the SFTX of the singlet axial current and the topological charge density was calculated through NLO.

In this work we extend the analysis of Ref. [114] by calculating SFTX of the operators appearing in the chiral anomaly of massless QCD to NNLO. This allows us to test the t-independence of the topological charge at higher orders and to provide matching coefficients that can connect lattice results at finite flow time to the physical $t \to 0$ limit. Using recent four-loop results for the renormalization of the axial current, we furthermore obtain the flowed anomalous dimension governing the t-dependence of the anomaly operators through order a_s^3.

The remainder of this chapter is organized as follows: in section 4.1 we review the subtleties of the definition of γ_5 in dimensional regularization as a consequence of the NNT. In section 4.2 we introduce the relevant operators appearing in the anomaly relation of the unflowed theory and discuss their renormalization. We consider the effect of the GFF on the anomaly in section 4.3 and discuss the definition of the flowed operators and the application of the method of projectors in section 4.4. Our results are presented and discussed in section 4.5 and used to calculate the flowed anomalous dimensions in section 4.6.

4.1 Treatment of γ_5 in dimensional regularization

In this section we recapitulate the properties of γ_5 in Euclidean spacetime and its treatment in dimensional regularization which is required to obtain the correct chiral anomaly. In four-dimensional Euclidean spacetime, γ_5 is defined by

$$\gamma_5 = \gamma_1\gamma_2\gamma_3\gamma_4 = \frac{1}{4!}\epsilon_{\mu\nu\rho\sigma}\gamma_\mu\gamma_\nu\gamma_\rho\gamma_\sigma \tag{4.1.1}$$

and we have $\{\gamma_\mu, \gamma_5\} = 0\ \forall\mu$. From this it follows that

$$\mathrm{tr}(\gamma_5\gamma_\mu\gamma_\nu\gamma_\rho\gamma_\sigma) = 4!\epsilon_{\mu\nu\rho\sigma}\,. \tag{4.1.2}$$

It is well-known that there is no definition of γ_5 in dimensional regularization which satisfies all the four-dimensional Dirac algebra relations. For example, requiring that

$$\{\gamma_\mu, \gamma_5\} = 0 \tag{4.1.3}$$

holds for general d implies

$$(d-4)\,\mathrm{tr}(\gamma_5\gamma_\mu\gamma_\nu\gamma_\rho\gamma_\sigma) = 0\,, \tag{4.1.4}$$

which is consistent with the non-zero value of the trace at $d = 4$, but requires the trace to vanish for any $d \neq 4$. Since in dimensional regularization all results are meromorphic functions in d, we cannot recover the four-dimensional theory from its extension to d dimensions if we have to deal with γ_5. In particular, the scheme where γ_5 anticommutes, commonly referred to as the naive dimensional regularization (NDR) scheme, does preserve chiral symmetry but does not reproduce the correct chiral anomaly relation given in Eq. (4.2.6), which relies on the relation Eq. (4.1.2).

Another way to define γ_5 is to give up chiral symmetry in d dimensions by dropping the requirement $\{\gamma_\mu, \gamma_5\} = 0$ and instead reproduce the correct chiral anomaly in $d = 4$ dimensions. This approach is taken by dimensional reduction [115] which has been developed in the context of supersymmetry (since supersymmetry is broken by dimensional regularization), and by the 't Hooft-Veltmann (HV) scheme which was introduced together with dimensional regularization itself in Ref. [116]. In this scheme, the full $d = 4 - 2\epsilon$ dimensional spacetime is decomposed into a direct sum of a 4-dimensional and a -2ϵ dimensional spacetime. γ_5 is then defined as a purely four-dimensional object,

$$\gamma_5 = \gamma_1\gamma_2\gamma_3\gamma_4\,, \tag{4.1.5}$$

even at $d \neq 4$.

Alternatively, we can define γ_5 as

$$\gamma_5 = \frac{1}{4!}\epsilon_{\mu\nu\rho\sigma}\gamma_\mu\gamma_\nu\gamma_\rho\gamma_\sigma\,, \tag{4.1.6}$$

where, however, the Levi-Civita tensor is now assumed to only live in the four-dimensional subspace, effectively projecting out the four-dimensional Dirac matrices from the product. Assuming that all γ_5 have been rewritten in this way, the Levi-Civita tensors can be contracted in four dimensions and the resulting determinant of metric tensors can then be continued to d dimensions. The rest of the calculation, involving contractions with momenta and Dirac matrices, can then be performed fully in d dimensions. We refer to this procedure as the Larin scheme [117].

Note that while the Larin scheme does not lead to a vanishing anomaly like the NDR scheme, it still does not lead to the correct anomaly as long as we use the MS scheme or modified minimal subtraction ($\overline{\text{MS}}$). However, it is possible to restore the anomaly by introducing a finite renormalization of the axial vector current [117].

The complications in defining γ_5 in dimensional regularization are a special case of the NNT [113]. In its general form it is a no-go theorem concerning the regularization of a gauge theory with chiral fermions. It states that there cannot exist a regularization of such a theory which satisfies all of these conditions:

1. invariance under the global part of the gauge symmetry,
2. different numbers of left- and right-chiral Weyl fermions,
3. bilinearity of the action in the Weyl fields and
4. the theory gives rise to the correct chiral anomaly.

Note that the first two conditions together imply that the gauge group is a chiral transformation. For our purposes, where the numbers of left- and right-chiral fermions are the same and the gauge group is vectorial, we should thus adjust the list of conditions by replacing the first two by the requirement of invariance under a global chiral transformation. Since the QCD action is bilinear in the fermion fields for any regularization we consider, the NNT implies that there is no regularization which preserves both chiral symmetry and the chiral anomaly.

Applied to dimensional regularization, the NDR scheme leads to a vanishing anomaly (such that it cannot be restored even by a finite renormalization) while satisfying all other conditions. The Larin scheme with an additional finite renormalization, on the other hand, satisfies all conditions except for invariance under the global chiral symmetry since γ_5 no longer anticommutes in $d \neq 4$ dimensions.

4.2 The chiral anomaly

In this chapter we consider a Yang-Mills theory with n_f massless quarks given by the Lagrangian 2.1.1. The Lagrangian is symmetric under vectorial and (in four dimensions) chiral SU(N) transformations,

$$\text{SU}(N)_V : \psi \to e^{i\alpha}\psi\,, \tag{4.2.1}$$

$$\text{SU}(N)_A : \psi \to e^{i\alpha\gamma^5}\psi\,, \tag{4.2.2}$$

leading to two classically conserved currents, the singlet vector current

$$j_V^{\text{s},\mu} = \overline{\psi}\gamma^\mu\psi\,, \tag{4.2.3}$$

which is also conserved at quantum-level, as well as the singlet axial current

$$j_A^{\mathrm{s},\mu} = \overline{\psi}[\gamma^\mu, \gamma_5]\psi\,, \tag{4.2.4}$$

where a summation over flavor indices is implied and the commutator $[\gamma^\mu, \gamma_5]$ guarantees hermiticity of the singlet axial current in schemes with a non-anticommuting γ_5. The singlet axial current is anomalously non-conserved due to the breaking of chiral invariance by dimensional regularization in the Larin scheme. We refer to these currents as *singlet* since they transform as singlets under the flavor group.

We follow Refs. [117, 118] in rewriting the singlet axial current as

$$j_A^{\mathrm{s},\mu} = \frac{1}{3!}\epsilon_{\mu\nu\rho\sigma}\overline{\psi}\gamma_\nu\gamma_\rho\gamma_\sigma\psi\,. \tag{4.2.5}$$

The non-conservation of the axial current manifests itself in the anomalous Ward identity

$$\partial j_{A,\mathrm{R}}^{\mathrm{s}} = a_s\frac{n_\mathrm{f}T_\mathrm{R}}{4}q_R\,, \tag{4.2.6}$$

where

$$\partial j_{A,\mathrm{R}}^{\mathrm{s}} \equiv \partial_\mu j_{A,\mathrm{R}}^{\mathrm{s},\mu} \tag{4.2.7}$$

is the divergence of the renormalized axial current and q_R is the renormalized topological charge density. The bare singlet axial current is given by Eq. (4.2.5) and the bare topological charge density is

$$q = \epsilon_{\mu\nu\rho\sigma}G^a_{\mu\nu}G^a_{\rho\sigma}\,. \tag{4.2.8}$$

The bare operators are related to the renormalized ones by [117, 119]

$$\begin{pmatrix} q_\mathrm{R} \\ \partial j_{A,\mathrm{R}}^{\mathrm{s}} \end{pmatrix} = Z\begin{pmatrix} q \\ \partial j_A^{\mathrm{s}} \end{pmatrix}\,, \qquad Z = \begin{pmatrix} Z_s & Z_{qA} \\ 0 & Z_A^{\mathrm{s}} \end{pmatrix}\,, \tag{4.2.9}$$

where Z_s is the gauge coupling renormalization constant given in appendix B and the renormalization constant Z_A^{s} is split into an MS part and a finite part which serves the purpose to restore the anomaly relation in the Larin scheme,

$$Z_A^{\mathrm{s}} = Z_A^{\mathrm{s,MS}}Z_A^{\mathrm{s,f}}\,. \tag{4.2.10}$$

Both the MS and the finite part were calculated in Ref. [117] through NNLO (or higher). The MS part is given by

$$Z_A^{\mathrm{s,MS}} = 1 - a_s\frac{\gamma_{A,0}^{\mathrm{s}}}{\epsilon} + a_s^2\left[\frac{1}{2\epsilon^2}\left((\gamma_{A,0}^{\mathrm{s}})^2 + \beta_0\gamma_{A,0}^{\mathrm{s}}\right) - \frac{\gamma_{A,1}^{\mathrm{s}}}{2\epsilon}\right] + \mathcal{O}(a_s^3) \tag{4.2.11}$$

where $\gamma_{A,i}^{\mathrm{s}}$ are the coefficients of the anomalous dimension

$$\gamma_A^{\mathrm{s}} = a_s\beta(a_s)\frac{\mathrm{d}}{\mathrm{d}a_s}\log Z_A^{\mathrm{s,MS}}(a_s) = \sum_{n=0}^{\infty}a_s^{n+1}\gamma_{A,n}^{\mathrm{s}}\,, \tag{4.2.12}$$

with the first two coefficients given by

$$\gamma_{A,0}^{\mathrm{s}} = 0\,, \qquad \gamma_{A,1}^{\mathrm{s}} = -\frac{11}{12}C_\mathrm{A}C_\mathrm{F} - \frac{5}{12}C_\mathrm{F}T_\mathrm{R}n_\mathrm{f}\,. \tag{4.2.13}$$

The finite renormalization is given by

$$Z_A^{\mathrm{s,f}} = 1 - a_sC_\mathrm{F} + a_s^2\left(\frac{11}{8}C_\mathrm{F}^2 - \frac{107}{144}C_\mathrm{F}C_\mathrm{A} + \frac{31}{144}C_\mathrm{F}T_\mathrm{R}n_\mathrm{f}\right) + \mathcal{O}(a_s^3)\,. \tag{4.2.14}$$

4.3 General properties of the anomaly in the Gradient Flow

Let us consider how the conditions of the NNT are affected by the GFF which introduces the flow time t as a new UV regulator. The Lagrangian (2.1.13) of flowed QCD has terms bilinear in ψ and $\overline{\psi}$ (from the regular QCD Lagrangian) as well as mixed terms with Lagrange multipliers which are only linear in $\overline{\psi}$, ψ. However, the flowed Lagrangian is bilinear in the combined fields $(\overline{\boldsymbol{\psi}}, \overline{\boldsymbol{\eta}})$ and $(\boldsymbol{\psi}, \boldsymbol{\eta})$.

The GFF is constructed in such a way that it introduces a soft UV cutoff in a way that preserves all original symmetries of the theory, in particular Lorentz and gauge symmetry. It does not affect the chiral symmetry either. However, note that the Lagrange multipliers have opposite chirality compared to the fermion fields since the fermion flow equation has a trivial Dirac structure. The GFF still relies on dimensional regularization. As we have seen before, IR divergences related to UV divergences of unflowed composite operators still remain in SFTX calculations. Thus, we cannot fully replace dimensional regularization by regularization with t and chiral symmetry thus remains broken even at $t > 0$.

Since in the chiral theory left- and right-handed fermions are decoupled, we can define any numbers of chiral fermions. In particular, we can consider a theory of only left-chiral fermions (or only right-chiral ones). It remains to examine the effect of the GFF on the chiral anomaly.

In the GFF approach, the topological charge and the axial current are replaced by their corresponding flowed versions by replacing the QCD fields by flowed fields. The flowed operators are then related to the unflowed ones by means of the SFTX. As a consequence of the general properties of the GFF, the flowed topological charge is free of UV divergences and can be calculated on the lattice. A remarkable property of the flowed topological charge is that in the continuum limit it is independent of t. This has been shown in Ref. [120] (also see Ref. [114]). By means of the flow equations it can be shown that the identity

$$\partial_t \boldsymbol{q}(t,x) = \partial_\mu \boldsymbol{W}_\mu(t,x) \tag{4.3.1}$$

holds, where $\boldsymbol{q}(t,x)$ is the flowed topological charge density defined in Eq. (4.4.9) and

$$\boldsymbol{W}_\mu(t,x) = 4\epsilon_{\mu\nu\rho\sigma}\partial_t \boldsymbol{G}^a_\nu(t,x)\boldsymbol{G}^a_{\rho\sigma}(t,x) \tag{4.3.2}$$

is a gauge invariant current. Partial integration then implies that the topological charge is independent of t up to surface terms which vanish in perturbation theory [120]. Thus, the limit $t \to 0$ is particularly well-behaved despite the discretized topological charge having a remaining t dependence due to lattice artifacts.

As mentioned above, the flowed operators must be related to the unflowed ones by an SFTX, the coefficients of which have been obtained through NLO in Ref. [114]. Our aim is to extend this calculation to NNLO and to examine the effects of the GFF on the anomaly.

4.4 The flowed axial currents and chiral anomaly

In this section, we consider the SFTX of the topological charge density and the divergences of the singlet and non-singlet axial currents.

The SFTX of the singlet and non-singlet axial currents themselves have already been obtained in Ref. [47] through NNLO, where the results presented in this chapter, which

I have calculated independently, have been used as a check. Concerning the singlet and non-singlet axial currents, the results of Ref. [47] are expected to hold for their divergences, too, because of the identity

$$P_{\partial\mathcal{O}}[\partial X] = P_{\mathcal{O}}[X]\,, \tag{4.4.1}$$

where the projectors are assumed to be naive, so no orthogonalization has been performed. It follows from the fact that the total derivative introduces a total momentum which is canceled again by the momentum-derivative of the projector. Here, we check that this indeed holds for the divergence of the singlet and non-singlet axial currents through NNLO explicitly and also take the mixing with the topological charge density into account.

We assume that the theory is symmetric under a flavor group with traceless generators h^a. We first define diagonal and non-diagonal currents by

$$j^\mu_{A,rs} = \frac{1}{3!}\epsilon_{\mu\nu\rho\sigma}\overline{\psi}_r\gamma_\nu\gamma_\rho\gamma_\sigma\psi_s\,, \tag{4.4.2}$$

$$j^\mu_{A,rr} = \frac{1}{3!}\epsilon_{\mu\nu\rho\sigma}\overline{\psi}_r\gamma_\nu\gamma_\rho\gamma_\sigma\psi_r\,, \tag{4.4.3}$$

where $r \neq s$ are flavor indices and no summation over these is implied. We can now define the non-singlet current by

$$j_A^{\mathrm{ns},\mu} = \sum_{r\neq s} h^a_{rs} j^\mu_{A,rs} + \sum_r h^a_{rr} j^\mu_{A,rr}\,, \tag{4.4.4}$$

where we suppress the index a on the LHS since we chose a specific flavor generator from now on. We also assume that the generators are normalized such that

$$\mathrm{tr}\Big(h^a h^b\Big) = \delta^{ab} \tag{4.4.5}$$

in order to simplify the projectors (see below). The singlet current, on the other hand, is defined by

$$j_A^{\mathrm{s},\mu} = \sum_r j^\mu_{A,rr}\,, \tag{4.4.6}$$

just as before. Note that all of the above operators are considered bare. As implied by Eq. (4.2.9), the divergence of the singlet current renormalizes multiplicatively including an additional finite renormalization due to the Larin scheme. The current itself renormalizes with the same renormalization constant. The non-singlet current renormalizes multiplicatively, too,

$$j_{A,\mathrm{R}}^{\mathrm{ns},\mu} = Z_A^{\mathrm{ns}} j_A^{\mathrm{ns},\mu}\,, \tag{4.4.7}$$

where the renormalization constant is split up into an MS and a finite part again,

$$Z_A^{\mathrm{ns}} = Z_A^{\mathrm{ns,MS}} Z_A^{\mathrm{ns,f}}\,. \tag{4.4.8}$$

The renormalization constants are given in Ref. [117] (see also Ref. [47]). In the Larin scheme this finite renormalization is chosen in such a way that matrix elements of the non-singlet axial current match those of the vector current since the absence of fermion loops guaranteed by the tracelessness of the flavor generator allows us to use the NDR scheme. Thus, in this case the schemes should give the same result. Effectively, the finite renormalization for the non-singlet axial current restores the anti-commutativity of γ_5 which is broken in the Larin scheme.

We can now define flowed versions of the above currents and the topological charge density by replacing the fields by their flowed counterparts,

$$\boldsymbol{q}(t,x) = \epsilon_{\mu\nu\rho\sigma} Z_s \boldsymbol{G}^a_{\mu\nu}(t,x) \boldsymbol{G}^a_{\rho\sigma}(t,x)\,, \tag{4.4.9}$$

$$\boldsymbol{j}^{rs,\mu}_A(t,x) = \frac{1}{3!} \overset{\circ}{Z}_{\boldsymbol{\psi}} \partial_\mu \epsilon_{\mu\nu\rho\sigma} \overline{\boldsymbol{\psi}}_r(t,x) \gamma_\nu\gamma_\rho\gamma_\sigma \boldsymbol{\psi}_s(t,x)\,, \tag{4.4.10}$$

$$\boldsymbol{j}^{rr,\mu}_A(t,x) = \frac{1}{3!} \overset{\circ}{Z}_{\boldsymbol{\psi}} \partial_\mu \epsilon_{\mu\nu\rho\sigma} \overline{\boldsymbol{\psi}}_r(t,x) \gamma_\nu\gamma_\rho\gamma_\sigma \boldsymbol{\psi}_r(t,x)\,, \tag{4.4.11}$$

where the flowed fields are understood to be bare. The flowed singlet and non-singlet axial currents are constructed from these in the same way as in the unflowed case.

The SFTX of the divergence of the non-singlet current is given by

$$\partial \boldsymbol{j}^{\mathrm{ns}}_A = \zeta^{\mathrm{ns,B}}_A \partial j^{\mathrm{ns}}_A + \mathcal{O}(t)\,. \tag{4.4.12}$$

It can only mix with itself as there is no other dimension four operator with the same flavor group structure. The renormalized mixing coefficient is then given by

$$\zeta^{\mathrm{ns}}_A = (Z^{\mathrm{ns}}_A)^{-1} \zeta^{\mathrm{ns,B}}_A\,. \tag{4.4.13}$$

The singlet current mixes with the topological charge under the flow,

$$\begin{pmatrix} \boldsymbol{q} \\ \partial \boldsymbol{j}^{\mathrm{s}}_A \end{pmatrix} = \zeta^{\mathrm{B}} Z^{-1} \begin{pmatrix} q \\ \partial j^{\mathrm{s}}_A \end{pmatrix}, \qquad \zeta^{\mathrm{B}} = \begin{pmatrix} \zeta^{\mathrm{B}}_q & \zeta^{\mathrm{B}}_{qA} \\ \zeta^{\mathrm{B}}_{Aq} & \zeta^{\mathrm{s,B}}_A \end{pmatrix} + \mathcal{O}(t)\,, \tag{4.4.14}$$

where Z is defined in Eq. (4.2.9) and we can obtain the renormalized mixing matrix by

$$\zeta = \zeta^{\mathrm{B}} Z^{-1} = \begin{pmatrix} \zeta_q & \zeta_{qA} \\ \zeta_{Aq} & \zeta^{\mathrm{s}}_A \end{pmatrix}. \tag{4.4.15}$$

As has been outlined in section 2.6, the mixing coefficients are accessible to perturbative calculations using the method of projectors. For the operators considered here, no nuisance operators need to be taken into account and orthonormal projectors onto the diagonal ($r = s$) or off-diagonal ($r \neq s$) currents and the topological charge are directly given by

$$P^{rs}_{\partial j}[X] = \frac{\mathrm{i}}{4N_{\mathrm{c}}} \frac{1}{d(d-1)(d-2)(d-3)} \epsilon_{\mu\nu\rho\sigma} \frac{\partial}{\partial q_2^\mu} \langle \overline{\psi}_{i,r}(q_1) \psi_{i,s}(q_2) | \gamma_\nu\gamma_\rho\gamma_\sigma X | 0 \rangle^{\mathrm{1PI,\,amp}}_{q_1,q_2,m_{\mathrm{B}}=0}\,, \tag{4.4.16}$$

$$P_q[X] = \frac{1}{4N_{\mathrm{A}}} \frac{1}{d(d-1)(d-2)(d-3)} \epsilon_{\mu\nu\rho\sigma} \frac{\partial^2}{\partial q_1^\rho \partial q_2^\sigma} \langle G^a_\mu(q_1) G^a_\nu(q_2) | X | 0 \rangle^{\mathrm{1PI,\,amp}}_{q_1,q_2,m_{\mathrm{B}}=0}\,. \tag{4.4.17}$$

Note again that products of Levi-Civita tensors are reduced in four dimensions. We thus have

$$\epsilon_{\mu\nu\rho\sigma}\epsilon_{\mu'\nu'\rho'\sigma'} = \delta^{[\mu}_{\mu'}\delta^{\nu}_{\nu'}\delta^{\rho}_{\rho'}\delta^{\sigma]}_{\sigma'}\,, \qquad \epsilon_{\mu\nu\rho\sigma}\epsilon_{\mu\nu'\rho'\sigma'} = \delta^{[\nu}_{\nu'}\delta^{\rho}_{\rho'}\delta^{\sigma]}_{\sigma'}\,, \tag{4.4.18}$$

$$\epsilon_{\mu\nu\rho\sigma}\epsilon_{\mu\nu\rho'\sigma'} = 2\delta^{[\rho}_{\rho'}\delta^{\sigma]}_{\sigma'}\,, \qquad \epsilon_{\mu\nu\rho\sigma}\epsilon_{\mu\nu\rho\sigma'} = 6\delta_{\sigma\sigma'}\,, \tag{4.4.19}$$

$$\epsilon_{\mu\nu\rho\sigma}\epsilon_{\mu\nu\rho\sigma} = 24\,, \tag{4.4.20}$$

where [...] denotes unnormalized antisymmetrization and the Kronecker deltas are to be understood as d-dimensional again. Note that the d-dependent normalization factors in the projectors arise from the contractions of these Kronecker deltas in d dimensions.

We can now obtain the matching coefficient of the non-singlet current by projecting onto the diagonal and off-diagonal parts and contracting with a flavor generator,

$$\zeta_A^{\mathrm{ns,B}} = \sum_{rs} h^a_{sr} P^{rs}_{\partial j}[\partial \boldsymbol{j}^{\mathrm{ns}}_A]\,, \tag{4.4.21}$$

where a is fixed to the same value as in the flowed operator. Since all terms depending on the generator h^a drop out due to normalization and its effect then only amounts to removing all triangle-like contributions where the fermion lines of the operator and the projector are not connected, the matching coefficient is also given by

$$\zeta_A^{\mathrm{ns,B}} = P^{rs}_{\partial j}[\partial \boldsymbol{j}^{rs}_A]\,, \tag{4.4.22}$$

where $r \neq s$. We implemented the projector in this way since it does not require the additional implementation of flavor generators.

For the singlet current, we can either directly calculate the full projection or we make use of the fact that the diagrams contributing to the singlet projection split into triangle-like diagrams and non-singlet diagrams where the fermion line of the projector is connected to the operator. The non-singlet contribution is already given by $\zeta_A^{\mathrm{ns,B}}$, so we only need to calculate the triangle-like part

$$\zeta_A^{\Delta,\mathrm{B}} = P^{rr}_{\partial j}[\partial \boldsymbol{j}^{ss}_A]\,, \tag{4.4.23}$$

where $r \neq s$, and then obtain

$$\zeta_A^{\mathrm{s,B}} = \zeta_A^{\mathrm{ns,B}} + n_{\mathrm{f}} \zeta_A^{\Delta,\mathrm{B}}\,. \tag{4.4.24}$$

Some sample diagrams appearing in the SFTX of the singlet and non-singlet current are shown in Fig. 4.1.

4.5 Results

For the divergence of the non-singlet axial current, we obtain the same mixing coefficient as is given in Ref. [47] for the non-singlet axial current itself. We also find

$$\zeta_{Aq}(t) = 0 + \mathcal{O}(a_s^3) \tag{4.5.1}$$

This can be understood by writing the topological charge as divergence of the Chern-Simons current, which is not BRST invariant. Thus, it cannot contribute to the SFTX of the singlet axial current. Due to (4.4.1), this also holds for the divergences of the currents.

For the flowed topological charge we find

$$\zeta_q(t) = 1 + \mathcal{O}(a_s^3)\,, \tag{4.5.2}$$

which is in agreement with Ref. [114]. It is expected that $\zeta_q = 1$ holds to all orders since t-independence of this coefficient it is crucial for the t-independence of the flowed

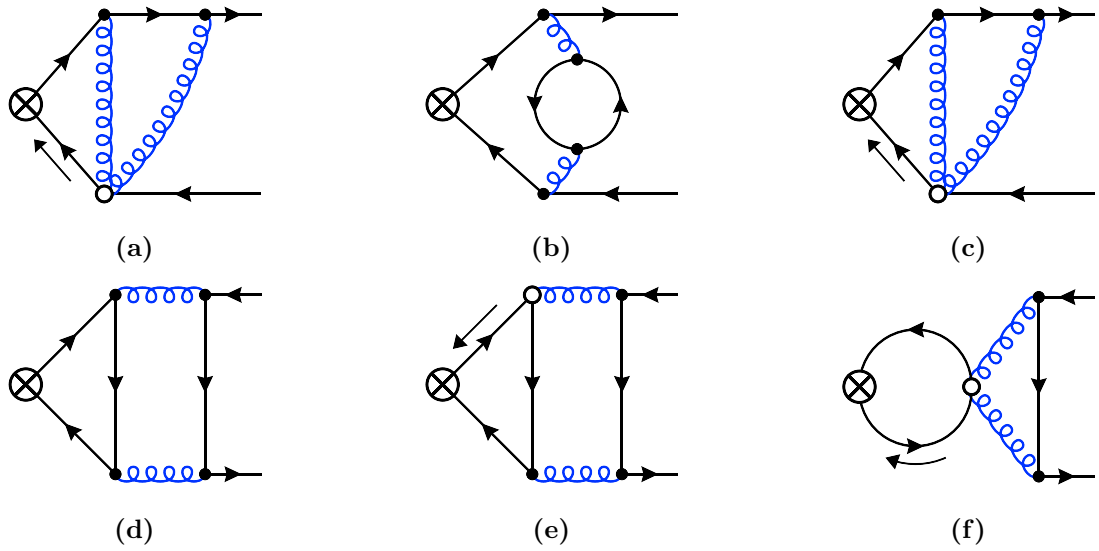

Figure 4.1: Sample diagrams appearing in the SFTX of the axial currents. Diagrams (a), (b) and (c) contribute to the the non-singlet current while (d) and (e) contribute to the triangle-like term of the singlet current. Diagrams of the form of (f) vanish.

topological charge. Since $\boldsymbol{q}(t)$ is the divergence of a gauge invariant current, it is independent of t for $t > 0$ as we have seen in Eq. (4.3.1). If we now check the t-dependence using the SFTX, we find

$$\partial_t Q(t) = \frac{1}{64\pi^2} \int_x \left(\partial_t \zeta_q(t) q_{\mathrm{R}}(x) + \partial_t \zeta_{qA}(t) \partial j^{\mathrm{s}}_A(x) \right) \stackrel{!}{=} 0 \,. \tag{4.5.3}$$

Perturbatively, the second term vanishes when integrated over since it is a total derivative, so we conclude that $\partial_t \zeta_q(t) = 0$ which is satisfied for our NNLO result. While q is a total derivative, too, we cannot set its integral to zero because it is the divergence of a gauge-variant current and its integral is a topological invariant.

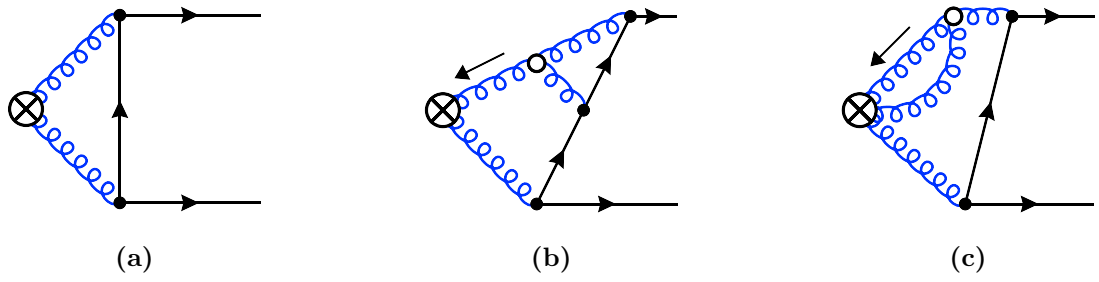

Figure 4.2: Sample diagrams contributing to the coefficient ζ_{qA}.

The two nontrivial elements of the mixing matrix $\zeta(t)$ are the self-projection $\zeta^{\mathrm{s}}_A(t)$ of the singlet axial current and its contribution $\zeta_{qA}(t)$ to the SFTX of the topological charge density. They are given by

$$\zeta_A^{\mathrm{s}}(t) = 1 + a_s C_{\mathrm{F}} \left(\frac{1}{8} - \log 2 - \frac{3}{4}\log 3\right) + a_s^2 \Bigg\{ C_{\mathrm{F}}^2 \Bigg(- \frac{41}{128} - \frac{5}{32}\zeta_2 + \frac{3}{8}\log 2 + \frac{1}{4}\log^2 2 - \frac{3}{32}\log 3 + \frac{3}{2}\mathrm{Li}_2(1/4)\Bigg) + C_{\mathrm{A}} C_{\mathrm{F}} \Bigg(- \frac{763}{384} - \frac{5}{32}\zeta_2 - \frac{13}{4}\log 2 + \frac{1}{4}\log^2 2 + \frac{27}{8}\log 3 + \frac{21}{16}\mathrm{Li}_2(1/4)\Bigg) + C_{\mathrm{F}} T_{\mathrm{R}} n_{\mathrm{f}} \Bigg(- \frac{1}{96} + \frac{\zeta_2}{4} + \frac{9}{2}\log 2 - \frac{9}{4}\log 3 + \frac{15}{8}\mathrm{Li}_2(1/4)\Bigg) + L_{\mu t}\Bigg[C_{\mathrm{A}} C_{\mathrm{F}} \left(\frac{11}{96} - \frac{11}{12}\log 2 - \frac{11}{16}\log 3\right) + C_{\mathrm{F}} T_{\mathrm{R}} n_{\mathrm{f}} \left(\frac{17}{24} + \frac{1}{3}\log 2 + \frac{1}{4}\log 3\right)\Bigg] + \frac{c_\chi^{(2)}}{16} \Bigg\}, \tag{4.5.4}$$

$$\zeta_{qA}(t) = -a_s C_{\mathrm{F}} \left(\frac{9}{2} + 3L_{\mu t}\right) + a_s^2 \Bigg\{ \frac{45}{16} C_{\mathrm{F}}^2 + C_{\mathrm{F}} C_{\mathrm{A}} \Bigg(- \frac{2789}{144} - \frac{299}{6}\log 2 + \frac{165}{4}\log 3 + \frac{5}{4}\mathrm{Li}_2(1/4)\Bigg) + C_{\mathrm{F}}\,\mathrm{tr}\, n_{\mathrm{f}} \left(\frac{139}{36} + \zeta_2\right) + L_{\mu t}\left[\frac{9}{4} C_{\mathrm{F}}^2 - \frac{85}{6} C_{\mathrm{A}} C_{\mathrm{F}} + \frac{10}{3} C_{\mathrm{F}} T_{\mathrm{R}} n_{\mathrm{f}}\right] + L_{\mu t}^2 \left[- \frac{11}{4} C_{\mathrm{A}} C_{\mathrm{F}} + C_{\mathrm{F}} T_{\mathrm{R}} n_{\mathrm{f}}\right] \Bigg\}. \tag{4.5.5}$$

Here we have used the ringed scheme and applied the finite renormalization of the Larin scheme. Some sample diagrams contributing to ζ_{qA} are shown in Fig. 4.2. Note that the ringed scheme only affects $\zeta_A^{\mathrm{s}}(t)$ since it is a projection of the only operator involving flowed fermions. The coefficient $c_\chi^{(2)}$ is given in Eq. (2.11.10). We abbreviate it here since it is only known numerically. Note, however, that it contributes additional terms to all color structures.

Note that the mixing coefficient $\zeta_{qA}(t)$ is allowed to depend on the flow time without spoiling the flow-time independence of $\boldsymbol{q}(t)$ since the divergence of the axial current does not contribute to the topological charge.

As expected, the result for $\zeta_A^{\mathrm{s}}(t)$ agrees with the result obtained in Ref. [47] for the SFTX of the singlet axial current itself. This provides a check of Eq. (4.4.1). $\zeta_A^{\mathrm{s}}(t)$ also agrees with the NLO results of Ref. [114], as does our result for $\zeta_{qA}(t)$, for which the NNLO contribution, however, is new.

As a check, both coefficients were calculated in general R_ξ gauge through NNLO and are independent of the gauge fixing parameter. The logarithmic terms are consistent with the RG equation (2.11.19).

4.6 Flowed anomalous dimensions

Since there are no power-divergences in t, we can calculate the flowed anomalous dimension from the results obtained through $\mathcal{O}(t^0)$ consistently. It is given by

$$\begin{aligned}\boldsymbol{\gamma}(t) &= \left(t\frac{\mathrm{d}}{\mathrm{d}t}\zeta(t)\right)\zeta^{-1}(t) \\ &= -\left(a_s\beta\frac{\partial}{\partial a_s}\zeta(t)\right)\zeta^{-1}(t) - \zeta(t)\gamma\zeta^{-1}(t) + \left[\left(a_s\beta(a_s)\frac{\partial}{\partial a_s} + t\frac{\mathrm{d}}{\mathrm{d}t}\right)F\right]F^{-1}\end{aligned} \tag{4.6.1}$$

where the second line can be derived from Eq. (2.11.19) and

$$F = \mathrm{diag}(Z_s, \mathring{Z}_{\boldsymbol{\psi}}) \tag{4.6.2}$$

is the matrix of flowed field renormalizations, implying that the last term in the equation before amounts to a diagonal matrix with $\beta(a_s)$ and $\mathring{\gamma}_{\boldsymbol{\psi}} = 1$ on the diagonals.

We find the flowed anomalous dimension matrix to have the form

$$\boldsymbol{\gamma} = \begin{pmatrix} 0 & \boldsymbol{\gamma}_{qA} \\ 0 & \boldsymbol{\gamma}_A \end{pmatrix} . \tag{4.6.3}$$

It is particularly convenient to choose the ringed scheme here since this allows us to calculate the flowed anomalous dimension to order a_s^3. This is because the unflowed anomalous dimensions start at order a_s^1 and the factor $a_s\beta(a_s)$ starts at order a_s^2 in the limit $\epsilon \to 0$. The flowed fermion field renormalization is only known to a_s^2, but in the ringed scheme, this does not matter as its anomalous dimension vanishes. The beta function, currently known to a_s^5 [121], is only needed to a_s^3 for this calculation.

We also need the unflowed anomalous dimension matrix to a_s^3. It is of the form

$$\gamma = \begin{pmatrix} \gamma_q & \gamma_{qA} \\ 0 & \gamma_A \end{pmatrix} . \tag{4.6.4}$$

For the singlet axial current, γ_A has been obtained to this order in Refs. [117, 122]. In Ref. [117] it was shown, however, that the off-diagonal element of the anomalous dimension matrix is given by

$$\gamma_{qA}(t) = \frac{\gamma_A}{c_{\mathrm{an}}(a_s)} \tag{4.6.5}$$

where $c_{\mathrm{an}}(a_s)$ is the one-loop exact coefficient appearing in the anomaly relation which we define later in Eq. (4.7.2). Since it is proportional to a_s, γ_A is required to order a_s^4 in order to obtain the full matrix to order a_s^3. The required four loop result has been obtained rather recently in Ref. [123]. The remaining diagonal element of the anomalous dimension matrix related to the topological charge is given by [117]

$$\gamma_q = -\beta(a_s) . \tag{4.6.6}$$

As a check we recalculate the flowed anomalous dimension for the singlet axial current with the same methods and setup and find agreement with Ref. [47] to order a_s^3. The result for the off-diagonal element is new. It is given by

$$\begin{aligned}
\boldsymbol{\gamma}_{qA}(t) = {} & -3a_sC_{\mathrm{F}} + a_s^2\Bigg\{C_{\mathrm{F}}^2\bigg(\frac{21}{8} - 3\log 2 - \frac{9}{4}\log 3\bigg) - \frac{85}{6}C_{\mathrm{A}}C_{\mathrm{F}} + \frac{10}{3}C_{\mathrm{F}}T_{\mathrm{R}}n_{\mathrm{f}} \\
& L_{\mu t}\bigg[- \frac{11}{2}C_{\mathrm{A}}C_{\mathrm{F}} + 2C_{\mathrm{F}}T_{\mathrm{R}}n_{\mathrm{f}}\bigg]\Bigg\} + a_s^3\Bigg\{\frac{3}{16}C_{\mathrm{F}}c_\chi^{(2)} + C_{\mathrm{F}}n_{\mathrm{f}}^2T_{\mathrm{R}}^2\bigg(- \frac{161}{72} - \zeta_2\bigg) \\
& + C_{\mathrm{A}}C_{\mathrm{F}}T_{\mathrm{R}}n_{\mathrm{f}}\bigg(\frac{1153}{36} + \frac{11}{4}\zeta_2 + 9\zeta_3 + \frac{299}{6}\log 2 - \frac{165}{4}\log 3 - \frac{5}{4}\mathrm{Li}_2(1/4)\bigg) \\
& + C_{\mathrm{A}}^2C_{\mathrm{F}}\bigg(- \frac{9793}{144} - \frac{3289}{24}\log 2 + \frac{1815}{16}\log 3 + \frac{55}{16}\mathrm{Li}_2(1/4)\bigg) \\
& + C_{\mathrm{A}}C_{\mathrm{F}}^2\bigg(\frac{4127}{384} - \frac{15}{32}\zeta_2 - \frac{287}{12}\log 2 + \frac{3}{4}\log^2 2 - \frac{1}{2}\log 3 + \frac{63}{16}\mathrm{Li}_2(1/4)\bigg)
\end{aligned}$$

$$
\begin{aligned}
&+ C_{\mathrm{F}}^3\bigg(- \frac{417}{128} - \frac{15}{32}\zeta_2 + \frac{33}{8}\log 2 - \frac{9}{4}\log^2 2 + \frac{63}{32}\log 3 - \frac{9}{2}\log 2\log 3 \\
&- \frac{27}{16}\log^2 3 + \frac{9}{2}\mathrm{Li}_2(1/4)\bigg) + C_{\mathrm{F}}^2 T_{\mathrm{R}} n_{\mathrm{f}}\bigg(\frac{221}{96} + \frac{3}{4}\zeta_2 - 9\zeta_3 + \frac{101}{6}\log 2 \\
&- \frac{17}{4}\log 3 + \frac{45}{8}\mathrm{Li}_2(1/4)\bigg) + L_{\mu t}\bigg[- \frac{1037}{24} C_{\mathrm{A}}^2 C_{\mathrm{F}} + \frac{155}{6} C_{\mathrm{A}} C_{\mathrm{F}} T_{\mathrm{R}} n_{\mathrm{f}} \\
&- \frac{10}{3} C_{\mathrm{F}} T_{\mathrm{R}}^2 n_{\mathrm{f}}^2 + C_{\mathrm{A}} C_{\mathrm{F}}^2\bigg(\frac{231}{32} - \frac{33}{4}\log 2 - \frac{99}{16}\log 3\bigg) + C_{\mathrm{F}}^2 T_{\mathrm{R}} n_{\mathrm{f}}\bigg(- \frac{9}{8} \\
&+ 3\log 2 + \frac{9}{4}\log 3\bigg)\bigg] + L_{\mu t}^2\bigg[- \frac{121}{16} C_{\mathrm{A}}^2 C_{\mathrm{F}} + \frac{11}{2} C_{\mathrm{A}} C_{\mathrm{F}} T_{\mathrm{R}} n_{\mathrm{f}} - C_{\mathrm{F}} T_{\mathrm{R}}^2 n_{\mathrm{f}}^2\bigg]\bigg\}\,,
\end{aligned}
\tag{4.6.7}
$$

where $\zeta_3 = \zeta(3) = 1.202\ldots$ is a value of the Riemann zeta function and we have given the dependence on $L_{\mu t}$ (which is defined in Eq. (2.11.9)) explicitly.

Note that the flowed anomalous dimension of the axial current is RG invariant in the ringed scheme, but $\boldsymbol{\gamma}_{qA}(t)$ is not: Since in the GFF the only renormalization required at $t > 0$ is the flowed field and the coupling renormalization, we can infer that for the flowed axial current we have

$$
\mu^2 \frac{\mathrm{d}}{\mathrm{d}\mu^2} \boldsymbol{j}_A^{\mathrm{s}}(t,x) = \bigg[\mu^2 \frac{\mathrm{d}}{\mathrm{d}\mu^2} \log \mathring{Z}_{\boldsymbol{\psi}}\bigg]\, \boldsymbol{j}_{A,\mathrm{B}}^{\mathrm{s}}(t,x) = 0 \tag{4.6.8}
$$

since in the ringed scheme the flowed fermion field is invariant under the RGE. We have used the fact that we can write

$$
\boldsymbol{j}_A^{\mathrm{s}} = \mathring{Z}_{\boldsymbol{\psi}} \boldsymbol{j}_{A,\mathrm{B}}^{\mathrm{s}} \tag{4.6.9}
$$

where $\boldsymbol{j}_{A,\mathrm{B}}^{\mathrm{s}}$ is independent of μ. Taking a flow-time derivative, using the definition of the flowed anomalous dimension and assuming that it commutes with the μ derivative, we can then derive from this that $\boldsymbol{\gamma}_A$ is independent of μ.

For the off-diagonal element of the flowed anomalous dimension, we can start from the relation

$$
\mu^2 \frac{\mathrm{d}}{\mathrm{d}\mu^2} \boldsymbol{q}(t,x) = \bigg[\mu^2 \frac{\mathrm{d}}{\mathrm{d}\mu^2} \log Z_s\bigg]\, \boldsymbol{q}(t,x) = -\beta \boldsymbol{q}(t,x)\,. \tag{4.6.10}
$$

Taking a flow-time derivative of this expression and proceeding as before yields the relation

$$
\mu^2 \frac{\mathrm{d}}{\mathrm{d}\mu^2} \boldsymbol{\gamma}_{qA}(t) = -\beta \boldsymbol{\gamma}_{qA}(t)\,, \tag{4.6.11}
$$

which is satisfied by our result.

4.7 Flowed anomaly relation

We can write the anomaly relation in a general form as

$$
0 = \partial j_{A,\mathrm{R}}^{\mathrm{s}}(x) + c_{\mathrm{an}}(a_s) q_{\mathrm{R}}(x)\,, \tag{4.7.1}
$$

where in our convention

$$
c_{\mathrm{an}}(a_s) = -a_s \frac{n_{\mathrm{f}} T_{\mathrm{R}}}{4}\,. \tag{4.7.2}
$$

Using the SFTX, we can rewrite the anomaly in terms of flowed operators,

$$
0 = \partial \boldsymbol{j}_A^{\mathrm{s}}(t,x) + \boldsymbol{c}_{\mathrm{an}}(a_s,t) \boldsymbol{q}(t,x)\,, \tag{4.7.3}
$$

where

$$\boldsymbol{c}_{\mathrm{an}}(a_s,t)=\frac{\zeta_A^{\mathrm{s}}c_{\mathrm{an}}(a_s)}{\zeta_q-c_{\mathrm{an}}(a_s)\zeta_{qA}}\,. \tag{4.7.4}$$

The denominator has the form $1-\mathcal{O}(a_s^2)$ and thus only the LO coefficient of ζ_{qA} contributes to the NNLO flowed anomaly coefficient. For the ratio of the anomaly coefficients we then obtain

$$\frac{\boldsymbol{c}_{\mathrm{an}}(a_s,t)}{c_{\mathrm{an}}(a_s)}=\zeta_A^{\mathrm{s}}(t)+a_s^2C_{\mathrm{F}}T_{\mathrm{R}}n_{\mathrm{f}}\left(\frac{9}{8}+\frac{3}{4}L_{\mu t}\right)+\mathcal{O}(a_s^3)\,, \tag{4.7.5}$$

where again the ringed scheme and the finite renormalization of the Larin scheme are applied.

It is worth noting that when the result is expressed in terms of the Gradient Flow coupling a_s^{GF} defined in Eq. (2.11.22), almost all $L_{\mu t}$ dependence vanishes and only a term

$$\frac{3}{2}a_s^2C_{\mathrm{F}}T_{\mathrm{R}}n_{\mathrm{f}}L_{\mu t}\in\boldsymbol{c}_{\mathrm{an}}(a_s,t) \tag{4.7.6}$$

remains. This remaining term can be traced back to the sign of the logarithmic term in the triangle contribution by which the matching coefficient of the singlet axial current differs from the non-singlet one. If the sign of this term would be reversed, all logarithms would cancel in the result for the flowed anomaly coefficient if it is expressed in terms of a_s^{GF}. However, after careful consideration, the sign seems to be correct and the $L_{\mu t}$ dependence does in fact remain in the anomaly coefficient.

From the flowed anomaly one can derive a relation among the flowed anomaly coefficient and the flowed anomalous dimensions which we use as a check. Taking a derivative of the anomaly relation with respect to $L_{\mu t}$ we arrive at

$$\frac{1}{\boldsymbol{c}_{\mathrm{an}}(a_s,t)}t\frac{\mathrm{d}}{\mathrm{d}t}\boldsymbol{c}_{\mathrm{an}}(a_s,t)-\boldsymbol{\gamma}_A(t)-\boldsymbol{c}_{\mathrm{an}}(a_s,t)\boldsymbol{\gamma}_{qA}(t)=0\,. \tag{4.7.7}$$

Since $\boldsymbol{c}_{\mathrm{an}}(a_s,t)$ starts at order a_s^1, we can only check this relation to order a_s^2 where we find it to be satisfied. It also requires the logarithmic term in Eq. (4.7.6) to remain in the flowed anomaly coefficient.

We see that the flowed coefficient reproduces $c_{\mathrm{an}}(a_s)$ only at leading order, implying on first glance that the GFF violates one-loop exactness of the anomaly relation. However, we can of course change the finite and t-dependent renormalization of the flowed fermion, i.e., replace the ringed scheme by a scheme in which the anomaly relation is restored. This new scheme is given by

$$\hat{\boldsymbol{\psi}}=\hat{Z}_{\boldsymbol{\psi}}^{1/2}\boldsymbol{\psi}_{\mathrm{B}}\,,\qquad\text{where}\quad\hat{Z}_{\boldsymbol{\psi}}=\frac{c_{\mathrm{an}}(a_s)}{\boldsymbol{c}_{\mathrm{an}}(a_s,t)}\zeta_{\boldsymbol{\psi}}Z_{\boldsymbol{\psi}}\,. \tag{4.7.8}$$

Note, however, that in this scheme, the flowed fermion is not independent of μ anymore since the flowed anomaly coefficient is μ-dependent.

The flowed anomaly relation might offer some interesting applications on the lattice. If a lattice fermion regularization is used which allows one to calculate the divergence of the singlet axial current, then together with the topological charge density one can infer the anomaly coefficient at $t>0$. By the above result, this coefficient is linked to α_s, so this might offer a new way to determine α_s at low energies from lattice data.

4.8 Conclusion

We have calculated the SFTX of the operators appearing in the chiral anomaly of massless QCD through NNLO and calculated the flowed anomalous dimension matrix to order a_s^3. We could verify that the the topological charge is t-independent perturbatively through NNLO. In addition, we formulated a flowed version of the anomaly relation and calculated the coefficient relating the flowed topological charge to the flowed singlet axial current, which in the unflowed theory is one-loop exact. The GFF introduces an additional UV regulator which does not break chiral symmetry, while still relying on dimensional regularization as an intermediate step and as an IR regulator. As such, it is interesting to observe how it relates to the NNT. At $t > 0$ we find that the flowed anomaly relation is no longer one-loop exact. The higher order contributions can be removed, however, by a t-dependent finite renormalization.

Chapter 5

The flowed Standard Model

The GFF has already been successfully applied to numerous problems in QCD. As a by-product of the perturbative GFF one also obtains the anomalous dimensions of the operators involved in the calculations. This includes NNLO anomalous dimensions of dimension-six four-quark operators [20, 124], the dimension-five chromomagnetic operator which we considered in the last chapter, the dimension-four operators appearing in the QCD Lagrangian [46] and the QCD energy-momentum tensor [14]. One might thus wonder if the GFF could not be used as a method to obtain the operator renormalization in particular in the context of effective field theories.[1]

In SMEFT, pushing the known NLO anomalous dimension to NNLO accuracy is of interest because one can improve the precision of SMEFT contributions to LHC processes or low-energy precision observables and investigate the structure of the SMEFT mixing pattern [127] which has been observed to have interesting characteristics such as non-trivial scheme-dependent zeros at NNLO [128] or holomorphy of the NLO anomalous dimensions [129]. Also, higher-order contributions can be used to estimate the theoretical accuracy [130].

Higher-order contributions to the anomalous dimensions also introduce new mixing among the operators. Thus, more operators contribute to a single observable which induces new correlations of Wilson coefficients and thus constrains the fits to experimental data. The effect of RG running has proven significant at NLO [131] and NNLO anomalous dimensions have been obtained in some sectors of the SMEFT [126], namely for the case of non-leptonic $\Delta F = 2$ operators (where only QCD effects are taken into account) [132] and for a SU(N) gauge theory including Dirac-fermions and scalars [133].

Concerning the calculational tools, the GFF based renormalization method would add to a list of already existing methods to calculate the NLO and NNLO anomalous dimensions of SMEFT operators. On-shell methods and unitary cuts have been used at one-loop [134, 135] and two-loop order [133, 136]. The R^* formalism [137–140] together with the background field method [141, 142] have been applied to the dimension six gluonic operator through 3-loop [127]. At NLO the full 2499×2499 anomalous dimension matrix of dimension six SMEFT operators has been calculated in the background field gauge [143–145] and there are ongoing efforts aimed at calculating the full NNLO anomalous dimensions of SMEFT using various methods [34].

A GFF based calculation of the NNLO anomalous dimensions could provide a strong check and, depending on the relative calculational efforts, might be a viable alternative to existing methods.

[1] For an introduction to and review of the SMEFT see Refs. [125, 126].

In this chapter, we consider a flavor-conserving version of the SM where we have set all Yukawa couplings to zero in a first approach. Since Yukawa couplings have not yet been considered in the GFF, we aim at first studying them separately and add them to the model considered in this chapter in the future. We will introduce the flow equations for all the fields and, by calculating suitable quantities, we determine the anomalous dimensions of the flowed fields, the ringed scheme conversion factors and the vacuum energy renormalization.

5.1 The flowed Standard Model Lagrangian

For the rest of the chapter we consider a flavor-conserving version of the SM (i.e., we set the Yukawa couplings to zero) with n_{g} generations of fermions and one scalar in the unbroken phase with mass m. Although we only consider one scalar as there is only one Higgs field in the SM, we introduce the marker variable n_{h} multiplying each scalar loop. Note that a proper treatment of multiple scalars requires slight modifications of the Feynman rules (see appendix C.3). Our notation for the field content is shown in Table 5.1.

Instead of the SM gauge groups we consider the more general group

$$\mathrm{SU}(N_3) \times \mathrm{SU}(N_2) \times \mathrm{U}(1)\,, \tag{5.1.1}$$

where the SM gauge group is recovered by $N_2 = 2$ and $N_3 = 3$. Note that anomaly cancellation requires $N_2 = 2$ (cf. section 5.2), but we keep $\mathrm{SU}(N_2)$ general in order to distinguish the contributions of different gauge groups more clearly.

Since the scalar sector of the SM is related to scalar QCD, the results presented in this chapter partially overlap with the ones published in Ref. [146] where we have considered a flowed massless SU(N) theory with scalars and fermions. The results we will give here were, however, calculated independently by me and were used to check the results presented in Ref. [146] which were calculated by Jonas T. Kohnen and Niels Felten.

The full covariant derivative in the fundamental representation is

$$D_\mu = \partial_\mu + g_1^{\mathrm{B}} Y B_\mu + g_2^{\mathrm{B}} W_\mu^i \tau^i + g_3^{\mathrm{B}} G_\mu^a t^a\,, \tag{5.1.2}$$

with the weak hypercharge operator Y, the $\mathrm{SU}(N_2)$ generators τ^i and the $\mathrm{SU}(N_3)$ generators t^a. The conventions regarding the Lie algebra can be found in Appendix A.1. The field strength tensors are given by

$$B_{\mu\nu} = \partial_{[\mu} B_{\nu]}\,, \quad W^i_{\mu\nu} = \partial_{[\mu} W^i_{\nu]} + g_2^{\mathrm{B}} f_2^{ijk} W^j_\mu W^k_\nu\,, \quad G^a_{\mu\nu} = \partial_{[\mu} G^a_{\nu]} + g_3^{\mathrm{B}} f_3^{abc} G^b_\mu G^c_\nu\,, \tag{5.1.3}$$

where $[\dots]$ denotes unnormalized antisymmetrization in the indices. With this, we can write the flavor-conserving SM Lagrangian as

$$\begin{aligned}\mathcal{L}_{\mathrm{SM}} = {} & \bar{q}_L \not{D} q_L + \bar{u}_R \not{D} u_R + \bar{d}_R \not{D} d_R + \bar{l}_L \not{D} l_L + \bar{e}_R \not{D} e_R \\ & - \frac{1}{4} B_{\mu\nu} B_{\mu\nu} - \frac{1}{4} W^i_{\mu\nu} W^i_{\mu\nu} - \frac{1}{4} G^a_{\mu\nu} G^a_{\mu\nu} \\ & + (D_\mu \phi)^\dagger (D_\mu \phi) - m_{\mathrm{B}}^2 \phi^\dagger \phi - \frac{\lambda^{\mathrm{B}}}{4} (\phi^\dagger \phi)^2 \\ & + \mathcal{L}_{\mathrm{gh}} + \mathcal{L}_{\mathrm{gf}}\,,\end{aligned} \tag{5.1.4}$$

where the gauge fixing terms are

$$\mathcal{L}_{\mathrm{gf}} = -\frac{1}{2\xi_B} (\partial_\mu B_\mu)^2 - \frac{1}{2\xi_W} (\partial_\mu W^i_\mu)^2 - \frac{1}{2\xi_G} (\partial_\mu G^a_\mu)^2\,, \tag{5.1.5}$$

Fundamental field	Representation	Y	Flowed field
ϕ	$\mathrm{SU}(N_2)_L^F \otimes \mathrm{U}(1)_Y^F$	y_h	$Z_{\boldsymbol{\phi}}^{1/2}\boldsymbol{\phi}_\mathrm{B}$
u_R	$\mathrm{SU}(N_2)_L^F \otimes \mathrm{SU}(N_3)_C^F$	y_u	$Z_{\boldsymbol{u}}^{1/2}(\boldsymbol{u}_R)_\mathrm{B}$
d_R	$\mathrm{SU}(N_2)_L^F \otimes \mathrm{SU}(N_3)_C^F$	y_d	$Z_{\boldsymbol{d}}^{1/2}(\boldsymbol{d}_R)_\mathrm{B}$
q_L	$\mathrm{SU}(N_2)_L^F \otimes \mathrm{SU}(N_3)_C^F \otimes \mathrm{U}(1)_Y^F$	y_q	$Z_{\boldsymbol{q}}^{1/2}(\boldsymbol{q}_L)_\mathrm{B}$
l_L	$\mathrm{SU}(N_2)_L^F \otimes \mathrm{U}(1)_Y^F$	y_l	$Z_{\boldsymbol{l}}^{1/2}(\boldsymbol{l}_L)_\mathrm{B}$
e_R	$\mathrm{U}(1)_Y^F$	y_e	$Z_{\boldsymbol{e}}^{1/2}(\boldsymbol{e}_R)_\mathrm{B}$
B	$\mathbb{1}$	0	$Z_1^{1/2}\boldsymbol{B}_\mathrm{B}$
W	$\mathrm{SU}(N_2)_L^A$	0	$Z_2^{1/2}\boldsymbol{W}_\mathrm{B}$
G	$\mathrm{SU}(N_3)_L^A$	0	$Z_3^{1/2}\boldsymbol{G}_\mathrm{B}$

Table 5.1: Overview of SM fields, their representation and weak hypercharge Y as well as the corresponding renormalized flowed fields written as products of flowed field renormalization constants and bare flowed fields. The values of the weak hypercharge guaranteeing anomaly cancellation are given in Eqs. (5.2.6) to (5.2.7). Z_1, Z_2 and Z_3 are the gauge coupling renormalization constants of our model (cf. appendix C.1).

and the ghost Lagrangian is given by

$$\mathcal{L}_\mathrm{gh} = \sum_{i=2,3} \mathrm{tr}\, \bar{c}_i \partial_\mu [D_\mu, c_i]\,, \tag{5.1.6}$$

with the $\mathrm{SU}(N_2)$ ghost c_2 and the $\mathrm{SU}(N_3)$ ghost c_3. As in QCD, it is convenient to define the couplings

$$a_1^\mathrm{B} = \frac{\left(g_1^\mathrm{B}\right)^2}{4\pi^2}\,, \quad a_2^\mathrm{B} = \frac{\left(g_2^\mathrm{B}\right)^2}{4\pi^2}\,, \quad a_3^\mathrm{B} = \frac{\left(g_3^\mathrm{B}\right)^2}{4\pi^2}\,, \quad a_4^\mathrm{B} = \frac{\lambda^\mathrm{B}}{4\pi^2}\,. \tag{5.1.7}$$

While the three gauge couplings renormalize multiplicatively like in QCD, the scalar self-coupling λ has additive counter terms which are not proportional to λ (for details on the renormalization, see appendix C.1). This follows from the appearance of divergent one-loop diagrams as the one shown in Fig 5.1 in the scalar four-point function.

We can now introduce flow equations analogously to the QCD ones. Thus, for the gauge fields we have

$$0 = \partial_t \boldsymbol{X}_\mu - [\boldsymbol{D}_\nu, \boldsymbol{X}_{\nu\mu}] - \kappa[\boldsymbol{D}_\mu, \partial_\nu \boldsymbol{X}_\nu] \equiv \boldsymbol{F}_X^\mu\,, \qquad \boldsymbol{X}_\mu(0,x) = X_\mu(x)\,, \tag{5.1.8}$$

with $\boldsymbol{X} \in \{\boldsymbol{B}, \boldsymbol{W}, \boldsymbol{G}\}$. We choose the same κ for all gauge fields for simplicity. In the end, we will set $\kappa = 1$ for all calculations. For $\boldsymbol{W}_\mu^i$ and $\boldsymbol{G}_\mu^a$ this equation takes the same form as the QCD one since the generators of different groups commute. Thus, these gauge fields flow independently of each other. For the B boson the situation is even simpler. Since U(1) is abelian, the adjoint covariant derivative is just the partial derivative and the flow equation for $\boldsymbol{B}_\mu$ reduces to the heat equation,

$$0 = \partial_t \boldsymbol{B}_\mu - \left[\partial^2 \delta_{\mu\nu} + (\kappa - 1)\partial_\mu \partial_\nu\right] \boldsymbol{B}_\nu\,. \tag{5.1.9}$$

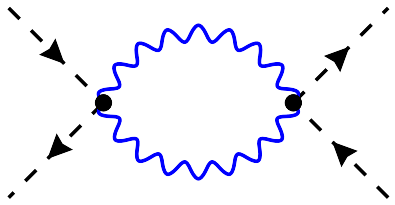

Figure 5.1: A diagram contributing to the non-multiplicative renormalization of the scalar self-coupling in the SM.

This can be solved exactly. The solution in the case $\kappa = 1$ is particularly simple,

$$\boldsymbol{B}_\mu(t,p) = B_\mu(p)e^{-tp^2}\,. \tag{5.1.10}$$

Because of the linearity of the flow equation, no B boson flow lines are required as they only serve the purpose of perturbatively solving the flow equation in diagrammatic form.

The fermion flow equations are formally the same as the QCD ones,

$$0 = \partial_t \boldsymbol{f} - \Big[\boldsymbol{D}^2 - \kappa(\partial_\mu \boldsymbol{D}_\mu - \partial^2)\Big]\boldsymbol{f} = \boldsymbol{F}_f\,, \tag{5.1.11}$$

$$0 = \partial_t \bar{\boldsymbol{f}} - \bar{\boldsymbol{f}}\Big[\overleftarrow{\boldsymbol{D}}^2 + \kappa(\partial_\mu \boldsymbol{D}_\mu - \partial^2)\Big] = \bar{\boldsymbol{F}}_f\,, \tag{5.1.12}$$

$$\boldsymbol{f}(0,x) = f(x)\,, \qquad \bar{\boldsymbol{f}}(0,x) = \bar{f}(x)\,, \tag{5.1.13}$$

with $f \in \{u_R, d_R, q_L, l_L, e_R\}$. Flow equations for scalar fields have already been considered in the context of other theories in Refs. [146–148]. Here, we chose the flow equations

$$0 = \partial_t \boldsymbol{\phi} - \Big[\boldsymbol{D}^2 - \kappa(\partial_\mu \boldsymbol{D}_\mu - \partial^2)\Big]\boldsymbol{\phi} = \boldsymbol{F}_\phi\,, \tag{5.1.14}$$

$$0 = \partial_t \boldsymbol{\phi}^\dagger - \boldsymbol{\phi}^\dagger\Big[\overleftarrow{\boldsymbol{D}}^2 + \kappa(\partial_\mu \boldsymbol{D}_\mu - \partial^2)\Big] = \boldsymbol{F}_\phi^\dagger\,, \tag{5.1.15}$$

$$\boldsymbol{\phi}(0,x) = \phi(x)\,, \qquad \boldsymbol{\phi}^\dagger(0,x) = \phi^\dagger(x)\,. \tag{5.1.16}$$

Just as in QCD, we now introduce Lagrange multiplier fields to implement the flow equations in the Lagrangian. We assign a multiplier field to each SM field by

$$f_R \to \boldsymbol{\lambda}_L^f\,, \qquad f_L \to \boldsymbol{\lambda}_R^f\,, \qquad \phi \to \boldsymbol{\lambda}^\phi\,, \tag{5.1.17}$$

$$W_\mu^a \to \boldsymbol{V}_\mu^a\,, \qquad G_\mu^a \to \boldsymbol{L}_\mu^a\,, \tag{5.1.18}$$

where f is a fermion. Note that for the fermions, the multiplier fields have opposite chirality since the flow equations have a trivial Dirac structure. The B boson does not require a multiplier field since its flow equation is solved exactly.

The flow part of the Lagrangian added to the SM Lagrangian then reads

$$\mathcal{L}_{\text{fl}} = \int_0^\infty \mathrm{d}t \left[\sum_f \left(\bar{\boldsymbol{F}}_f \boldsymbol{\lambda}^f + \bar{\boldsymbol{\lambda}}^f \boldsymbol{F}_f\right) + \boldsymbol{F}_W^{a,\mu}\boldsymbol{V}_\mu^a + \boldsymbol{F}_G^{a,\mu}\boldsymbol{L}_\mu^a + \boldsymbol{\mathcal{L}}_{\text{fl-gh}}\right]\,, \tag{5.1.19}$$

where $\boldsymbol{\mathcal{L}}_{\text{fl-gh}}$ contains the two flowed ghosts which are implemented just as in QCD. Note that there are no flowed antighosts again, these are instead interpreted as Lagrange multipliers. Also, flowed ghosts will again not contribute to any matrix elements as long as there are no ghosts in external states or operator insertions.

5.2 Anomaly cancellation

In the SM, there can in general appear gauge anomalies which would render the theory unphysical. They are, however, canceled by summing the anomalous triangle diagrams shown in Fig. 5.2 over all fermions appearing in the loops. Then, the axial contributions from different flavors cancel each other and the total amplitude for the gauge anomaly vanishes.

One can also turn this around and require the cancellation of the gauge anomalies, leading to a quantization of the weak hypercharge [149]. Since we work in a more general gauge group, we derive the cancellation conditions in their general form. The pure SU(N_3) anomaly cancellation condition requires

$$N_2 = 2\,, \tag{5.2.1}$$

since the elements of the left-handed quark multiplet have to combine with the two right-handed quarks in order to cancel the anomaly. However, we will still treat N_2 as a general parameter in the following in order to distinguish the contributions of the different gauge groups more clearly. For $N_2 = 2$, the pure SU(N_2) gauge anomaly vanishes due to the vanishing anomaly coefficient

$$\mathrm{tr}\Big(\tau^i\{\tau^j,\tau^k\}\Big) = 0\,. \tag{5.2.2}$$

Requiring the axial part of the triple B boson triangle diagram to vanish, we obtain the cubic equation

$$N_2 y_\mathrm{l}^3 + N_3 N_2 y_\mathrm{q}^3 = y_\mathrm{e}^3 + N_3(y_\mathrm{u}^3 + y_\mathrm{d}^3)\,, \tag{5.2.3}$$

while the two mixed diagrams with one B boson and two W bosons or gluons yield the linear equations

$$N_3 y_\mathrm{q} + y_\mathrm{l} = 0\,, \qquad y_\mathrm{u} + y_\mathrm{d} = N_2 y_\mathrm{q}\,. \tag{5.2.4}$$

Since there are five fermion hypercharges, a fourth condition is needed in order to fix the hypercharges up to one undetermined parameter[2]. One may choose the condition resulting from the requirement that the gravitational anomaly (with one B boson and two gravitons) has to vanish, too,

$$N_3 N_2 y_\mathrm{q} + N_2 y_\mathrm{l} = N_3(y_\mathrm{u} + y_\mathrm{d}) + y_\mathrm{e}\,. \tag{5.2.5}$$

Note that the above equations are all homogeneous in the hypercharges. Thus, there is only one parameter remaining which the hypercharges depend on linearly and which can thus be absorbed into the $U(1)$ generator. The ratios of the hypercharges are therefore fixed. Leaving the electron hypercharge as a free parameter, we find the solution

$$\frac{y_\mathrm{l}}{y_\mathrm{e}} = \frac{1}{2}\,, \qquad \frac{y_\mathrm{q}}{y_\mathrm{e}} = -\frac{1}{2N_3}\,, \tag{5.2.6}$$

$$\frac{y_\mathrm{u}}{y_\mathrm{e}} = \frac{N_3 - 1}{2N_3}\,, \qquad \frac{y_\mathrm{d}}{y_\mathrm{e}} = -\frac{N_3 + 1}{2N_3}\,, \tag{5.2.7}$$

where we have inserted $N_2 = 2$. This yields the SM values for $y_\mathrm{e} = -1$ and $N_3 = 3$. Since the theory is symmetric under $u_R \leftrightarrow d_R$, there is also a solution with the charges of the right handed quarks interchanged, of course.

[2] As has been shown in Ref. [150], it is also possible to derive the SM values of the hypercharges from requiring gauge anomaly cancellation and charge quantization, using Fermat's last theorem. This does not generalize to the more general gauge groups considered here in a straightforward way, however.

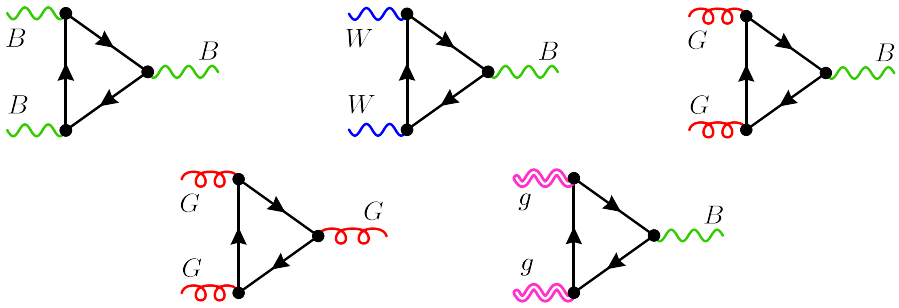

Figure 5.2: Diagrams requiring anomaly cancellation. Gravitons are displayed as double-line waves. The three-gluon diagram leads to the requirement $N_2 = 2$ which automatically renders the three-W diagram non-anomalous. The triangle diagrams not shown here vanish due to the generators of the non-abelian gauge groups being traceless.

As far as the effect of the GFF on anomaly cancellation is concerned, every triangle diagram vanishes as soon as at least one of its vertices is at $t > 0$ since this creates a closed loop of flow-lines. Thus, the flowed theory is still free of gauge anomalies if the unflowed one is. Note that this argument does not apply to non-minimal Gradient Flows (cf. section 2.3).

However, as explained in the next chapter in more detail, we will calculate the SFTX of various flowed fermionic operators with fixed flavor. Insertions of such operators generate non-vanishing anomalous triangle diagrams. The anomaly here again only cancels if all possible operator insertions are summed up. Since in any application this should be the case, we can neglect the anomalous contributions in such diagrams. We thus only calculate non-singlet type diagrams and can apply the NDR scheme.

5.3 Overview of quantities

A main objective of this chapter is to determine the renormalization constants of the flowed fields through NNLO. At NLO, mixing of different sectors is impossible and the fermion renormalization constants can thus be inferred from the QCD ones. At NNLO, however, mixed contributions of different gauge groups and the scalar sector lead to non-trivial new results.

Concerning the fermions, different quantities can be used to extract the renormalization constants. The original NLO calculation by Lüscher [9] in flowed QCD relied on an explicit calculation of the 1-loop self-energy diagrams contributing to $\langle \overline{\chi}(t,x)\chi(s,y)\rangle$. In Ref. [14], the NNLO flowed fermion field renormalization in QCD was determined analytically by taking advantage of the fact that the NNLO mixing of the operators appearing in the QCD energy-momentum tensor were known. Alternatively, one can calculate the VEV

$$\left\langle Z_\chi \overline{\chi}_\mathrm{B} \overleftrightarrow{\not{D}} \chi_\mathrm{B} \right\rangle\Big|_{m=0} \tag{5.3.1}$$

which must be finite by multiplicative renormalization with Z_χ alone. However, the NNLO contributions to this VEV are of 3-loop order and can thus only be calculated numerically with the methods currently available.

An alternative which allows one to obtain analytical results without having to consider operator mixing is provided by the SFTX of operators which are finite (or renormalize trivially) already in the unflowed theory. For fermions in our model, the fermionic non-singlet vector current is suited for this purpose. Since the non-singlet vector current is the conserved current of the flavor group, it is a finite operator. Furthermore, it allows us to safely use anticommuting γ_5. Since we are neglecting Yukawa couplings, we consider the generations as different flavors. We use the same strategy to obtain the mixing coefficient here as described in section 4.4, so we do not need to consider explicit flavor generators and instead we define the non-singlet vector current as

$$j_f^\mu \equiv \bar{f}_1 \gamma^\mu f_2 \,, \tag{5.3.2}$$

where f_1 and f_2 are fermions of different generations which transform under the same representation of the symmetry groups and have the same charges, such that the current is well-defined and gauge invariant.

Note that the above vector current is only finite for each fermion separately since we omit the Yukawa couplings. In this case, we have an additional global $\mathrm{U}(1)^5$ symmetry, where each factor transforms one of the five fermion species. The SM Yukawa interactions break this symmetry into a product of only two U(1) groups,

$$\mathrm{U}(1)^5 \overset{\text{Yukawa}}{\longrightarrow} \mathrm{U}(1)_{\text{leptons}} \otimes \mathrm{U}(1)_{\text{quarks}} \,. \tag{5.3.3}$$

This implies that the lepton currents can mix with each other under renormalization, as can the quark currents. A selection of diagrams responsible for mixing of the currents under the Gradient Flow is shown in Fig. 5.3. Approaching the extension of the GFF to the SM via the flavor-conserving version of the SM thus provides a clear intermediate step: it helps establish the structure of the GFF extension and enables various checks before moving on to the full SM in future work.

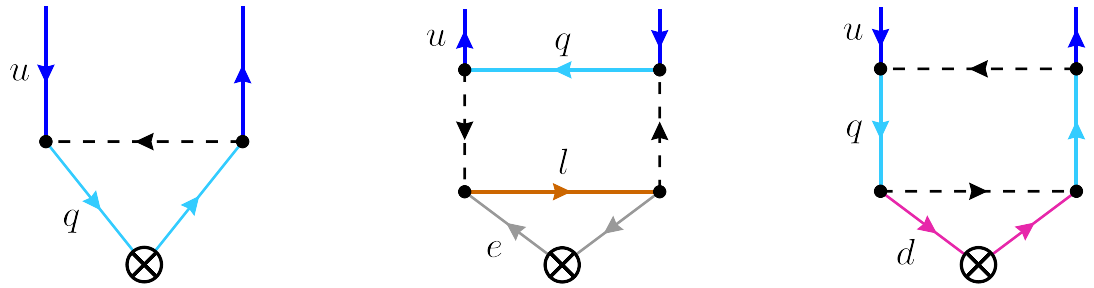

Figure 5.3: Sample diagrams leading to a mixing of different vector currents through Yukawa interactions.

The flowed fermionic vector currents

$$\boldsymbol{j}_f^\mu \equiv \bar{\boldsymbol{f}}_1 \gamma^\mu \boldsymbol{f}_2 \tag{5.3.4}$$

are defined as usual by replacing the unflowed fields with their renormalized flowed counterparts. Its SFTX is given by

$$\boldsymbol{j}_f^\mu(t,x) = v_f(t) j_f^\mu(x) + \mathcal{O}(t) \,, \tag{5.3.5}$$

and we can extract the flowed fermion renormalization through NNLO analytically from the requirement that $v_f(t)$ be finite.

Regarding the scalars, we can use the finite vector current defined by

$$j^\mu_\phi \equiv \phi^\dagger \overleftrightarrow{D}^\mu \phi \tag{5.3.6}$$

and its SFTX

$$\boldsymbol{j}^\mu_\phi(t,x) = v_\phi(t) j^\mu_\phi(x) + \mathcal{O}(t)\,, \tag{5.3.7}$$

to extract the flowed scalar field renormalization $Z_{\boldsymbol{\phi}}$.

Just as in QCD, we can also define a ringed scheme in the SM which allows us to obtain RG invariant quantities. We define the operators

$$S(x) = \phi^\dagger(x)\phi(x)\,, \quad \text{and} \qquad K_f(x) = \bar{f}(x) \overleftrightarrow{\not{D}} f(x)\,. \tag{5.3.8}$$

The SFTX of their flowed counterparts (again defined with renormalized flowed fields) is given by

$$\boldsymbol{K}_f(t,x) = \Big(K^f_0(t) + K^f_m(t) m^2\Big)\mathbb{1} + K^f_1(t) S(x) + \mathcal{O}(t)\,, \tag{5.3.9}$$

$$\boldsymbol{S}(t,x) = \Big(S_0(t) + S_m(t) m^2\Big)\mathbb{1} + S_1(t) S(x) + \mathcal{O}(t)\,. \tag{5.3.10}$$

where the unflowed operators on the RHS are understood to be renormalized. The relation of the bare and renormalized SFTX coefficients is described in section 5.7. The finite renormalizations $\zeta_{\boldsymbol{f}}$ and $\zeta_{\boldsymbol{\phi}}$ of the fermion and the scalar fields, respectively, are then implicitly defined by

$$\zeta_{\boldsymbol{f}} K^{f,\mathrm{MS}}_0(t) = K^{f,\mathrm{LO}}_0(t)\,, \qquad \zeta_{\boldsymbol{\phi}} S^{\mathrm{MS}}_0(t) = S^{\mathrm{LO}}_0(t)\,, \tag{5.3.11}$$

where the superscript MS implies that the quantity is renormalized in the MS scheme. $\boldsymbol{K}^{f,\mathrm{LO}}_0$ and $S^{\mathrm{LO}}_0(t)$ are the respective scheme-independent LO coefficients.

The gauge boson field renormalization is given by the renormalization of the corresponding couplings just as in QCD. We check this explicitly by considering the flowed operators

$$\boldsymbol{X}^2 \equiv \operatorname{tr} \boldsymbol{X}_{\mu\nu}\boldsymbol{X}_{\mu\nu} \tag{5.3.12}$$

for $\boldsymbol{X} = \boldsymbol{B}, \boldsymbol{W}, \boldsymbol{G}$ (defined with renormalized flowed fields). They also allow a definition of the SM couplings in a GFF scheme, cf. Eq. (2.11.22). Their SFTX is given by

$$\boldsymbol{X}^2(t,x) = \Big(X_0(t) + X_m(t) m^2\Big)\mathbb{1} + X_1(t) S(x) + \mathcal{O}(t)\,. \tag{5.3.13}$$

The flowed quartic scalar operator is given by

$$\boldsymbol{H} \equiv \lambda(\boldsymbol{\phi}^\dagger\boldsymbol{\phi})^2\,, \tag{5.3.14}$$

(see section 5.8), where the flowed fields are understood to be renormalized. Its SFTX in terms of renormalized operators is given by

$$\boldsymbol{H}(t,x) = \Big(H_0(t) + H_m(t) m^2\Big)\mathbb{1} + H_1(t) S(x) + \mathcal{O}(t)\,. \tag{5.3.15}$$

The last quantity we want to derive is the vacuum energy renormalization which appears in the renormalization of the SFTX coefficients multiplying the operator $m^2\mathbb{1}$. We derive it from the renormalization of the coefficient $S_m(t)$. Several checks are provided by the renormalization of $K^f_m(t)$, $X_m(t)$ (with $X = B, W, G$) and $H_m(t)$.

An overview of all the 36 quantities calculated in this chapter can be found in Tab. 5.2.

$Z_{\mathcal{O}}$	$\mathcal{O}$	$\mathbb{1}$	m^2	S	j^μ_ϕ	j^μ_u	j^μ_d	j^μ_q	j^μ_l	j^μ_e
$Z_{\boldsymbol{\phi}}$	$\boldsymbol{S}$	S_0	S_m	S_1	0	0	0	0	0	0
$Z_{\boldsymbol{\phi}}$	$\boldsymbol{j}^\mu_\phi$	0	0	0	v_ϕ	0	0	0	0	0
$Z_{\boldsymbol{u}}$	$\boldsymbol{j}^\mu_u$	0	0	0	0	v_u	0	0	0	0
$Z_{\boldsymbol{d}}$	$\boldsymbol{j}^\mu_d$	0	0	0	0	0	v_d	0	0	0
$Z_{\boldsymbol{q}}$	$\boldsymbol{j}^\mu_q$	0	0	0	0	0	0	v_q	0	0
$Z_{\boldsymbol{l}}$	$\boldsymbol{j}^\mu_l$	0	0	0	0	0	0	0	v_l	0
$Z_{\boldsymbol{e}}$	$\boldsymbol{j}^\mu_e$	0	0	0	0	0	0	0	0	v_e
$Z_{\boldsymbol{u}}$	$\boldsymbol{K}_u$	K^u_0	K^u_m	K^u_1	0	0	0	0	0	0
$Z_{\boldsymbol{d}}$	$\boldsymbol{K}_d$	K^d_0	K^d_m	K^d_1	0	0	0	0	0	0
$Z_{\boldsymbol{q}}$	$\boldsymbol{K}_q$	K^q_0	K^q_m	K^q_1	0	0	0	0	0	0
$Z_{\boldsymbol{l}}$	$\boldsymbol{K}_l$	K^l_0	K^l_m	K^l_1	0	0	0	0	0	0
$Z_{\boldsymbol{e}}$	$\boldsymbol{K}_e$	K^e_0	K^e_m	K^e_1	0	0	0	0	0	0
Z_1	$\boldsymbol{B}^2$	B_0	B_m	B_1	0	0	0	0	0	0
Z_2	$\boldsymbol{W}^2$	W_0	W_m	W_1	0	0	0	0	0	0
Z_3	$\boldsymbol{G}^2$	G_0	G_m	G_1	0	0	0	0	0	0
$Z^2_{\boldsymbol{\phi}}\frac{\lambda}{\lambda_{\mathrm{B}}}$	$\boldsymbol{H}$	H_0	H_m	H_1	0	0	0	0	0	0

Table 5.2: Overview of the quantities calculated in this chapter. The first column shows the flowed operator renormalization constants defined by $\mathcal{O} = Z_{\mathcal{O}}\mathcal{O}_{\mathrm{B}}$, where the renormalized flowed operators $\mathcal{O}$ shown in the second column are defined with renormalized couplings and flowed fields while $\mathcal{O}_{\mathrm{B}}$ is defined with the corresponding bare couplings and flowed fields. The bottom right part of the table separated by double lines shows the coefficient in the SFTX of the flowed operator in the second column multiplying the unflowed operator shown in the first row.

5.4 Gauge boson action densities

We consider the VEVs of the action densities B_0, W_0, G_0 defined in Eq. (5.3.13) through NNLO which here implies 3-loop order. They can be used to define the gauge couplings in a GFF scheme in analogy to QCD (see Eq. (2.11.22)). Through NLO we used general R_ξ gauge for each boson and confirmed that the results are gauge independent. At 3-loop order we chose Feynman gauge since keeping general R_ξ gauge leads to many more integrals which have to be evaluated numerically. We checked, however, that all the VEVs are consistent when mapping different gauge groups onto each other and that in the case of QCD they agree with the literature [17].

The results depend on the logarithm $L_{\mu t}$ defined in Eq. (2.11.9), but this dependence can be reconstructed from the result for $L_{\mu t} = 0$ using RG equations. Let

$$A_1 = B_0\,, \quad A_2 = W_0\,, \quad \text{and} \quad A_3 = G_0\,. \tag{5.4.1}$$

Since A_i is renormalized by multiplicative renormalization with a gauge coupling renormalization constant, its anomalous dimension is proportional to the corresponding beta function defined in appendix C.1. We thus find from Eqs. (2.11.19) and (2.11.20) that

$$\mu^2 \frac{\mathrm{d}}{\mathrm{d}\mu^2}(a_i A_i) = \left(\sum_{j=1}^{4} \beta^{(j)} \frac{\partial}{\partial a_j} + \frac{\partial}{\partial L_{\mu t}}\right)(a_i A_i) = 0 \tag{5.4.2}$$

for all three gauge boson action densities. We normalize the VEVs to their LO values by

$$\hat{A}_i = \frac{A_i}{A_i^{\mathrm{LO}}}\,, \quad i = 1,2,3\,, \tag{5.4.3}$$

where the leading-order contributions are

$$A_1^{\mathrm{LO}} = \frac{3}{32\pi^2}\,, \qquad A_2^{\mathrm{LO}} = \frac{3N_{\mathrm{A2}}}{32\pi^2}\,, \qquad A_3^{\mathrm{LO}} = \frac{3N_{\mathrm{A3}}}{32\pi^2}\,, \tag{5.4.4}$$

and expand the $\hat{A}_i$ in the couplings and the logarithmic terms as

$$\hat{A}_i = 1 + \sum_{n=1}^{\infty} \sum_{l=0}^{n} \sum_{i_1 \ldots i_n} \hat{A}^l_{i,i_1\ldots i_n} a_{i_1} \ldots a_{i_n} L^l_{\mu t}\,. \tag{5.4.5}$$

Note that writing the expansion in this way implies that the coefficients $\hat{A}^l_{i,i_1\ldots i_n}$ can always be chosen to be symmetric in $i_1 \ldots i_n$. In order to reduce redundancy, in the results we will give the coefficients multiplying particular products of couplings. These coefficients can be obtained from the $\hat{A}^l_{i,i_1\ldots i_n}$ by summing over all permutations of $i_1 \ldots i_n$, denoted as $\hat{A}^l_{i,(i_1\ldots i_n)}$ (the exact definition of this notation is given in Eq. (C.1.11)). For consistency of notation, we will always write $(i_1 \ldots i_n)$ in the results even if there are no index permutations other than the trivial one.

At orders beyond N^{4}LO this notation has the disadvantage that at least one index i_k always has to appear twice since there are only four couplings. At these orders a multi-index notation would thus be preferable.

With the beta functions as defined in appendix C.1, the logarithmic terms through NNLO are given by

$$\hat{A}^1_{i,j} = -\delta_{ij}\beta_0^{(i)}\,, \qquad \hat{A}^2_{i,jk} = \delta_{ij}\delta_{jk}\left(\beta_0^{(i)}\right)^2\,,$$

$$\hat{A}^1_{i,jk} = -\beta^{(i)}_{1,jk} - 2\delta_{ij}\delta_{ik}\beta^{(i)}_0 \hat{A}^0_{i,i}\,, \tag{5.4.6}$$

where no summation over multiple indices is implied. We calculated the analytic NLO as well as the numerical NNLO results.

Through NNLO, many results in our model share a similar structure and can partially be inferred from known QCD results and diagrammatic considerations. We therefore distinguish the numerical coefficients from the group and coupling structure. For this, we have to introduce some notation.

For a fermion or scalar field $F \in \{u, d, q, l, e, \phi\}$ we use these conventions:

- $\delta_2^F = 1$ if F transforms in the fundamental representation of $\mathrm{SU}(N_2)$, else $\delta_2^F = 0$
- $\delta_3^F = 1$ if F transforms in the fundamental representation of $\mathrm{SU}(N_3)$, else $\delta_3^F = 0$
- $\delta_H^F = 1$ if $F = \phi$, else $\delta_H^F = 0$

Whenever a fermion loop is inserted into a B boson propagator, we will encounter the combination

$$\Sigma_{\mathrm{yf}} = \sum_{f \text{ ferm.}} y_f^2 N_2^{\delta_2^f} N_3^{\delta_3^f} = \left(y_{\mathrm{u}}^2 + y_{\mathrm{d}}^2\right) N_3 + y_{\mathrm{q}}^2 N_2 N_3 + y_{\mathrm{l}}^2 N_2 + y_{\mathrm{e}}^2\,. \tag{5.4.7}$$

Note that one can rewrite the sum over the weak hypercharges in terms of group factors and only one hypercharge using the anomaly cancellation conditions, leading to

$$\Sigma_{\mathrm{yf}} = \left(\frac{3}{2} + \frac{1}{N_3} + \frac{N_3}{2}\right) y_{\mathrm{e}}^2 \overset{N_3=3}{=} \frac{10}{3} y_{\mathrm{e}}^2\,, \tag{5.4.8}$$

where we have assumed $N_2 = 2$. With these conventions, we can write the vacuum expectation values of the B boson action density as

$$\begin{aligned}
\hat{A}^0_{1,(1)} &= -X_{\mathrm{ng}} n_{\mathrm{g}} \Sigma_{\mathrm{yf}} - X_{\mathrm{nh}} n_{\mathrm{h}} N_2 y_{\mathrm{h}}^2\,,\\
\hat{A}^0_{1,(11)} &= n_{\mathrm{h}} N_2 y_{\mathrm{h}}^4 \left(X_{\mathrm{nh2}} n_{\mathrm{h}} N_2 + X_{\mathrm{cfh}}\right) + X_{\mathrm{ngh}} \Sigma_{\mathrm{yf}} n_{\mathrm{g}} n_{\mathrm{h}} y_{\mathrm{h}}^2 N_2 + X_{\mathrm{ng2}} n_{\mathrm{g}}^2 \Sigma_{\mathrm{yf}}^2\\
&\quad + X_{\mathrm{cfg}} n_{\mathrm{g}} \sum_{f \text{ ferm.}} y_f^4 N_2^{\delta_2^f} N_3^{\delta_3^f}\,,\\
\hat{A}^0_{1,(12)} &= -N_{\mathrm{A2}} T_2 \Big(X_{\mathrm{cfg}} n_{\mathrm{g}} \left(y_{\mathrm{l}}^2 + y_{\mathrm{q}}^2 N_{\mathrm{c}}\right) + X_{\mathrm{cfh}} n_{\mathrm{h}} y_{\mathrm{h}}^2\Big)\,,\\
\hat{A}^0_{1,(13)} &= -X_{\mathrm{cfg}} N_{\mathrm{A3}} T_3 n_{\mathrm{g}} \left(y_{\mathrm{u}}^2 + y_{\mathrm{d}}^2 + y_{\mathrm{q}}^2 N_2\right)\,.
\end{aligned} \tag{5.4.9}$$

where the $X_{\dots}$ are numerical coefficients. For $L_{\mu t} = 0$, they are given by

$$X_{\mathrm{ca}} = \frac{13}{9} + \frac{11}{6}\log 2 - \frac{3}{4}\log 3\,, \tag{5.4.10}$$

$$X_{\mathrm{ng}} = -\frac{1}{9}\,, \qquad X_{\mathrm{nh}} = -\frac{5}{36}\,, \tag{5.4.11}$$

$$X_{\mathrm{ca2}} = 1.748\,, \qquad X_{\mathrm{cag}} = -0.9864\,, \tag{5.4.12}$$

$$X_{\mathrm{cah}} = -0.7639\,, \qquad X_{\mathrm{cfg}} = 0.1531\,, \tag{5.4.13}$$

$$X_{\mathrm{cfh}} = -0.3453\,, \qquad X_{\mathrm{ng2}} = 0.03025\,, \tag{5.4.14}$$

$$X_{\mathrm{nh2}} = 0.02376\,, \qquad X_{\mathrm{ngh}} = 0.04878\,. \tag{5.4.15}$$

For the numerical coefficients we display four significant digits. The numerical accuracy can be estimated from the cancellation of the poles in the renormalized results through order $\mathcal{O}(10^{-6})$. The numerical evaluation (see section 2.9) also produces a numerical error which is multiplied by a marker variable. These errors are simply added together and thus do not reflect a proper error propagation. However, for the coefficient X_{ca2} these added errors amount to a value of 0.0001, which is larger than the pole cancellation by two orders of magnitude and should thus be considered a more proper estimate of the actual numerical error of this coefficient. This does still not, however, affect the four significant digits (implying three decimal places for this coefficient) we display.

For the W boson action density, we obtain

$$\begin{aligned}
\hat{A}^0_{2,(2)} &= X_{\mathrm{ca}}C_{\mathrm{A2}} + X_{\mathrm{ng}}\big(1+N_3\big)n_{\mathrm{g}}T_2 + X_{\mathrm{nh}}n_{\mathrm{h}}T_2\,,\\
\hat{A}^0_{2,(12)} &= -\Big(X_{\mathrm{cfg}}\big(y_l^2 + N_3 y_q^2\big)n_{\mathrm{g}} + X_{\mathrm{cfh}}y_{\mathrm{h}}^2 n_{\mathrm{h}}\Big)T_2\,,\\
\hat{A}^0_{2,(22)} &= X_{\mathrm{ca2}}C_{\mathrm{A2}}^2 + C_{\mathrm{A2}}T_2\Big(X_{\mathrm{cag}}n_{\mathrm{g}}\big(1+N_3\big) + X_{\mathrm{cah}}n_{\mathrm{h}}\Big)\\
&\quad + C_{\mathrm{F2}}T_2\Big(X_{\mathrm{cfg}}n_{\mathrm{g}}\big(1+N_3\big) + X_{\mathrm{cfh}}n_{\mathrm{h}}\Big)\\
&\quad + T_2^2\Big(X_{\mathrm{ng2}}\big(1+N_3\big)^2 n_{\mathrm{g}}^2 + X_{\mathrm{ngh}}\big(1+N_3\big)n_{\mathrm{g}}n_{\mathrm{h}} + X_{\mathrm{nh2}}n_{\mathrm{h}}^2\Big)\,,\\
\hat{A}^0_{2,(23)} &= X_{\mathrm{cfg}}N_{\mathrm{A3}}T_2T_3n_{\mathrm{g}}\,,
\end{aligned} \tag{5.4.16}$$

and for the gluonic one we have

$$\begin{aligned}
\hat{A}^0_{3,(3)} &= X_{\mathrm{ca}}C_{\mathrm{A2}} + X_{\mathrm{ng}}\big(2+N_2\big)n_{\mathrm{g}}T_3\,,\\
\hat{A}^0_{3,(13)} &= -X_{\mathrm{cfg}}\big(y_u^2 + y_{\mathrm{d}}^2 + N_2 y_q^2\big)n_{\mathrm{g}}T_3\,,\\
\hat{A}^0_{3,(23)} &= X_{\mathrm{cfg}}N_{\mathrm{A2}}T_2T_3n_{\mathrm{g}}\,,\\
\hat{A}^0_{3,(33)} &= X_{\mathrm{ca2}}C_{\mathrm{A3}}^2 + T_3n_{\mathrm{g}}\big(2+N_2\big)\big(X_{\mathrm{cag}}C_{\mathrm{A3}} + X_{\mathrm{cfg}}C_{\mathrm{F3}}\big) + X_{\mathrm{ng2}}T_3^2\big(2+N_2\big)^2 n_{\mathrm{g}}^2\,,
\end{aligned} \tag{5.4.17}$$

At NLO all three results have terms proportional to n_{g} or n_{h} (arising from diagrams like (b) and (c) in Fig. 5.4), while the W boson and the gluon also have terms proportional to C_{A3} or C_{A2}, respectively, arising from diagrams like (a). These are missing for the B boson due to the abelian nature of the corresponding gauge group. For the same reason, up to pinching and flow lines, the only NNLO diagrams contributing to the B boson result are (g) (where the fermion loops can be replaced by scalar ones, too), (h) and (d) (replacing the gluon with a B boson). The scalar does not contribute to the gluon action density through NNLO since all such contributions as the one in diagram (f) are of higher order. The numbers of diagrams contributing to the coefficients are shown in Tab. 5.3.

Interestingly, there are no contributions by diagrams like (i) which are proportional to a_4. They do not vanish algebraically, however, but only after inserting the numerical values for the 3-loop integrals. This is in agreement with the fact that there are no contributions of the scalar self-coupling to the beta functions of the gauge bosons through NNLO in the SM [151].

5.5 Flowed fermion field renormalizations

In this section we consider the SFTX of the flowed fermionic vector currents $\boldsymbol{j}_f^\mu$ defined in Eq. (5.3.4) in order to derive the flowed fermion field renormalizations in the MS

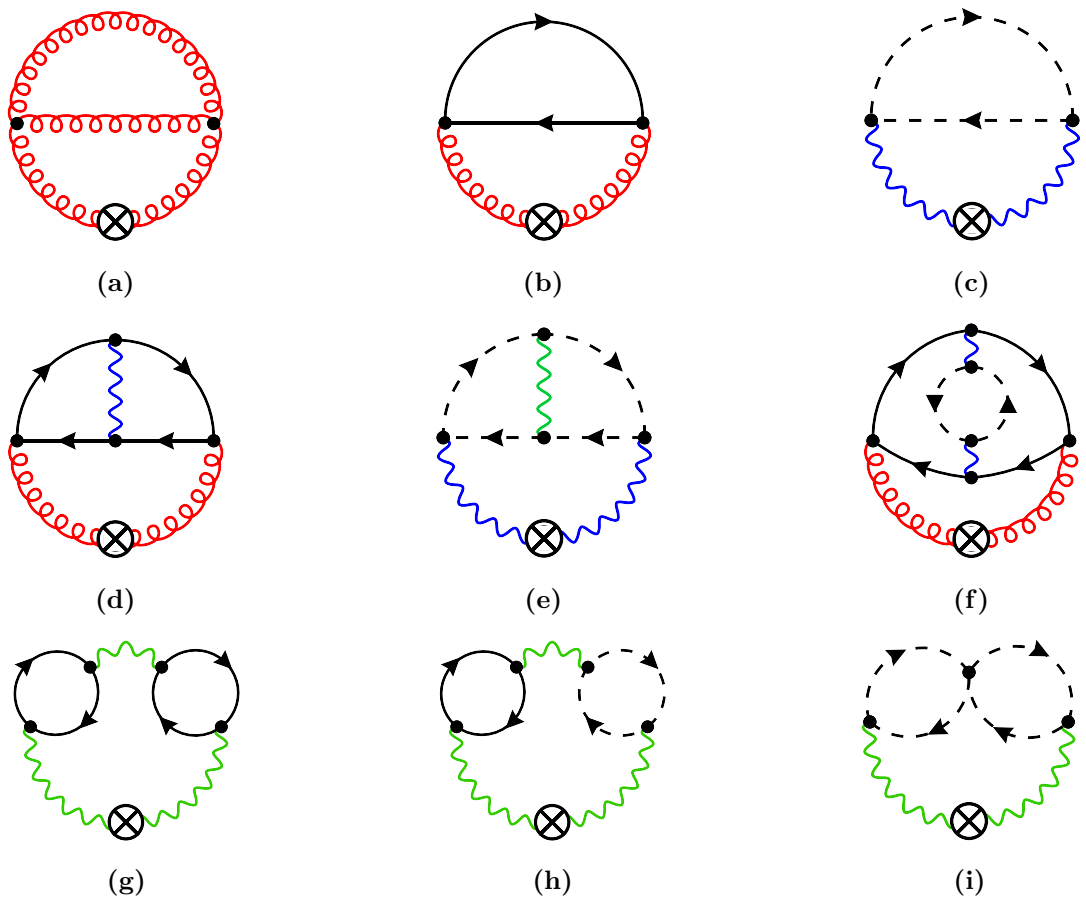

Figure 5.4: Some diagrams contributing to the gauge boson action densities. The B boson is displayed in green, the W boson in blue and the gluon in red. Solid lines with arrows represent fermions and dashed ones represent the scalar boson. The crossed vertex is the vertex of the respective flowed action density. Note that Diagram (f) only arises at $\mathrm{N^3LO}$ while Diagram (i) vanishes.

Quantity	NLO	NNLO
B_0	31 (7)	1067 (167)
W_0	28 (14)	1192 (330)
G_0	27 (13)	1099 (263)

Table 5.3: Numbers of diagrams contributing to the VEVs of the gauge boson action densities. We show the full number of diagrams as well as the number of diagrams which do not vanish due to closed flow-line loops in parentheses. For the coefficients B_m, BW_m and G_m the numbers are the same. Note that here, omitting diagrams with closed flow-line loops greatly reduces the number of diagrams to compute.

scheme as well as a conversion factor to a new non-minimal scheme which we call the caron scheme. Deriving the field renormalization from the SFTX of the vector currents (instead of the fermion kinetic operators) offers the benefit that the NNLO results can be calculated analytically through a 2-loop calculation. However, we also consider the VEVs of the fermion kinetic operators in order to derive the conversion factors to the ringed scheme and to check the field renormalization obtained from the vector currents.

Again, the NLO results can directly be inferred from the known QCD ones since there is no mixing of different sectors through NLO. We still show these redundant results for completeness, though. The numbers of diagrams contributing to each coefficient are shown in Tab. 5.4. Sample diagrams contributing at NLO and NNLO are displayed in Fig. 5.5.

The relation between the anomalous dimensions and the renormalization constants is given in appendix C.2. Using Eq. (2.11.19) and the fact that the vector currents are RG invariant, we find that

$$\left(\sum_{i=1}^{4}\beta^{(i)}\frac{\partial}{\partial a_i}+\frac{\partial}{\partial L_{\mu t}}\right)\log v_f(t)=\left(\sum_{i=1}^{4}\beta^{(i)}\frac{\partial}{\partial a_i}+\frac{\partial}{\partial L_{\mu t}}\right)\log Z_{\boldsymbol{f}}^{\mathrm{MS}}=-\gamma^f\,. \tag{5.5.1}$$

Normalizing the flowed fermions with the flow-time dependent coefficients might offer an alternative to the ringed scheme which we call the caron scheme, defined by

$$\check{\boldsymbol{f}}=\check{Z}_{\boldsymbol{f}}^{1/2}\boldsymbol{f}\,,\qquad \check{Z}_{\boldsymbol{f}}=\frac{Z_{\boldsymbol{f}}^{\mathrm{MS}}}{v_f(t)}\,. \tag{5.5.2}$$

From Eq. (5.5.1) it follows that, in the caron scheme, the anomalous dimension of the flowed fermion is canceled. We have verified this explicitly and confirmed that the μ-dependence of the caron field renormalizations vanishes through NNLO. It should be noted, however, that since this scheme relies on the limit $t\to 0$, it may be less well suited for lattice applications than the ringed scheme.

Consider an SFTX of an operator which is bilinear in a fermion or scalar field (which we call F). Let $X(t)$ be the SFTX coefficient multiplying a finite unflowed operator (like a vector current or the identity). We expand the coefficient as

$$X(t)=X_{\mathrm{lo}}+\sum_{i=1}^{4}\left(X_{0,i}+X_{1,i}L_{\mu t}\right)a_i+\sum_{i,j=1}^{4}\left(X_{0,ij})+X_{1,ij}L_{\mu t}+X_{2,ij}L_{\mu t}^2\right)a_ia_j+\mathcal{O}(t)\,. \tag{5.5.3}$$

Due to the non-renormalization of the RHS of the SFTX, the logarithmic terms can be derived using the RGE by

$$X_{1,j}=-\gamma_j\,, \tag{5.5.4}$$

$$X_{1,(jk)}=-\gamma_{(jk)}-\frac{1}{2}\left(X_{0(j}\gamma_{k)}+X_{0(k}\gamma_{j)}\right)+\sum_{l=1}^{4}\beta^{(l)}_{0,(jk)}X_{0,l}\,, \tag{5.5.5}$$

$$X_{2,(jk)}=\frac{1}{2}\left[\gamma_{(j}\gamma_{k)}-\sum_{l=1}^{4}\beta^{(l)}_{0,(jk)}\gamma_l\right]\,, \tag{5.5.6}$$

where γ is the anomalous dimension of the flowed operator which in the cases considered here amounts to the field anomalous dimension of the flowed version of F. However, we still give the logarithmic terms explicitly for convenience.

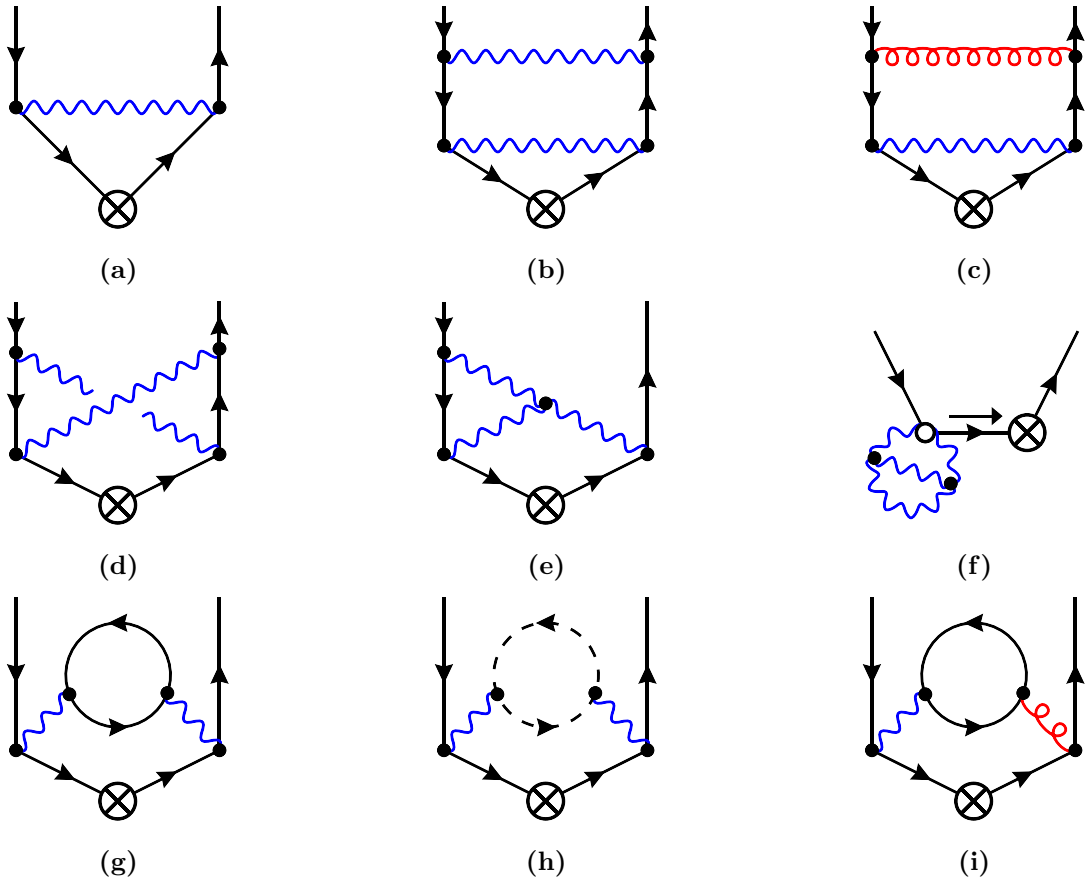

Figure 5.5: Sample diagrams contributing to the factors in Eq. (5.5.7). Note that diagram (i) vanishes.

We can write the SFTX coefficients in a general way for all vector currents considering the diagrammatic structure through NNLO:

$$X_{0,1} = -X_{\text{nlo}} y_F^2\,, \qquad X_{0,2} = X_{\text{nlo}} C_{\text{F2}} \delta_2^F\,, \qquad X_{0,3} = X_{\text{nlo}} C_{\text{F3}} \delta_3^F\,, \qquad X_{0,4} = 0\,, \tag{5.5.7}$$

$$X_{0,(11)} = y_F^4 X_{\text{diag}} + y_F^2 \left(n_{\text{g}} X_{\text{mixG}} \Sigma_{\text{yf}} + X_{\text{mixH}} N_2 n_{\text{h}} y_{\text{h}}^2 \right), \tag{5.5.8}$$

$$X_{0,(12)} = -2\delta_2^F y_F^2 C_{\text{F2}} X_{\text{diag}}\,, \tag{5.5.9}$$

$$X_{0,(13)} = -2\delta_3^F y_F^2 C_{\text{F3}} X_{\text{diag}}\,, \tag{5.5.10}$$

$$X_{0,(14)} = -y_f^2 n_{\text{h}} (N_2 + 1) X_{\text{sc-mix}}\,, \tag{5.5.11}$$

$$X_{0,(22)} = \delta_2^F \left(C_{\text{F2}} T_2 n_{\text{g}} (1 + N_3) X_{\text{mixG}} + C_{\text{F2}} C_{\text{A2}} \overline{X}_{\text{diag}} + C_{\text{F2}}^2 X_{\text{diag}} + C_{\text{F2}} T_2 n_{\text{h}} X_{\text{mixH}} \right), \tag{5.5.12}$$

$$X_{0,(23)} = 2\delta_2^F \delta_3^F C_{\text{F2}} C_{\text{F3}} X_{\text{diag}}\,, \tag{5.5.13}$$

$$X_{0,(24)} = C_{\text{F2}} n_{\text{h}} X_{\text{sc-mix}}\,, \tag{5.5.14}$$

$$X_{0,(33)} = \delta_3^F \left(C_{\text{F3}} T_3 n_{\text{g}} (2 + N_2) X_{\text{mixG}} + C_{\text{F3}} C_{\text{A3}} \overline{X}_{\text{diag}} + C_{\text{F3}}^2 X_{\text{diag}} \right), \tag{5.5.15}$$

$$X_{0,(34)} = 0\,, \tag{5.5.16}$$

$$X_{0,(44)} = \delta_H^F X_{\text{sc-sc}} (N_2 + 1) n_{\text{h}}^2\,. \tag{5.5.17}$$

We will see that this or a similar general form of the SFTX coefficients can be obtained for all results in this chapter.

For the fermionic vector currents, i.e., with $X = v_f$, we find

$$X_{\text{lo}} = 1\,, \qquad X_{\text{nlo}} = \frac{1}{8} - \frac{3}{4}L_{\mu t}\,, \qquad X_{\text{sc-mix}} = 0\,, \qquad X_{\text{sc-sc}} = 0\,, \tag{5.5.18}$$

$$X_{\text{diag}} = -\frac{41}{128} - \frac{5}{32}\zeta_2 + \frac{1}{2}\log 2 + \frac{1}{4}\log^2 2 + \frac{3}{2}\text{Li}_2(1/4) + \frac{\log 2}{2}L_{\mu t} + \frac{9}{32}L_{\mu t}^2\,, \tag{5.5.19}$$

$$\begin{aligned}\overline{X}_{\text{diag}} = &-\frac{763}{384} - \frac{5}{32}\zeta_2 - \frac{13}{4}\log 2 + \frac{1}{4}\log^2 2 + \frac{27}{8}\log 3 + \frac{21}{16}\text{Li}_2(1/4) \\ &- \left(\frac{53}{24} + \frac{1}{2}\log 2\right) L_{\mu t} - \frac{11}{32}L_{\mu t}^2\,,\end{aligned} \tag{5.5.20}$$

$$X_{\text{mixG}} = \frac{35}{192} + \frac{1}{16}\zeta_2 + \frac{5}{24}L_{\mu t} + \frac{1}{16}L_{\mu t}^2\,, \qquad X_{\text{mixH}} = \frac{65}{384} + \frac{1}{32}\zeta_2 + \frac{1}{6}L_{\mu t} + \frac{1}{32}L_{\mu t}^2\,. \tag{5.5.21}$$

We obtain the flowed field renormalization constant from requiring that $v_f(t)$ be finite. We can then infer the anomalous dimension γ^f through Eq. (5.5.1). It can be expanded as

$$\gamma^f = \sum_{i=1}^{4} \gamma_i^f a_i + \sum_{i,j=1}^{4} \gamma_{ij}^f a_i a_j + \mathcal{O}(a_k^3)\,. \tag{5.5.22}$$

The coefficients of the anomalous dimension take the same form as the general coefficient $X(t)$ in Eq. (5.5.7), i.e., we can set $\gamma_i^f = X_{0,i}$ and $\gamma_{ij}^f = X_{0,ij}$ (and the logarithmic terms vanish, of course) and obtain

$$X_{\text{lo}} = 0\,, \qquad X_{\text{nlo}} = \frac{3}{4}\,, \qquad X_{\text{diag}} = -\frac{3}{32} - \frac{1}{2}\log 2\,, \qquad X_{\text{mixG}} = -\frac{11}{48}\,, \tag{5.5.23}$$

$$X_{\text{mixH}} = -\frac{17}{96}\,, \qquad \overline{X}_{\text{diag}} = \frac{223}{96} - \frac{1}{2}\log 2\,, \qquad X_{\text{sc-mix}} = X_{\text{sc-sc}} = 0\,. \tag{5.5.24}$$

Projecting this result onto scalar QCD (sQCD) (i.e., only taking the SU(N_2) part of our model with q_L and ϕ and omitting all the other fields), we can compare our result with Ref. [146] and find agreement. There, however, the flowed fermion renormalization was determined from the finiteness of $\boldsymbol{K}_f(t)$, which as a VEV requires a 3-loop calculation for NNLO accuracy and thus only numerical results could be obtained at NNLO in Ref. [146]. Analytical results in QCD have been obtained previously in Ref. [14] using the non-renormalization property of the energy-momentum tensor, so only the contribution of the scalar was not known analytically in Ref. [146]. Using the finiteness of the vector current in order to determine the flowed fermion renormalization instead, we obtain analytical results through NNLO here, allowing us to identify the numerical coefficient in Eq. (3.18) in Ref. [146] as

$$0.1771 \to \frac{17}{96} = 0.17708\ldots\,. \tag{5.5.25}$$

Note that the last digit on the LHS has been rounded.

The conversion factors $\zeta_{\boldsymbol{f}}$ for the ringed scheme can be obtained from the SFTX of the flowed fermion kinetic operators given in Eq. (5.3.9). They are given by the VEV normalized by its LO value,

$$\zeta_{\boldsymbol{f}} = \frac{(K_0^f)_{\text{LO}}}{K_0^f} = \frac{1}{\hat{K}_0^f}\,. \tag{5.5.26}$$

$\hat{K}_0^f$ has the same structure as $X(t)$ in Eq. (5.5.7), so with $\hat{K}_0^f$ as $X(t)$ we obtain

$$X_{\text{lo}} = 1\,, \qquad X_{\text{nlo}} = \log 2 + \frac{3}{4}\log 3 - \frac{3}{3}L_{\mu t}\,, \tag{5.5.27}$$

$$X_{\text{diag}} = 0.4021 - 0.6975\,L_{\mu t} + 0.2812\,L_{\mu t}^2\,, \tag{5.5.28}$$

$$X_{\text{mixG}} = 0.1225 - 0.02368\,L_{\mu t} + 0.06250\,L_{\mu t}^2\,, \tag{5.5.29}$$

$$X_{\text{mixH}} = 0.02340 + 0.05065\,L_{\mu t} + 0.03125\,L_{\mu t}^2\,, \tag{5.5.30}$$

$$\overline{X}_{\text{diag}} = 1.487 - 0.5856\,L_{\mu t} - 0.3437\,L_{\mu t}^2\,, \tag{5.5.31}$$

$$X_{\text{sc-mix}} = 0\,, \qquad X_{\text{sc-sc}} = 0\,, \tag{5.5.32}$$

where we displayed the logarithmic terms again for convenience although they can be derived from Eq. (5.5.4). The precision estimated from pole cancellation is $\mathcal{O}(10^{-8})$ for the above numerical coefficients.

Note that using the vector currents in order to derive the flowed field renormalization constants allows us in principle to calculate these through N^3LO numerically with the methods currently available. However, the numbers of three-loop diagrams and the corresponding integrals are large. For the most simple case, the electron vector current, there are 78362 diagrams and 5989 scalar integrals which need to be evaluated. For the most complicated case, the quark doublet vector current, there are already 693941 diagrams. We thus leave this calculation to future work.

5.6 Flowed scalar field renormalization

An analogue of the ringed scheme for the scalar field is provided by the definition

$$\mathring{Z}_\phi \langle \phi^\dagger(t,x)\phi(t,x)\rangle \equiv \frac{N_2}{32\pi^2 t}\,, \qquad \mathring{Z}_\phi = \zeta_\phi Z_\phi^{\text{MS}}\,. \tag{5.6.1}$$

Note that for scalars we do not run into problems by using the scalar bilinear to define the ringed scheme, while for fermions this would cause complications if the fermions are massless (as in the model we consider in this chapter) since such a term would break chiral symmetry. We can thus infer ζ_ϕ from the VEV of the scalar bilinear (see Eq. (5.3.9)) by

$$\zeta_\phi = S_0^{\text{LO}}/S_0 = 1/\hat{S}_0\,. \tag{5.6.2}$$

The logarithmic terms of $\hat{S}_0$ can be determined in the same way as the ones of the vector currents in Eq. (5.5.4) since the unflowed operator $\mathbb{1}$ has no anomalous dimension. We still display them for convenience, however. Note that due to the anomalous dimension of the flowed scalar field vanishing at 1-loop order, the only logarithmic terms are linear ones at NNLO. With $\hat{S}_0$ as $X(t)$ in Eqs. (5.5.7) to (5.5.17), we find

$$X_{\text{lo}} = 1\,, \qquad X_{\text{nlo}} = 1 + 2\log 2\,, \tag{5.6.3}$$

$$X_{\text{diag}} = 2.481 + 0.5764\,L_{\mu t}\,, \qquad X_{\text{mixG}} = -0.5425 - 0.3354\,L_{\mu t}\,, \tag{5.6.4}$$

$$X_{\text{mixH}} = -0.4551 - 0.1673\,L_{\mu t}\,, \qquad \overline{X}_{\text{diag}} = 4.267 + 1.194\,L_{\mu t}\,, \tag{5.6.5}$$

$$X_{\text{sc-mix}} = 0\,, \qquad X_{\text{sc-sc}} = -0.02539 - 0.007812\,L_{\mu t}\,. \tag{5.6.6}$$

As a check, we compare this with the sQCD results obtained in Ref. [146] and find the results to agree.

The numerical accuracy estimated from the cancellation of poles is $\mathcal{O}(10^{-4})$, which is rather large. However, the coefficient $X_{\text{sc-sc}}$ which might be affected in its last digit agrees

with the four significant digits given in Ref. [146] where the result has been computed with higher accuracy.

For an analogue of the caron scheme, we can use the SFTX of the flowed Noether current,

$$\boldsymbol{j}^\mu_\phi(t,x) = v_\phi(t) j^\mu_\phi(x) + \mathcal{O}(t)\,, \tag{5.6.7}$$

and define

$$\check{\boldsymbol{\phi}} = \check{Z}^{1/2}_{\boldsymbol{\phi}} \boldsymbol{\phi}\,, \qquad \check{Z}_{\boldsymbol{\phi}} = \frac{Z^{\mathrm{MS}}_{\boldsymbol{\phi}}}{v_\phi(t)}\,. \tag{5.6.8}$$

v_ϕ has again the same structure as $X(t)$ in Eqs. (5.5.7) to (5.5.17), and with v_ϕ as $X(t)$ we obtain

$$X_{\mathrm{lo}} = 1\,, \qquad X_{\mathrm{nlo}} = 0\,, \tag{5.6.9}$$

$$X_{\mathrm{diag}} = \frac{111}{128} - \frac{1}{8}\zeta_2 + \frac{13}{2}\log 2 - \frac{7}{8}\log^2 2 - \frac{33}{8}\log 3 + \frac{9}{8}\log 2 \log 3 - \frac{9}{32}\log^2 3 + \frac{3}{2}\mathrm{Li}_2(1/4) + \left(\frac{11}{4}\log 2 - \frac{3}{32} - \frac{9}{8}\log 3\right) L_{\mu t}\,, \tag{5.6.10}$$

$$X_{\mathrm{mixG}} = \frac{5}{64} + \frac{1}{16} L_{\mu t}\,, \qquad X_{\mathrm{mixH}} = \frac{7}{128} + \frac{1}{32} L_{\mu t}\,, \tag{5.6.11}$$

$$\overline{X}_{\mathrm{diag}} = -\frac{231}{256} - \frac{1}{8}\zeta_2 - \frac{19}{8}\log 2 + \frac{11}{8}\log^2 2 + \frac{21}{16}\log 3 - \frac{9}{8}\log 2 \log 3\,, \tag{5.6.12}$$

$$+ \frac{9}{32}\log^2 3 + \frac{9}{32}\mathrm{Li}_2(1/4) + \left(-\frac{65}{64} - \frac{7}{4}\log 2 + \frac{9}{8}\log 3\right) L_{\mu t}\,, \tag{5.6.13}$$

$$X_{\text{sc-mix}} = -\frac{3}{16} - \frac{1}{32}\zeta_2 + \frac{9}{32}\mathrm{Li}_2(1/4)\,, \qquad X_{\text{sc-sc}} = -\frac{7}{512} - \frac{1}{128} L_{\mu t}\,. \tag{5.6.14}$$

As was the case for the fermions, the scalar field anomalous dimension behaves exactly like the flowed fermion ones concerning the discussion after Eq. (5.5.22). Thus, with γ^ϕ as X, we obtain

$$X_{\mathrm{lo}} = 0\,, \qquad X_{\mathrm{nlo}} = 0\,, \qquad X_{\mathrm{diag}} = \frac{3}{32} - \frac{11}{4}\log 2 + \frac{9}{8}\log 3\,, \tag{5.6.15}$$

$$X_{\mathrm{mixG}} = -\frac{1}{16}\,, \qquad X_{\mathrm{mixH}} = -\frac{1}{32}\,, \tag{5.6.16}$$

$$\overline{X}_{\mathrm{diag}} = \frac{65}{64} + \frac{7}{4}\log 2 - \frac{9}{8}\log 3\,, \qquad X_{\text{sc-mix}} = 0\,, \tag{5.6.17}$$

$$X_{\text{sc-sc}} = \frac{1}{128}\,, \tag{5.6.18}$$

which agrees with the logarithmic terms in the result above. The numbers of diagrams contributing to v_ϕ at NLO and NNLO are shown in Tab. 5.4.

5.7 Vacuum energy renormalization

In this section we consider the vacuum energy renormalization which is needed for the renormalization of the matching coefficients with the dimension two scalar operators $m^2\mathbb{1}$ and $\phi^\dagger\phi$.

Let $\boldsymbol{\mathcal{O}}_{\mathrm{B}}$ be some flowed operator which is a singlet under all symmetries of the theory (so in our case $\boldsymbol{S}$, $\boldsymbol{H}$, $\boldsymbol{B}^2$, $\boldsymbol{W}^2$, $\boldsymbol{G}^2$ or $\boldsymbol{K}_f$) and which is defined using bare flowed fields and bare couplings. The renormalized flowed operator $\boldsymbol{\mathcal{O}}$ is defined with the

Quantity	NLO	NNLO
$v_u\,,\ v_d$	20	1536 (940)
v_q	30	3085 (2061)
v_l	20	1564 (968)
v_e	10	498 (258)
v_ϕ	29	3267 (2423)

Table 5.4: Numbers of diagrams contributing to the SFTX of the fermionic and scalar vector currents. We show the full number of diagrams as well as the number of diagrams which do not vanish due to closed flow-line loops in parentheses.

corresponding renormalized flowed fields and renormalized couplings. Let us denote the mass dimensions of these operators by

$$[\boldsymbol{\mathcal{O}}_{\mathrm{B}}(t,x)] = n - a\epsilon\,, \qquad [\boldsymbol{\mathcal{O}}(t,x)] = n - b\epsilon\,, \tag{5.7.1}$$

where n, a and b are integers. For $\boldsymbol{S}$, $\boldsymbol{B}^2$, $\boldsymbol{W}^2$, $\boldsymbol{G}^2$ and $\boldsymbol{K}_f$ we have $a = b = 2$, while for $\boldsymbol{H}$ we have $a = 2$ and $b = 4$ due to the presence of λ_{B} in $\boldsymbol{H}_{\mathrm{B}}$. The bare SFTX is then given by

$$\boldsymbol{\mathcal{O}}_{\mathrm{B}}(t,x) = \Big[C_0^{\mathrm{B}}(t) + m_{\mathrm{B}}^2 C_m^{\mathrm{B}}(t)\Big]\mathbb{1} + C_S^{\mathrm{B}}(t)\Big[\phi^\dagger(x)\phi(x)\Big]_{\mathrm{B}} + \dots\,, \tag{5.7.2}$$

where we have omitted the mixing with unflowed operators of mass dimension larger than two. The coefficients $C_i^{\mathrm{B}}(t)$ can have non-integer mass dimension. The renormalized SFTX on the other hand is given by

$$\boldsymbol{\mathcal{O}}(t,x) = \Big[C_0(t) + m^2 C_m(t)\Big]\mathbb{1}\mu^{-b\epsilon} + C_S(t)\Big[\phi^\dagger(x)\phi(x)\Big]_{\mathrm{R}}\mu^{(2-b)\epsilon} + \dots\,, \tag{5.7.3}$$

where the renormalized coefficients are given by

$$C_0(t) = Z_{\boldsymbol{\mathcal{O}}}\mu^{a\epsilon}C_0^{\mathrm{B}}(t)\,, \qquad C_S(t) = Z_{\boldsymbol{\mathcal{O}}}\frac{\mu^{(a-2)\epsilon}}{Z_m}C_S^{\mathrm{B}}(t)\,, \tag{5.7.4}$$

$$C_m(t) = Z_{\boldsymbol{\mathcal{O}}}\left(\mu^{a\epsilon}Z_m C_m^{\mathrm{B}}(t) + \frac{\mu^{(a-2)\epsilon}Z_0}{Z_m}C_S^{\mathrm{B}}(t)\right)\,. \tag{5.7.5}$$

Due to the factors $\mu^{a\epsilon}$ and $\mu^{(a-2)\epsilon}$ they are ensured to have integer mass dimension. $Z_{\boldsymbol{\mathcal{O}}}$ is the product of flowed field and coupling renormalization constants needed to renormalize $\boldsymbol{\mathcal{O}}_{\mathrm{B}}$ (cf. Tab. 5.2), Z_m is the scalar mass renormalization and Z_0 is the vacuum energy renormalization. The relations between the bare and renormalized coefficients can be derived using the methods developed in Refs. [100, 101]. In particular, we used the fact that the unflowed scalar bilinear operator $S(x)$ renormalizes like the inverse squared scalar mass.

Apart from an additional global factor $1/\epsilon$, Z_0 has the same general form as the other renormalization constants. The necessity of the extra divergent factor becomes clear if

we consider the loop orders of the quantities in the above relation: Since $C_m(t)$ is derived from a VEV and $C_S(t)$ is derived from a two-point function, the loop order of $C_m(t)$ exceeds the one of $C_S(t)$ by one for fixed order in the couplings. Thus, higher poles can appear in $C_m(t)$ which require counter-terms of the same order, generated by the extra $1/\epsilon$ in Z_0.

For QCD, the vacuum energy renormalization has been first derived in [101] through NLO (two-loop order) and is by now known through five-loop order [103]. We give it through NNLO in Eq. (3.2.5). For the SM, however, we have not found any results in the literature and thus derived Z_0 through NNLO ourselves from the finiteness condition on the coefficients $C_m(t)$. The various operators for which we calculated this coefficient provide a strong check of our calculation. Furthermore, this shows that the GFF can be applied to derive unflowed renormalization constants in a rather straightforward way.

The anomalous dimension of the vacuum energy is given by

$$\gamma_0 = (2\gamma_m - \epsilon)Z_0 + \sum_{i=1}^{4} \beta^{(i)} \frac{\partial Z_0}{\partial a_i} \equiv \frac{N_2 n_\mathrm{h}}{(4\pi)^2} \left(\gamma_{0,0} + \sum_{i=1}^{4} \gamma_0^i a_i + \sum_{i,j=1}^{4} \gamma_0^{ij} a_i a_j \right) + \mathcal{O}(a_i^3) \,. \tag{5.7.6}$$

The equivalent formula for QCD has been derived in Ref. [101]. Note that there γ_m is the anomalous dimension of the fermion mass. Since we only have a scalar mass, γ_m comes with a factor 2 instead of 4 in our case.

The vacuum energy renormalization constant is given by

$$\begin{aligned} Z_0 = -\frac{N_2 n_\mathrm{h}}{(4\pi)^2} \frac{1}{\epsilon} \Bigg\{ & \gamma_{0,0} + \sum_{i=1}^{4} a_i \left(\frac{\gamma_0^i}{2} + \frac{\gamma_m^i}{\epsilon} \right) \\ & + \sum_{i,j=1}^{4} a_i a_j \left[\frac{1}{3} \gamma_0^{ij} + \frac{1}{\epsilon} \left(\frac{1}{3} \gamma_m^{\{ij\}} - \frac{1}{6} \sum_{l=0}^{4} \beta_{0,ij}^{(l)} \gamma_0^l + \frac{1}{6} \gamma_m^{\{i} \gamma_0^{j\}} \right) \right. \\ & \left. \left. \frac{1}{\epsilon^2} \left(\frac{1}{3} \gamma_m^{\{i} \gamma_m^{j\}} - \frac{1}{3} \sum_{l=1}^{4} \beta_{0,ij}^{(l)} \gamma_m^l \right) \right] \right\} + \mathcal{O}(a_i^3) \,, \end{aligned} \tag{5.7.7}$$

where we have used the general form of the beta functions defined in Eq. (C.1.8) and $x_{\{i} y_{j\}} \equiv x_i y_j + x_j y_i$ denotes unnormalized symmetrization. We can check the above formula by projecting it onto QCD. Due to our conventions for the sign of the anomalous dimension of the mass and the fact that in our case the mass is that of a scalar, we can reproduce the QCD formula for Z_0 symbolically as given in Ref. [46] in the case of only one coupling (a gauge one) and with the replacement $\gamma_m \to -2\gamma_m$. Note, however, that due to the different massive particles we cannot compare the numerical results for Z_0 by inserting the values of γ_m and γ_0 since these are different in our model.

The normalized anomalous dimension $\gamma_0/\gamma_0^\mathrm{LO}$ has the same form as $X(t)$ in Eqs. (5.5.7) to (5.5.17), where we have to choose $F = \phi$ as the field. With $\gamma_0/\gamma_0^\mathrm{LO}$ as $X(t)$ we thus obtain

$$X_\mathrm{lo} = 1 \,, \qquad X_\mathrm{nlo} = 2 \,, \tag{5.7.8}$$

$$X_\mathrm{diag} = 1.309 \,, \qquad X_\mathrm{mixG} = -0.5312 \,, \tag{5.7.9}$$

$$X_\mathrm{mixH} = -0.6718 \,, \qquad \overline{X}_\mathrm{diag} = 1.970 \,, \tag{5.7.10}$$

$$X_\text{sc-mix} = 0 \,, \qquad X_\text{sc-sc} = 0.1875 \,. \tag{5.7.11}$$

5.8 Quartic scalar operator

In section 5.4 we have calculated the VEVs of the gauge boson action densities which can be used to define the gauge couplings in a GFF scheme just like in flowed QCD. In our model, however, there is the scalar self-coupling as well, for which we have not defined a flowed version yet. We can define it to be the quantity $H_0(t)$, the vacuum expectation value of the scalar self-coupling term which appears in the Lagrangian. The renormalized quartic scalar VEV is obtained as described in section 5.7.

From the RG invariance of the bare version of this operator, we find the RGE

$$\mu^2 \frac{\mathrm{d}}{\mathrm{d}\mu^2} \log H_0(t) = \epsilon - 2\gamma_\phi + \frac{\beta^{(4)}}{a_4}\,, \tag{5.8.1}$$

which we use as a check. We also compare $\beta^{(4)}$ found from our results through NLO with the literature [152] and find agreement. The μ-dependence of $H_0(t)$ which persists even in the ringed or caron scheme is a disadvantage compared to the flowed gauge couplings since it prohibits a matching with lattice results. However, the quantity $\hat{H}_0(t) = H_0(t)/a_4$ is RG invariant and given by

$$\hat{H}_0(t) = \frac{N_2(1+N_2)n_\mathrm{h}^2}{256\pi^2}\Big(1 + 4.772\, a_2 C_{\mathrm{F}2} - 0.1834\, a_4 n_\mathrm{h} - 4.772\, a_1 y_\mathrm{h}^2\Big) + \mathcal{O}(a_i^3)\,. \tag{5.8.2}$$

This could be matched with a corresponding lattice evaluation of $\hat{H}_0(t)$ in order to extract the scalar self-coupling λ from lattice data. The above coefficients have a numerical uncertainty of $\mathcal{O}(10^{-9})$ estimated from polce cancellation.

5.9 Remaining SFTX coefficients

With Z_0 as obtained in the last section, we can renormalize all the remaining projections of the Lorentz singlet flowed operators onto the dimension two operators.

The flowed fermion kinetic operators only start to mix with $\phi^\dagger(x)\phi(x)$ at two-loop order since due to the absence of Yukawa couplings in our model the fermions do not directly couple to the scalar boson. Thus, the results are finite and free of logarithmic terms. They are given by

$$K_1^f(t) = \left(-\frac{3}{4} + 5\log 2 - \frac{9}{4}\log 3\right) n_\mathrm{g}\Big(a_1^2 y_\mathrm{h}^2 y_f^2 N_2^{\delta_2^f} N_3^{\delta_3^f} + a_2^2 \delta_2^f C_{\mathrm{F}2} N_3^{\delta_3^f} T_2\Big) + \mathcal{O}(a_i^3)\,. \tag{5.9.1}$$

Mixed terms $\sim a_1 a_2$ vanish due to the vanishing trace of the single $\mathrm{SU}(N_2)$ generator in the quark loop and the projector line.

The results for the mass terms of the VEV of the fermion kinetic operators are equally simple due to the fact that the scalar is the only massive particle and thus the mass only starts to contribute at three-loop order. The results are given by

$$K_m^f(t) = 0.006399 N_2 n_\mathrm{h} n_\mathrm{g}\Big(a_1^2 y_\mathrm{h}^2 y_f^2 N_2^{\delta_2^f} N_\mathrm{c}^{\delta_3^f} + a_2^2 \delta_2^f N_\mathrm{c}^{\delta_3^f} C_{\mathrm{F}2} T_2\Big) + \mathcal{O}(a_i^3)\,, \tag{5.9.2}$$

with a numerical uncertainty of $\mathcal{O}(10^{-7})$ estimated from pole cancellation.

Since the B and W bosons directly couple to the scalar, the mass starts to contribute to the VEVs of their action densities already at two-loop order. We obtain

$$B_m(t) = \frac{3 a_1 N_2 n_\mathrm{h} y_\mathrm{h}^2}{32\pi^2}\Big\{(2 + L_{\mu t}) + a_2 C_{\mathrm{F}2}\Big(3.393 + 1.999\, L_{\mu t}\Big)$$

$$+ a_1\Big(\big(-3.393 - 1.999\,L_{\mu t} + (1.163 + 0.7782\,L_{\mu t} + 0.1666\,L_{\mu t}^2)N_2 n_{\rm h}\big)y_{\rm h}^2 + \Big(1.658 + 1.221\,L_{\mu t} + 0.3333\,L_{\mu t}^2\Big)n_{\rm g}\Sigma_{\rm yf}\Big)\Big\} + \mathcal{O}(a_i^3)\,, \tag{5.9.3}$$

$$W_m(t) = -\frac{3a_2 N_2 C_{\rm F2} n_{\rm h}}{32\pi^2}\Big\{(2 + L_{\mu t}) + a_2\Big(\big(3.393 + 1.999\,L_{\mu t}\big)C_{\rm F2} + \big(14.45 + 9.888\,L_{\mu t} + 1.833\,L_{\mu t}^2\big)C_{\rm A2} - T_2\Big(\big(1.658 + 1.221\,L_{\mu t} + 0.3333\,L_{\mu t}^2 + (1.658 + 1.221\,L_{\mu t} + 0.3333 L_{\mu t}^2)N_3\big)n_{\rm g} + (1.163 + 0.7782\,L_{\mu t} + 0.1666\,L_{\mu t}^2)n_{\rm h}\Big)\Big) - a_1 y_{\rm h}^2\Big(3.393 + 1.999 L_{\mu t}\Big)\Big\} + \mathcal{O}(a_i^3)\,. \tag{5.9.4}$$

The numerical uncertainty of the above results estimated from pole cancellation is $\mathcal{O}(10^{-4})$ which might affect the last digit of the smallest numerical coefficients. Since the gluon does not directly couple to the scalar, scalar mass effects in its action density VEV must be mediated by a fermion loop. Thus, such contributions only start to contribute at four-loop order and we have

$$G_m(t) = 0 + \mathcal{O}(a_i^3)\,. \tag{5.9.5}$$

For the projection of the action densities onto the bilinear scalar operator we obtain

$$B_1(t) = \frac{3}{2}y_{\rm h}^2 a_1 + a_1^2 y_{\rm h}^2\Big\{\left(\frac{9}{4} + \frac{9}{8}L_{\mu t} + \left(\frac{2}{3} + \frac{1}{4}L_{\mu t}\right)N_2 n_{\rm h}\right)y_{\rm h}^2 + \left(\frac{5}{6} + \frac{1}{2}L_{\mu t}\right)n_{\rm g}\Sigma_{\rm yf}\Big\} - \frac{9}{4}a_1 a_2 y_{\rm h}^2 C_{\rm F2}\left(1 + \frac{1}{2}L_{\mu t}\right) + \frac{3}{8}a_1 a_4 y_{\rm h}^2 n_{\rm h}\left(1 + N_2 + \frac{1}{2}(1 + N_2)L_{\mu t}\right) + \mathcal{O}(a_i^3)\,, \tag{5.9.6}$$

$$W_1(t) = -\frac{3}{2}C_{\rm F2}a_2 + a_2^2 C_{\rm F2}\Big\{-\frac{28}{3}C_{\rm A2} + \frac{9}{4}C_{\rm F2} + \frac{2}{3}T_2 n_{\rm h} + \frac{5}{6}T_2(1 + N_3)n_{\rm g} + L_{\mu t}\Big(-\frac{11}{4}C_{\rm A2} + \frac{9}{8}C_{\rm F2} + \frac{1}{4}T_2 n_{\rm h} + \frac{1}{2}T_2(1 + N_3)n_{\rm g}\Big)\Big\} - a_1 a_2 y_{\rm h}^2 C_{\rm F2}\left(\frac{9}{4} + \frac{9}{8}L_{\mu t}\right) - a_2 a_4 C_{\rm F2} n_{\rm h}(1 + N_2)\left(\frac{3}{8} + \frac{3}{16}L_{\mu t}\right) + \mathcal{O}(a_i^3)\,,$$

$$G_1(t) = 0 + \mathcal{O}(a_i^3)\,, \tag{5.9.7}$$

where $G_1(t)$ vanishes through NNLO because the first diagrams contributing to it start to appear at three-loop order.

The projection of the scalar bilinear operator onto itself takes the form

$$S_1 = X_{\rm lo} + \big(-y_{\rm h}^2 a_1 + C_{\rm F2}a_2\big)X_{\rm nlo} + n_{\rm h}(1 + N_2)a_4 X_{\rm nlo4} + a_1^2\Big(y_{\rm h}^4 X_{\rm diag} + y_{\rm h}^2 n_{\rm g} X_{\rm mixG}\Sigma_{\rm yf} + n_{\rm h}N_2 y_{\rm h}^4 X_{\rm mixH}\Big) - 2a_1 a_2 y_{\rm h}^2 C_{\rm F2}X_{\rm diag} - y_{\rm h}^2 n_{\rm h}(1 + N_2)a_1 a_4 X_{\rm sc\text{-}mix} + a_2^2\Big(C_{\rm F2}T_2\big((1 + N_2)n_{\rm g}X_{\rm mixG} + n_{\rm h}X_{\rm mixH}\big) + C_{\rm F2}C_{\rm A2}\overline{X}_{\rm diag} + C_{\rm F2}^2 X_{\rm diag}\Big) + a_2 a_4 C_{\rm F2} n_{\rm h}(1 + N_2)X_{\rm sc\text{-}mix} + a_4^2(N_2 + 1)n_{\rm h}^2 X_{\rm sc\text{-}sc}\,, \tag{5.9.8}$$

which differs from Eq. (5.5.7) by some extra factors (N_2+1) and the appearance of a_4 at NLO. The factors are given by

$$X_{\rm lo} = 1\,, \qquad X_{\rm nlo} = -\frac{1}{4}(1+3L_{\mu t})\,, \qquad X_{\rm nlo4} = \frac{1}{8}(1+L_{\mu t})\,, \tag{5.9.9}$$

$$\begin{aligned} X_{\rm diag} = &-\frac{9}{32} - \frac{5}{32}\zeta_2 + \frac{43}{8}\log 2 - \frac{7}{8}\log^2 2 - \frac{39}{16}\log 3 + \frac{9}{8}\log 2\log 3 \\ &- \frac{9}{32}\log^2 3 + \frac{15}{8}{\rm Li}_2(1/4) + \left[-\frac{1}{8} + \frac{11}{4}\log 2 - \frac{9}{8}\log 3\right]L_{\mu t} + \frac{3}{32}L_{\mu t}^2\,, \end{aligned} \tag{5.9.10}$$

$$\begin{aligned} \overline{X}_{\rm diag} = &-\frac{397}{192} - \frac{7}{64}\zeta_2 - \frac{47}{8}\log 2 + \frac{11}{8}\log^2 2 + \frac{75}{16}\log 3 - \frac{9}{8}\log 2\log 3 + \frac{9}{32}\log^2 3 \\ &+ \frac{3}{4}{\rm Li}_2(1/4) + \left[-\frac{91}{48} - \frac{7}{4}\log 2 + \frac{9}{8}\log 3\right]L_{\mu t} - \frac{19}{64}L_{\mu t}^2\,, \end{aligned} \tag{5.9.11}$$

$$X_{\rm mixG} = \frac{5}{24}(1+L_{\mu t}) + \frac{1}{16}(\zeta_2 + L_{\mu t}^2)\,, \tag{5.9.12}$$

$$X_{\rm mixH} = -\frac{55}{96} - \frac{1}{32}\zeta_2 + \frac{11}{3}\log 2 - \frac{3}{2}\log 3 + \frac{7}{8}{\rm Li}_2(1/4) + \frac{5}{12}L_{\mu t} - \frac{5}{32}L_{\mu t}^2\,, \tag{5.9.13}$$

$$X_{\text{sc-mix}} = \frac{1}{2} + \frac{5}{8}\log 2 - \frac{9}{16}\log 3 - \frac{3}{8}{\rm Li}_2(1/4) + \frac{5}{16}L_{\mu t}\,, \tag{5.9.14}$$

$$X_{\text{sc-sc}} = -\frac{15}{128} - \frac{3}{128}\zeta_2 - \frac{3}{32}L_{\mu t} - \frac{3}{128}L_{\mu t}^2\,. \tag{5.9.15}$$

The normalized projection $S_m/S_m^{(0)}$ of the scalar bilinear onto m^2, where we define

$$S_m^{(0)} = \frac{N_2 n_{\rm h}}{(4\pi)^2}\,, \tag{5.9.16}$$

takes the same form as S_1 in Eq. (5.9.8), with

$$X_{\rm lo} = 1 + L_{\mu t}\,, \qquad X_{\rm nlo} = 4 + 5\log 2 - \frac{9}{2}\log 3 - 3{\rm Li}_2(1/4) + \frac{5}{2}L_{\mu t}\,, \tag{5.9.17}$$

$$X_{\rm nlo4} = 0\,, \tag{5.9.18}$$

$$X_{\rm diag} = 1.678 + 3.626\,L_{\mu t} + 0.6702\,L_{\mu t}^2 + 0.03125 L_{\mu t}^3\,, \tag{5.9.19}$$

$$\overline{X}_{\rm diag} = 3.820 + 2.472\,L_{\mu t} + 0.08539\,L_{\mu t}^2 - 0.09895\,L_{\mu t}^3\,, \tag{5.9.20}$$

$$X_{\rm mixG} = -1.219 - 0.5482\,L_{\mu t} - 0.1250\,L_{\mu t}^2 + 0.02083\,L_{\mu t}^3\,, \tag{5.9.21}$$

$$X_{\rm mixH} = -1.164 - 1.019\,L_{\mu t} - 0.2499\,L_{\mu t}^2 - 0.05208\,L_{\mu t}^3\,, \tag{5.9.22}$$

$$X_{\text{sc-mix}} = 0\,, \tag{5.9.23}$$

$$X_{\text{sc-sc}} = -0.1270 - 0.1127\,L_{\mu t} - 0.03125\,L_{\mu t}^2 - 0.007812\,L_{\mu t}^3\,, \tag{5.9.24}$$

where we have given four significant digits. For the the smallest coefficients, the last digit might be inaccurate, however, estimated from the cancellation of the poles which is only accurate through $\mathcal{O}(10^{-5})$ for $X_{\rm sc-sc}$ and through $\mathcal{O}(10^{-4})$ for the other coefficients. The actual uncertainty might be lower that this, however, so we also display digits affected by the pole cancellation uncertainty.

The projection $H_1(t)$ of the quartic scalar interaction term onto the scalar bilinear is given by

$$H_1(t) = -\frac{1}{16}a_4(N_2+1)n_{\rm h} - \frac{1}{64}a_4\Big(a_2 C_{\rm F2} - a_1 y_{\rm h}^2\Big)(N_2+1)n_{\rm h}(3 + 8\log 2 - 3L_{\mu t})$$

$$+\frac{1}{128}a_4^2(N_2+1)n_{\rm h}^2\Big(24\log 2-12\log 3-(N_2+1)(1+L_{\mu t})\Big)+\mathcal{O}(a_i^3)\,. \tag{5.9.25}$$

For the mass term, we obtain

$$\begin{aligned}H_m(t)=-\frac{a_4 n_{\rm h}^2}{256\pi^2}N_2(1+N_2)\Big\{&(1+L_{\mu t})+\Big(a_2C_{\rm F2}-a_1y_{\rm h}^2\Big)\Big(4.105+4.886\,L_{\mu t}\Big)\\&-\;a_4n_{\rm h}(1+N_2)\Big(0.5761+0.4315\,L_{\mu t}\Big)\Big\}\,.\end{aligned} \tag{5.9.26}$$

with an uncertainty of $\mathcal{O}(10^{-5})$ for the numerical coefficients, estimated from the cancellation of the poles.

Chapter 6

Conclusion

In this thesis, we applied the perturbative Gradient Flow formalism in QCD to the quark chromomagnetic dipole operator and the chiral anomaly. Furthermore, we developed an extension of the GFF to the flavor-conserving SM in the unbroken phase.

Using established methods for perturbative calculations in flowed QCD, we found that in the case of the CMDM operator we had to extend the basis of operators to include both operators which vanish by equations of motion as well as gauge-variant operators. This enabled us to extend the known NNLO results for the SFTX of the CMDM operator in the massless case presented in Ref. [98] and the NLO results in massive QCD [24] to NNLO with massive quarks. As a by-product, we found the dimension-five renormalization matrix of physical effective operators in QCD. Our results provide a significant step towards determining the SFTX of the CEDM which can then be combined with lattice data to increase the precision of the nEDM predictions from lattice simulations as required by the increased precision of upcoming experiments. Our results also show that the GFF can be successfully applied to effective operators at higher mass dimensions as is required for possible future applications in SMEFT renormalization.

We then studied the effect of the Gradient Flow on the operators appearing in the Adler-Bell-Jackiw anomaly in QCD. While we verified the topological charge density itself being independent of the flow time through NNLO up to total derivative terms which vanish when integrated, its mixing with the divergence of the singlet axial current is non-trivial. We derived a flowed version of the anomaly relation and considered the effect of the flow on the conditions in the NNT, finding that it breaks one-loop exactness by generating higher-order contributions to the flowed anomaly. While these additional terms can be removed by a t-dependent finite renormalization, the GFF still relies on dimensional regularization of IR divergencies. Thus, even when reproducing the correct anomaly relation, it still breaks chiral symmetry.

Furthermore, we developed a Gradient Flow formalism for a flavor-conserving version of the SM in the unbroken phase, the main new features being the presence of multiple gauge groups as well as a scalar field. We defined minimal flow equations respecting the symmetries of this modification of the SM and implemented them into our established setup used for perturbative calculations in flowed QCD. We calculated the renormalization constants of the fermion fields and the scalar through NNLO in all couplings and checked that in the case of multiple gauge groups the flowed gauge bosons do not require additional renormalization. We suggested a new scheme to define RG invariant flowed fermion and scalar fields by normalizing them with the SFTX matching coefficients of the flowed vector currents and calculated several quantities in order to check the validity

of our setup and the consistency of our results. Among these quantities were the vacuum expectation values of quark kinetic operators, the gauge boson action densities, the scalar bilinear and the scalar self-interaction term. In order to renormalize these, the vacuum energy renormalization of the flavor-conserving SM is required which we were able to derive from our results through NNLO. The flowed SM may provide a viable alternative for existing methods used to renormalize SMEFT operators through NNLO and could be used in future lattice simulations of the SM.

Appendix A

Conventions

A.1 Group theory

Conventions for QCD

We define the SU(N) Lie algebra for all groups considered in this thesis by

$$[t^a, t^b] = f^{abc} t^c \,, \tag{A.1.1}$$

where the structure constant is assumed to be real and equal to the one in the more common convention (here denoted with a hat) which has

$$[\hat{t}^a, \hat{t}^b] = \mathrm{i} f^{abc} \hat{t}^c \,. \tag{A.1.2}$$

The conventions are related by $t^a = \mathrm{i}\hat{t}^a$, implying that the t^a are anti-hermitian. Our results will depend on the group invariants: C_F and C_A are the quadratic Casimir operators in the fundamental and adjoint representation, respectively, while N_c and N_A are the dimensions of these representations. T_R is the trace normalization factor. The group invariants are implicitly defined by

$$t^a_{ij} t^a_{jk} = -C_\mathrm{F} \delta_{ik} \,, \qquad f^{abc} f^{acd} = C_\mathrm{A} \delta^{bd} \tag{A.1.3}$$

$$\mathrm{tr}\left(t^a t^b\right) = -T_\mathrm{R} \delta^{ab} \,, \qquad \delta_{ii} = N_\mathrm{c} \,, \quad \delta^{aa} = N_\mathrm{A} \,, \tag{A.1.4}$$

implying the relations

$$N_\mathrm{A} = N_\mathrm{c}^2 - 1 \,, \qquad C_\mathrm{F} = \frac{T_\mathrm{R} N_\mathrm{A}}{N_\mathrm{c}} = T_\mathrm{R} \frac{N_\mathrm{c}^2 - 1}{N_\mathrm{c}} \,, \qquad C_\mathrm{A} = 2 T_\mathrm{R} N_\mathrm{c} \,. \tag{A.1.5}$$

Note that the number of group factors in a term corresponds to the loop order.

Conventions for the flavor-symmetric version of the SM

Since the t^a in our QCD convention are anti-hermitian and traceless, they appear in group transformations as $e^{u^a t^a} \in \mathrm{SU}(N)$. We adapt this convention for the two non-abelian groups SU(N_2) and SU(N_3) in our simplified version of the SM. This implies that we can effectively replace SU(N) by U(1) by setting $t^a = \mathrm{i}$, with only one generator. This implies $N_\mathrm{A} = 1$ and $C_\mathrm{A} = 0$ as well as

$$T_\mathrm{R} = 1 \,, \qquad C_\mathrm{F} = 1 \,, \qquad N_\mathrm{c} = 1 \,, \tag{A.1.6}$$

and

$$D_\mu = \partial_\mu + g A_\mu^a t^a \quad \to \quad \partial_\mu + \mathrm{i} g A_\mu \,. \tag{A.1.7}$$

Thus, if we define the covariant derivative as in Eq. (5.1.2) (i.e., without the factor i), then g_1 must be imaginary. This is because $\mathrm{U}(1)^{\mathrm{i}\alpha}$ with $\alpha \in \mathbb{R}$ and the term proportional to g_1 in the covariant derivative has to cancel the imaginary contribution $\mathrm{i}\partial_\mu\alpha$ from the gauge transformation. Thus, in our results we have $a_1 \sim g_1^2 < 0$ and we obtain SM or QED results in the usual conventions only after the replacement $a_1 \to -a_1$.

Regarding the non-abelian groups, we denote the $\mathrm{SU}(N_2)$ generators by τ^i and the $\mathrm{SU}(N_3)$ generators by t^a. They obey the commutation relations

$$[\tau^i, \tau^j] = f_2^{ijk}\tau^k \,, \qquad [t^a, t^b] = f_3^{abc} t^c \,, \qquad [\tau^i, t^a] = 0 \,. \tag{A.1.8}$$

We denote the group invariants by an additional index 2 for $\mathrm{SU}(N_2)$ and 3 for $\mathrm{SU}(N_3)$ invariants. Thus, for $\mathrm{SU}(N_2)$ the Casimir operators are $C_{\mathrm{F}2}$ (fundamental) and $C_{\mathrm{A}2}$ (adjoint), while the dimensions of the representations are N_2 (fundamental) and $N_{\mathrm{A}2}$ (adjoint). For $\mathrm{SU}(N_3)$ the Casimir operators are $C_{\mathrm{F}3}$ (fundamental) and $C_{\mathrm{A}3}$ (adjoint), while the dimensions are N_3 (fundamental) and $N_{\mathrm{A}3}$ (adjoint). The relations among the invariants stated above for QCD apply to both $\mathrm{SU}(N_2)$ and $\mathrm{SU}(N_3)$ in the same form.

Since we use general group factors for $\mathrm{SU}(N_2)$ and $\mathrm{SU}(N_3)$, we can do cross-checks by mapping the gauge groups onto each other as depicted in Fig. A.1. For mixed $\mathrm{SU}(N_2)\otimes\mathrm{SU}(N_3)$ results, we can check symmetry in exchanging the gauge groups.

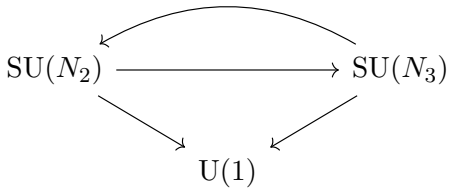

Figure A.1: Group mapping cross-checks for parts of the results obtained in the flavor-symmetric version of the SM.

Note that these symmetries do not apply to all results since the fermions and the scalar transforming in the fundamental representation are not symmetric with respect to swapping the gauge groups. In particular, the scalar does not couple to $\mathrm{SU}(N_3)$. This also implies that we obtain the already known results for scalar QCD [146] not from the actual QCD sector of the flavor-symmetric SM, but from the electroweak sector, and we have to map $\mathrm{SU}(N_2)\to\mathrm{SU}(3)$. Furthermore, we cannot reconstruct $\mathrm{SU}(N)$ results from $\mathrm{U}(1)$ since the invariant group factors become trivial for abelian groups.

A.2 Dirac algebra

In Euclidean space, the Dirac matrices γ_μ are hermitian,

$$(\gamma_\mu)^\dagger = \gamma_\mu \,, \tag{A.2.1}$$

and satisfy the anticommutation relation

$$\{\gamma_\mu, \gamma_\nu\} = 2\delta_{\mu\nu} \,, \tag{A.2.2}$$

implying $(\gamma_\mu)^2 = \mathbb{1}\ \forall\mu$. The fifth Dirac matrix in four dimensions, defined by

$$\gamma_5 = \gamma_1\gamma_2\gamma_3\gamma_4 = \frac{1}{4!}\epsilon_{\mu\nu\rho\sigma}\gamma_\mu\gamma_\nu\gamma_\rho\gamma_\sigma\,, \tag{A.2.3}$$

is hermitian as well, anticommutes with the other four Dirac matrices and satisfies the important properties

$$(\gamma_5)^2 = 1\,, \qquad \mathrm{tr}(\gamma_5) = 0\,. \tag{A.2.4}$$

Its generalization to $d = 4-2\epsilon$ dimensions depends on the scheme chosen and is discussed in more detail in chapter 4.1.

The spin generators which appear in the definition of the CMDM operator are given by

$$\sigma_{\mu\nu} = \frac{\mathrm{i}}{2}[\gamma_\mu, \gamma_\nu]\,. \tag{A.2.5}$$

Appendix B

QCD renormalization

We define the d-dimensional QCD beta function β through

$$\mu^2 \frac{\mathrm{d}}{\mathrm{d}\mu^2} a_s(\mu) \equiv a_s(\mu)\beta(a_s(\mu))\,, \tag{B.0.1}$$

where $a_s = g/(4\pi^2)$. It is expanded in the coupling as

$$\beta(a_s) = -\epsilon - \sum_{n=0}^{\infty} a_s^{n+1}\beta_n\,. \tag{B.0.2}$$

The coupling is renormalized in the MS scheme by

$$a_s^{\mathrm{B}} = \mu^{2\epsilon} Z_s a_s\,, \tag{B.0.3}$$

where

$$Z_s = 1 - a_s\frac{\beta_0}{\epsilon} + a_s^2\left(\frac{\beta_0^2}{\epsilon^2} - \frac{\beta_1}{2\epsilon}\right) + \mathcal{O}(a_s^3)\,, \tag{B.0.4}$$

with

$$\beta_0 = \frac{1}{4}\left(\frac{11}{3}C_{\mathrm{A}} - \frac{4}{3}n_{\mathrm{f}}T_{\mathrm{R}}\right)\,, \qquad \beta_1 = \frac{1}{16}\left(\frac{34}{3}C_{\mathrm{A}}^2 - 4C_{\mathrm{F}}T_{\mathrm{R}}n_{\mathrm{f}} - \frac{20}{3}C_{\mathrm{A}}T_{\mathrm{R}}n_{\mathrm{f}}\right)\,. \tag{B.0.5}$$

The fermion mass is renormalized by

$$m_{\mathrm{B}} = Z_m\,, \tag{B.0.6}$$

where

$$Z_m = 1 - a_s\frac{\gamma_{m,0}}{\epsilon} + a_s^2\left[\frac{\gamma_{m,0}}{2\epsilon^2}\left(\gamma_{m,0}+\beta_0\right) - \frac{\gamma_{m,1}}{2\epsilon}\right] + \mathcal{O}(a_s^3)\,. \tag{B.0.7}$$

Its anomalous dimension is defined by

$$\gamma_m \equiv -a_s\beta(a_s)\frac{\partial}{\partial a_s}\log Z_m \equiv -\sum_{n=0}^{\infty} a_s^{n+1}\gamma_{m,n}\,, \tag{B.0.8}$$

with

$$\gamma_{m,0} = \frac{3}{4}C_{\mathrm{F}}\,, \quad \gamma_{m,1} = \frac{3}{32}C_{\mathrm{F}}^2 + \frac{97}{96}C_{\mathrm{A}}C_{\mathrm{F}} - \frac{5}{24}C_{\mathrm{F}}T_{\mathrm{R}}n_f\,. \tag{B.0.9}$$

Appendix C

Flowed Standard Model

C.1 Coupling renormalization

The bare couplings in Eq. (5.1.7) can be written in the MS scheme as

$$a_i^{\mathrm{B}} = \mu^{2\epsilon} \mathfrak{a}_i^{\mathrm{B}} \tag{C.1.1}$$

with

$$\mathfrak{a}_i^{\mathrm{B}} = a_i + \sum_{n=2}^{\infty} \sum_{i_1,\ldots,i_n=1}^{4} z_{i_1\ldots i_n}^{(i)} a_{i_1} \ldots a_{i_n} \,, \tag{C.1.2}$$

where the dependence of the a_i on the MS renormalization scale μ is not written explicitly. For the gauge couplings, Eq. (C.1.2) simplifies to

$$\mathfrak{a}_i^{\mathrm{B}} = Z_i a_i \,, \quad i \in \{1,2,3\} \,, \tag{C.1.3}$$

but the scalar self-coupling a_4 renormalizes non-multiplicatively. For this reason we choose a convention for the definition of the beta functions different from QCD: The dependence of the couplings on μ is governed by the RG equation

$$\vec{\beta} \equiv \left(\beta^{(1)}, \ldots, \beta^{(i)}\right) \equiv \mu^2 \frac{\mathrm{d}}{\mathrm{d}\mu^2} \vec{a} \,, \tag{C.1.4}$$

where $\vec{a} = (a_1, a_2, a_3, a_4)$. From the RG invariance of $\vec{a}^{\mathrm{B}}$, one obtains the beta functions expressed in terms of the bare couplings,

$$\vec{\beta} = -\epsilon N \cdot \vec{\mathfrak{a}}^{\mathrm{B}} \,, \qquad \text{where} \quad (N^{-1})_{ij} \equiv \frac{\partial \mathfrak{a}_i^{\mathrm{B}}}{\partial a_j} \,. \tag{C.1.5}$$

Through NNLO, the gauge coupling beta functions do not depend on a_4. We can thus write them as

$$\beta^{(i)} = -\epsilon a_i - a_i^2 \beta_0^{(i)} - a_i^2 \sum_{j=1}^{3} \beta_{1,j}^{(i)} a_j + \mathcal{O}(a_i^4) \,, \qquad (i < 4) \,. \tag{C.1.6}$$

The beta function of the scalar self-coupling does depend on all couplings and can be written as

$$\beta^{(4)} = -\epsilon a_4 - \sum_{j,k=1}^{4} \beta_{0,jk}^{(4)} a_j a_k - \sum_{j,k,l=1}^{4} \beta_{1,jkl}^{(4)} a_j a_k a_l + \mathcal{O}(a_i^4) \,. \tag{C.1.7}$$

For compactness of notation, we might want to write the beta functions of all couplings in a formally equal form. We thus write them generally as

$$\beta^{(i)} = -\epsilon a_i - \sum_{j,k=1}^{4} \beta^{(i)}_{0,jk} a_j a_k - \sum_{j,k,l=1}^{4} \beta^{(i)}_{1,jkl} a_j a_k a_l + \mathcal{O}(a_i^4)\,, \tag{C.1.8}$$

which directly turns into the scalar self-coupling beta function for $i = 4$. For $i < 4$ we identify

$$\beta^{(i)}_{0,jk} = \delta_{ij}\delta_{ik}\beta^{(i)}_0\,, \qquad \beta^{(i)}_{1,jkl} = \delta_{ij}\delta_{ik}\beta^{(i)}_{1,l}\,, \tag{C.1.9}$$

where no summation over multiple indices is implied. Note that the coefficient multiplying a monomial of couplings in some perturbative result X is not directly related to an element of the coefficient tensor $x_{i_1\dots i_n}$ appearing in the perturbative expansion

$$X = \sum_{n=0}^{\infty} \sum_{i_1,\dots,i_n} x_{i_1\dots i_n} a_{i_1} \dots a_{i_n} \tag{C.1.10}$$

since the coefficient tensor is contracted with a symmetric product of couplings. We correct for this by always giving as results the unnormalized sum over all permutations of different coupling indices, i.e.,

$$x_{(i_1\dots i_n)} = \frac{1}{m_1!\dots m_k!} \sum_{\pi\in S_n} x_{\pi(i_1)\dots\pi(i_n)}\,, \tag{C.1.11}$$

where $\pi \in S_n$ is an element of the symmetric group of order n and the m_k are the multiplicities of indices i_k appearing more then once. For example, the coefficient multiplying $a_1^2 a_4$ in $\beta^{(4)}$ is given by

$$-\beta^{(4)}_{1,(114)} = -\left(\beta^{(4)}_{1,114} + \beta^{(4)}_{1,141} + \beta^{(4)}_{1,411}\right) = -\frac{3!}{2!}\beta^{(4)}_{1,114}\,, \tag{C.1.12}$$

where the last equality holds if $\beta^{(4)}_{1,ijk}$ is symmetric. Since it is always contracted with a symmetric coupling tensor, we always choose the coefficient tensors to be symmetric, too.

In terms of the beta functions, the renormalization constants of the gauge couplings are given by

$$Z_i = 1 - a_i\frac{\beta^{(i)}_0}{\epsilon} + a_i^2\frac{\left(\beta^{(i)}_0\right)^2}{\epsilon^2} - a_i\sum_{j=1}^{3} a_j\frac{\beta^{(i)}_{1,j}}{2\epsilon} + \mathcal{O}(a_k^3)\,. \tag{C.1.13}$$

For these, we have the relation

$$\mu^2\frac{\mathrm{d}}{\mathrm{d}\mu^2}\log Z_i = -\left.\frac{\beta^{(i)}}{a_i}\right|_{\epsilon=0}\,. \tag{C.1.14}$$

The numerical values of the beta function coefficients are the same as in QCD or scalar QCD through NNLO, with appropriate replacements of the group factors for $\mathrm{SU}(N_2)$ and $\mathrm{SU}(N_3)$ and the numbers of fermions and scalars.

The bare scalar self-coupling is given by

$$\mathfrak{a}_4^{\mathrm{B}} = a_4 + \sum_{i,j=1}^{4} a_i a_j\frac{\beta^{(4)}_{0,ij}}{\epsilon} + \sum_{ijk=1}^{4} a_i a_j a_k\left(-\frac{\beta^{(4)}_{2,ij}}{2\epsilon}\right)\,, \tag{C.1.15}$$

and the coefficients of the beta function through NLO are given by

$$\beta^{(4)}_{(11)} = -\frac{3y_{\rm h}^4}{4}\frac{1+N_2 n_{\rm h}}{n_{\rm h}(1+N_2)}\,, \qquad \beta^{(4)}_{(12)} = \frac{3y_{\rm h}^2 C_{\rm F2}}{2(1+N_2)n_{\rm h}}\,, \tag{C.1.16}$$

$$\beta^{(4)}_{(13)} = 0\,, \qquad \beta^{(4)}_{(14)} = \frac{3y_{\rm h}^2}{2}\,, \tag{C.1.17}$$

$$\beta^{(4)}_{(22)} = \frac{3(C_{\rm A2}C_{\rm F2} - 4C_{\rm F2}^2 - 4C_{\rm F2}T_{\rm R}n_{\rm h})}{16(1+N_2)n_{\rm h}}\,, \qquad \beta^{(4)}_{(23)} = 0\,, \tag{C.1.18}$$

$$\beta^{(4)}_{(24)} = -\frac{3C_{\rm F2}}{2}\,, \qquad \beta^{(4)}_{(33)} = \beta^{(4)}_{(34)} = 0\,, \tag{C.1.19}$$

$$\beta^{(4)}_{(44)} = -\frac{4+N_2}{2}n_{\rm h}\,. \tag{C.1.20}$$

Note that higher orders do not contribute to any results we calculated and that the variable $n_{\rm h}$ indicates the presence of scalar loops and does not directly correspond an actual number of degenerate scalar fields (cf. the discussion below (C.3.24)).

C.2 Anomalous dimensions

We consider a quantity $A^{\rm B} = Z_A A$ which we expand as

$$A = 1 + \sum_{n=1}^{2}\sum_{l=0}^{n}\sum_{i_1,\ldots,i_n=1}^{4} A_{l,i_1\ldots i_n} a_{i_1}\ldots a_{i_n} L_{\mu t}^{l} + \mathcal{O}(a_i^3)\,. \tag{C.2.1}$$

The anomalous dimension of A is then

$$\gamma \equiv -\mu^2\frac{{\rm d}\log Z}{{\rm d}\mu^2} = -\sum_{i=1}^{4}\beta^{(i)}\frac{\partial \log Z}{\partial a_i}\,, \tag{C.2.2}$$

where we expand γ as

$$\gamma = \sum_{i=1}^{4}\gamma_i a_i + \sum_{ij}\gamma_{ij}a_i a_j + \mathcal{O}(a_i^3)\,. \tag{C.2.3}$$

Then, Z can be expressed in terms of γ by

$$Z = 1 + \sum_{i=1}^{4} a_i\frac{\gamma_i}{\epsilon} + \sum_{i,j=1}^{4} a_i a_j\left[\frac{\gamma_{ij}}{2\epsilon} + \frac{1}{\epsilon^2}\left(\gamma_i\gamma_j - \sum_{l=1}^{4}\beta^{(l)}_{0,ij}\gamma_l\right)\right] + \mathcal{O}(a_k^3) \tag{C.2.4}$$

and the logarithmic terms of A are given by

$$A_{1,j} = -\gamma_j\,, \tag{C.2.5}$$

$$A_{1,jk} = -\gamma_{jk} - \frac{1}{2}\left(A_{0j}\gamma_k + A_{0k}\gamma_j\right) + \sum_{l=1}^{4}\beta^{(l)}_{0,jk}A_{0l}\,, \tag{C.2.6}$$

$$A_{2,jk} = \frac{1}{2}\left[\gamma_j\gamma_k - \sum_{l=1}^{4}\beta^{(l)}_{0,jk}\gamma_l\right]\,. \tag{C.2.7}$$

C.3 Feynman rules

We give the full set of Feynman rules for our flavor-symmetric version of the flowed SM. The rules for QCD can be derived from these by considering only the QCD sector.

The propagators and flow-lines for gauge bosons $X \in \{B, W, G\}$, fermions and the scalar are given by

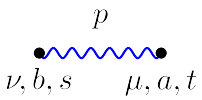

$$= \frac{\delta^{ab}}{p^2}\left[\left(\delta_{\mu\nu} - \frac{p_\mu p_\nu}{p^2}\right) e^{-(t+s)p^2} + \xi_X \frac{p_\mu p_\nu}{p^2} e^{-\kappa_X (t+s)p^2}\right], \tag{C.3.1}$$

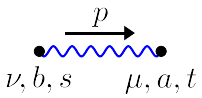

$$= \delta^{ab}\theta(t-s)\left[\left(\delta_{\mu\nu} - \frac{p_\mu p_\nu}{p^2}\right) e^{-(t-s)p^2} + \frac{p_\mu p_\nu}{p^2} e^{-\kappa_X (t-s)p^2}\right], \tag{C.3.2}$$

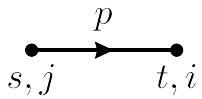

$$= \delta_{ij} \frac{-\mathrm{i}\not{p} + m_{\mathrm{B}}}{p^2 + m_{\mathrm{B}}^2} e^{-(t+s)p^2}, \tag{C.3.3}$$

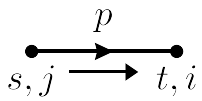

$$= \delta_{ij}\theta(t-s) e^{-(t-s)p^2}, \tag{C.3.4}$$

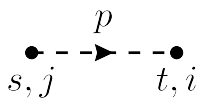

$$= \delta_{ij} \frac{1}{p^2 + m^2} e^{-(t+s)p^2}, \tag{C.3.5}$$

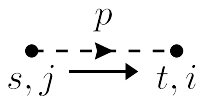

$$= \delta_{ij}\theta(t-s) e^{-(t-s)p^2}, \tag{C.3.6}$$

where for the gauge bosons the respective gauge group indices a and b have to be used (and $\delta^{ab} \to 1$ for the B-boson). The indices i, j for the scalar and fermion propagators and flow-lines represent all fundamental internal group indices of the corresponding fields, i.e., $i = (i_2, i_3)$ with i_2 a $\mathrm{SU}(N_2)$ and i_3 a $\mathrm{SU}(N_3)$ index for the quark doublet. For the electron, which has no indices, set $\delta_{ij} \to 1$. For all vertices we assume the momenta to be outgoing. The pure gauge vertices are given by

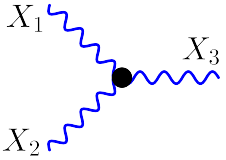

$$\begin{aligned} &= \mathrm{i} g_{\mathrm{B}} f^{a_1 a_2 a_3} \big(\delta_{\mu_1\mu_2}(p_1 - p_2)_{\mu_3} + \delta_{\mu_2\mu_3}(p_2 - p_3)_{\mu_1} \\ &\qquad + \delta_{\mu_3\mu_1}(p_3 - p_1)_{\mu_2}\big), \end{aligned} \tag{C.3.7}$$

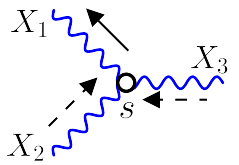

$$= -\mathrm{i}g_\mathrm{B} f^{\mu_1\mu_2\mu_3} \int_0^\infty \mathrm{d}s \Big(\delta_{\mu_2\mu_3}(p_3 - p_2)_{\mu_1} + 2\delta_{\mu_1\mu_2}(p_2)_{\mu_3} - 2\delta_{\mu_1\mu_3}(p_3)_{\mu_2} + (\kappa_X - 1)\big(\delta_{\mu_1\mu_3}(p_2)_{\mu_2} - \delta_{\mu_1\mu_2}(p_3)_{\mu_3}\big)\Big) \tag{C.3.8}$$

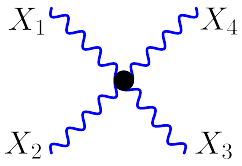

$$\begin{aligned} = -g_\mathrm{B}^2 \Big(& f^{a_1a_2e} f^{a_3a_3e} \big(\delta_{\mu_1\mu_3}\delta_{\mu_2\mu_4} - \delta_{\mu_1\mu_4}\delta_{\mu_2\mu_3}\big) \\ & + f^{a_1a_3e} f^{a_2a_4e} \big(\delta_{\mu_1\mu_2}\delta_{\mu_3\mu_4} - \delta_{\mu_1\mu_4}\delta_{\mu_2\mu_3}\big) \\ & + f^{a_1a_4e} f^{a_2a_3e} \big(\delta_{\mu_1\mu_2}\delta_{\mu_3\mu_4} - \delta_{\mu_1\mu_3}\delta_{\mu_2\mu_4}\big)\Big) \end{aligned} \tag{C.3.9}$$

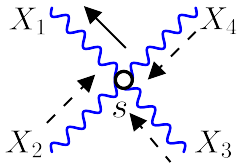

$$\begin{aligned} = -g_\mathrm{B}^2 \int_0^\infty \mathrm{d}s \Big(& f^{a_1a_2e} f^{a_3a_3e} \big(\delta_{\mu_1\mu_3}\delta_{\mu_2\mu_4} - \delta_{\mu_1\mu_4}\delta_{\mu_2\mu_3}\big) \\ & + f^{a_1a_3e} f^{a_2a_4e} \big(\delta_{\mu_1\mu_2}\delta_{\mu_3\mu_4} - \delta_{\mu_1\mu_4}\delta_{\mu_2\mu_3}\big) \\ & + f^{a_1a_4e} f^{a_2a_3e} \big(\delta_{\mu_1\mu_2}\delta_{\mu_3\mu_4} - \delta_{\mu_1\mu_3}\delta_{\mu_2\mu_4}\big)\Big) \end{aligned} \tag{C.3.10}$$

There are no pure gauge vertices with mixed gauge bosons since the gauge bosons are not charged with respect to the other groups. For the B-boson, no self-interactions exist (since for U(1) we have $f^{abc} = 0$ due to commutativity).

The four-boson rules (C.3.9) and (C.3.10) can cause some complications since they do not factorize into external and internal group factors. With previous setups, this problem was solved by introducing so-called σ-particles [36] which do not propagate, but only decompose the four-boson vertex into three three-boson subdiagrams (s-, t- and u-channel like). A disadvantage of this approach is that the number of diagrams is artificially enlarged. An improvement of the setup [83], simplified further by the replacement of `q2e` [79, 80] by `tapir` [78], allowed us to factorize the four-boson vertex using tensor structures which are only contracted after the combination of internal group factors and the Lorentz part of the calculation, whereby only the products in (C.3.9) survive.

The vertices connecting one gauge boson to a fermion or scalar field are given by

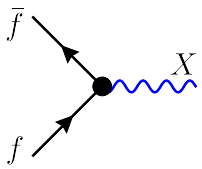

$$= g_X^\mathrm{B} (T_X^{a_X})_{i_{\bar{f}} i_f} \gamma^{\mu_X} P_f \,, \tag{C.3.11}$$

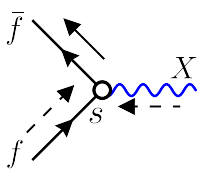

$$= \mathrm{i}g_X^\mathrm{B} T^{a_X}_{i_{\bar{f}} i_f} P_f \int_0^\infty \mathrm{d}s \left[2p_f^{\mu_X} + (1 - \kappa_X) p_X^{\mu_X} \right] , \tag{C.3.12}$$

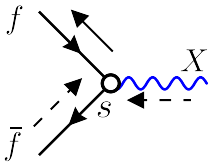

$$= -\mathrm{i}g_X^{\mathrm{B}} T^{a_X}_{i_{\bar{f}} i_f} P_{\bar{f}} \int_0^\infty \mathrm{d}s \, \left[2p_f^{\mu_X} + (1-\kappa_X) p_X^{\mu_X} \right] , \tag{C.3.13}$$

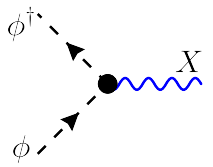

$$= \mathrm{i}g_X^{\mathrm{B}} T^{a_X}_{i_{\phi^\dagger} i_\phi} \left(p_\phi - p_{\phi^\dagger} \right)_{\mu_X} , \tag{C.3.14}$$

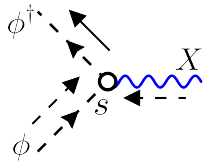

$$= \mathrm{i}g_X^{\mathrm{B}} T^{a_X}_{i_{\phi^\dagger} i_\phi} \int_0^\infty \mathrm{d}s \, \left[2p_\phi^{\mu_X} + (1-\kappa_X) p_X^{\mu_X} \right] , \tag{C.3.15}$$

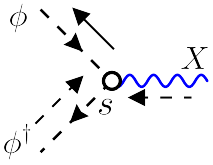

$$= -\mathrm{i}g_X^{\mathrm{B}} T^{a_X}_{i_{\phi^\dagger} i_\phi} \int_0^\infty \mathrm{d}s \, \left[2p_\phi^{\mu_X} + (1-\kappa_X) p_X^{\mu_X} \right] , \tag{C.3.16}$$

where P_f is the chiral projector corresponding to the chirality of the fermion, e.g., $P_u = P_R$ and $P_q = P_L$. The respective opposite projector corresponding to the anti-fermion is denoted as $P_{\bar{f}}$. The generator T is to be understood as a tensor product of unit matrices and the generator corresponding to the gauge boson coupling to the scalar or fermion field (including factors of the hypercharge if X is the B-boson). The fundamental indices of the group corresponding to X get attributed to the corresponding generator while any other fundamental group indices form Kronecker deltas. For example, if in Eq. (C.3.11) the fermion is a quark doublet with color and electroweak indices $i_{\bar{f}} = (i, I)$, $i_f = (j, J)$ and the boson is a gluon, then the rule is

$$g_X^{\mathrm{B}} (T_X^{a_X})_{i_{\bar{f}} i_f} \gamma^\mu = g_3^{\mathrm{B}} t^a_{ij} \delta_{IJ} \gamma^\mu , \tag{C.3.17}$$

where a and i, j are the $\mathrm{SU}(N_3)$ indices of the adjoint and fundamental representation, respectively, and I, J are the indices of the fundamental representation of $\mathrm{SU}(N_2)$. But if the boson is a B boson, then the rule is

$$g_X^{\mathrm{B}} (T_X^{a_X})_{i_{\bar{f}} i_f} \gamma^\mu = g_1^{\mathrm{B}} y_{\mathrm{q}} \delta_{ij} \delta_{IJ} \gamma^\mu . \tag{C.3.18}$$

Note that the flowed rules for the fermion and the scalar are identical up to the presence of a chiral projector in the fermion vertices since we chose the corresponding flow equations to be formally identical. In non-minimal flows there would appear more complicated Dirac structures in the fermion vertices.

For the vertices connecting two gauge bosons and two fermion or scalar fields we obtain

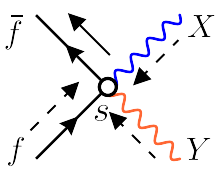

$$= g_X^{\mathrm{B}} g_Y^{\mathrm{B}} P_f \delta_{\mu_X \mu_Y} \left\{ t_X^{a_X}, t_Y^{a_Y} \right\}_{i_{\bar{f}} i_f} \int_0^\infty \mathrm{d}s , \tag{C.3.19}$$

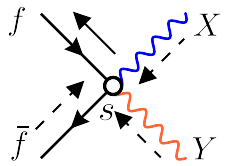

$$= g_X^{\mathrm{B}} g_Y^{\mathrm{B}} P_{\bar{f}} \delta_{\mu_X \mu_Y} \{ t_X^{a_X}, t_Y^{a_Y} \}_{i_{\bar{f}} i_f} \int_0^\infty \mathrm{d}s \,, \tag{C.3.20}$$

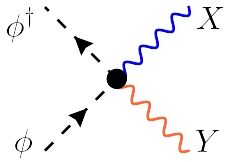

$$= g_X^{\mathrm{B}} g_Y^{\mathrm{B}} \delta_{\mu_X \mu_Y} \{ t_X^{a_X}, t_Y^{a_Y} \}_{i_{\phi^\dagger} i_\phi} \,, \tag{C.3.21}$$

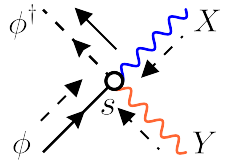

$$= g_X^{\mathrm{B}} g_Y^{\mathrm{B}} \delta_{\mu_X \mu_Y} \{ t_X^{a_X}, t_Y^{a_Y} \}_{i_{\phi^\dagger} i_\phi} \int_0^\infty \mathrm{d}s \,, \tag{C.3.22}$$

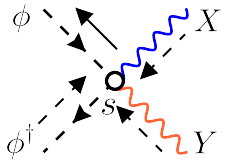

$$= g_X^{\mathrm{B}} g_Y^{\mathrm{B}} \delta_{\mu_X \mu_Y} \{ t_X^{a_X}, t_Y^{a_Y} \}_{i_{\phi^\dagger} i_\phi} \int_0^\infty \mathrm{d}s \,. \tag{C.3.23}$$

The anticommutator reduces to $2 t_X^{a_X} t_Y^{a_Y}$ if the gauge bosons are different and the fundamental indices are then distributed over their corresponding generators. If the bosons are equal, the pair of fundamental indices corresponding to the group of the gauge boson is attributed to the corresponding anticommutator of generators while the rest of the indices form Kronecker deltas as before. Note that for the fermion vertices, the diagrams where the flow-line has the same or opposite direction as the fermion line differ only in the chiral projector. For the scalars, the vertices are the same.

The scalar self-interaction vertex is given by

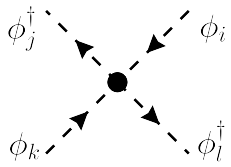

$$= \frac{1}{2} \lambda^{\mathrm{B}} \left(\delta_{ij} \delta_{kl} + \delta_{il} \delta_{jk} \right) , \tag{C.3.24}$$

where i, j, k, l are the fundamental $\mathrm{SU}(N_2)$ indices. Note that since we assume only one scalar particle to exist in the model, there is no Kronecker delta combination of flavor indices as there is for the $\mathrm{SU}(N_2)$ indices. If we would assume multiple flavors of scalar particles, such an additional flavor structure would appear. Also note, as explained in section 5.1, that n_{h} only serves as an indicator for scalar loops and does not represent an actual number of flavors. Otherwise, depending on the diagram structure, we would have to replace, e.g., $n_{\mathrm{h}} \to n_{\mathrm{h}} + 1$ (for a four-scalar vertex where two legs close to a loop) or $n_{\mathrm{h}}^2 \to n_{\mathrm{h}}(n_{\mathrm{h}} + 1)$ (if both pairs of legs form loops). Setting $n_{\mathrm{h}} = 1$ recovers the correct flavor-conserving SM results.

List of Acronyms

QCD quantum chromodynamics

GFF Gradient Flow formalism

IBP integration by parts

EOM equations of motion

BRST Becchi-Rouet-Stora-Tyutin

SM Standard Model

SFTX short-flow-time expansion

LO leading order

NLO next-to-leading order

NNLO next-to-next-to-leading order

UV ultraviolet

IR infrared

SMEFT Standard Model effective field theory

VEV vacuum expectation value

RG renormalization group

MS minimal subtraction

nEDM neutron electric dipole moment

BSM beyond the Standard Model

CEDM quark chromoelectric dipole moment

CMDM quark chromomagnetic dipole moment

RHS right-hand side

LHS left-hand side

RGE renormalization group equation

NNT Nielsen-Ninomiya theorem

NDR naive dimensional regularization

HV 't Hooft-Veltmann

$\overline{\text{MS}}$ modified minimal subtraction

Acknowledgements

I am very grateful to Prof. Dr. Robert V. Harlander for his guidance throughout my doctoral studies. His teaching and advice were invaluable and his sense of humor made many moments along the way more enjoyable. I also very much appreciate the countless stimulating and insightful discussions we had over the time as well as the opportunity to engage in outreach activities.

I thank Prof. Dr. Michał Czakon for agreeing to be the second referee of my thesis.

Furthermore, I thank my other collaborators Andrea Shindler, Fabian Lange, Jonas T. Kohnen, Nils Felten and Matthew D. Rizik for insightful discussions and their contributions to our joint projects. I would like to thank Jonas T. Kohnen, Robert Mason, Andrea Shindler, Nils Felten, Lars Georg and Lucas Cesinger for many fruitful discussions on the Gradient Flow and other topics. I would like to thank Òscar L. Crosas for an invaluable discussion at the Gradient Flow work shop in Zürich.

I also thank Magnus Schaaf and Felix Wilsch for the stimulating discussions on the Gradient Flow and effective field theories.

For proofreading my thesis, I would like to thank Jonas T. Kohnen, Robert Mason and Benedikt Gurdon.

I thank Anke Bachtenkirch, Silke Christ and Ina Vogel for their support regarding all administrative matters and Sven Yannick Klein and Dr. Uwe Kahlert for their IT support and their help with all kinds of technical problems.

Finally, I would like to thank my family and my parents in particular for their kind and reliable support.

All Feynman diagrams in this thesis were created with `FeynGame` [153–155].

I thank the Deutsche Forschungsgemeinschaft (DFG, German Research Foundation) for financial support through grant 460791904 and through grant 396021762 as part of the Collaborative Research Center TRR 257.

Bibliography

[1] M. F. Atiyah and R. Bott. "The Yang-Mills equations over Riemann surfaces". In: *Phil. Trans. Roy. Soc. Lond. A* 308 (1982), pp. 523–615.

[2] S. K. Donaldson. "Anti self-dual Yang-Mills connections over complex algebraic surfaces and stable vector bundles". In: *Proc. Lond. Math. Soc.* 50 (1985), pp. 1–26. DOI: 10.1112/plms/s3-50.1.1.

[3] K. H. Mutter and K. Schilling. "Determination of the Correlation Length by Varying the Boundary Conditions in Lattice Gauge Theories". In: *Phys. Lett. B* 117 (1982). Ed. by J. Julve and M. Ramón-Medrano, p. 75. DOI: 10.1016/0370-2693(82)90877-2.

[4] M. Albanese et al. "Glueball Masses and String Tension in Lattice QCD". In: *Phys. Lett. B* 192 (1987), pp. 163–169. DOI: 10.1016/0370-2693(87)91160-9.

[5] R. Narayanan and H. Neuberger. "Infinite N phase transitions in continuum Wilson loop operators". In: *JHEP* 03 (2006), p. 064. DOI: 10.1088/1126-6708/2006/03/064. arXiv: hep-th/0601210.

[6] M. Luscher. "Trivializing maps, the Wilson flow and the HMC algorithm". In: *Commun. Math. Phys.* 293 (2010), pp. 899–919. DOI: 10.1007/s00220-009-0953-7. arXiv: 0907.5491 [hep-lat].

[7] M. Lüscher. "Properties and uses of the Wilson flow in lattice QCD". In: *JHEP* 08 (2010). [Erratum: *JHEP* 03, 092 (2014)], p. 071. DOI: 10.1007/JHEP08(2010)071. arXiv: 1006.4518 [hep-lat].

[8] M. Lüscher and P. Weisz. "Perturbative analysis of the gradient flow in non-abelian gauge theories". In: *JHEP* 02 (2011), p. 051. DOI: 10.1007/JHEP02(2011)051. arXiv: 1101.0963 [hep-th].

[9] M. Luscher. "Chiral symmetry and the Yang–Mills gradient flow". In: *JHEP* 04 (2013), p. 123. DOI: 10.1007/JHEP04(2013)123. arXiv: 1302.5246 [hep-lat].

[10] S. Borsányi et al. "High-precision scale setting in lattice QCD". In: *JHEP* 09 (2012), p. 010. DOI: 10.1007/JHEP09(2012)010. arXiv: 1203.4469 [hep-lat].

[11] R. Sommer. "Scale setting in lattice QCD". In: *PoS* LATTICE2013 (2014), p. 015. DOI: 10.22323/1.187.0015. arXiv: 1401.3270 [hep-lat].

[12] H. Suzuki. "Energy–momentum tensor from the Yang–Mills gradient flow". In: *PTEP* 2013 (2013). [Erratum: *PTEP* 2015, 079201 (2015)], 083B03. DOI: 10.1093/ptep/ptt059. arXiv: 1304.0533 [hep-lat].

[13] M. Asakawa et al. "Thermodynamics of SU(3) gauge theory from gradient flow on the lattice". In: *Phys. Rev. D* 90.1 (2014). [Erratum: *Phys. Rev. D* 92, 059902 (2015)], p. 011501. DOI: 10.1103/PhysRevD.90.011501. arXiv: 1312.7492 [hep-lat].

[14] R. V. Harlander, Y. Kluth, and F. Lange. "The two-loop energy-momentum tensor within the gradient-flow formalism". In: *Eur. Phys. J. C* 78.11 (2018). [Erratum: *Eur. Phys. J. C* 79, 858 (2019)], p. 944. DOI: 10.1140/epjc/s10052-018-6415-7. arXiv: 1808.09837 [hep-lat].

[15] H. Suzuki and H. Takaura. "$t \to 0$ extrapolation function in the small flow time expansion method for the energy–momentum tensor". In: *PTEP* 2021.7 (2021), 073B02. DOI: 10.1093/ptep/ptab068. arXiv: 2102.02174 [hep-lat].

[16] T. Iritani et al. "Thermodynamics in quenched QCD: energy–momentum tensor with two-loop order coefficients in the gradient-flow formalism". In: *PTEP* 2019.2 (2019), 023B02. DOI: 10.1093/ptep/ptz001. arXiv: 1812.06444 [heplat].

[17] R. V. Harlander and T. Neumann. "The perturbative QCD gradient flow to three loops". In: *JHEP* 06 (2016), p. 161. DOI: 10.1007/JHEP06(2016)161. arXiv: 1606.03756 [hep-ph].

[18] A. Hasenfratz, C. Rebbi, and O. Witzel. "Gradient flow step-scaling function for SU(3) with Nf=8 fundamental flavors". In: *Phys. Rev. D* 107.11 (2023), p. 114508. DOI: 10.1103/PhysRevD.107.114508. arXiv: 2210.16760 [hep-lat].

[19] A. Hasenfratz et al. "Infrared fixed point of the SU(3) gauge theory with Nf=10 flavors". In: *Phys. Rev. D* 108.7 (2023), p. L071503. DOI: 10.1103/PhysRevD.108.L071503. arXiv: 2306.07236 [hep-lat].

[20] M. Black et al. "Using Gradient Flow to Renormalise Matrix Elements for Meson Mixing and Lifetimes". In: *PoS* LATTICE2023 (2024), p. 263. DOI: 10.22323/1.453.0263. arXiv: 2310.18059 [hep-lat].

[21] M. Black et al. "Gradient Flow Renormalisation for Meson Mixing and Lifetimes". In: *PoS* LATTICE2024 (2025), p. 243. DOI: 10.22323/1.466.0243. arXiv: 2409.18891 [hep-lat].

[22] A. J. Buras et al. "Connections between ϵ'/ϵ and rare kaon decays in supersymmetry". In: *Nucl. Phys. B* 566 (2000), pp. 3–32. DOI: 10.1016/S0550-3213(99)00645-8. arXiv: hep-ph/9908371.

[23] G. D'Ambrosio, G. Isidori, and G. Martinelli. "Direct CP violation in K→3π decays induced by SUSY chromomagnetic penguins". In: *Phys. Lett. B* 480 (2000), pp. 164–170. DOI: 10.1016/S0370-2693(00)00361-0. arXiv: hep-ph/9911522.

[24] E. Mereghetti et al. "One-loop matching for quark dipole operators in a gradient-flow scheme". In: *JHEP* 04 (2022). [Erratum: *JHEP* 03, 101 (2025)], p. 050. DOI: 10.1007/JHEP04(2022)050. arXiv: 2111.11449 [hep-lat].

[25] T. M. Ito et al. "Performance of the upgraded ultracold neutron source at Los Alamos National Laboratory and its implication for a possible neutron electric dipole moment experiment". In: *Phys. Rev. C* 97.1 (2018), p. 012501. DOI: 10.1103/PhysRevC.97.012501. arXiv: 1710.05182 [physics.ins-det].

[26] S. Ahmed et al. "First ultracold neutrons produced at TRIUMF". In: *Phys. Rev. C* 99.2 (2019), p. 025503. DOI: 10.1103/PhysRevC.99.025503. arXiv: 1809.04071 [physics.ins-det].

[27] C. Abel et al. "The n2EDM experiment at the Paul Scherrer Institute". In: *EPJ Web Conf.* 219 (2019). Ed. by T. Jenke et al., p. 02002. DOI: 10.1051/epjconf/201921902002. arXiv: 1811.02340 [physics.ins-det].

[28] E. Chanel et al. "The Pulsed Neutron Beam EDM Experiment". In: *EPJ Web Conf.* 219 (2019). Ed. by T. Jenke et al., p. 02004. DOI: 10.1051/epjconf/201921902004. arXiv: 1812.03987 [physics.ins-det].

[29] D. Wurm et al. "The PanEDM Neutron Electric Dipole Moment Experiment at the ILL". In: *EPJ Web Conf.* 219 (2019). Ed. by T. Jenke et al., p. 02006. DOI: 10.1051/epjconf/201921902006. arXiv: 1911.09161 [physics.ins-det].

[30] A. Serebrov. "Present status and future prospects of n-EDM experiment of PNPI-ILL-PTI collaboration". In: *PoS* INPC2016 (2017), p. 179. DOI: 10.22323/1.281.0179.

[31] M. W. Ahmed et al. "A New Cryogenic Apparatus to Search for the Neutron Electric Dipole Moment". In: *JINST* 14.11 (2019), P11017. DOI: 10.1088/1748-0221/14/11/P11017. arXiv: 1908.09937 [physics.ins-det].

[32] C.-Y. Seng. "Reexamination of The Standard Model Nucleon Electric Dipole Moment". In: *Phys. Rev. C* 91.2 (2015), p. 025502. DOI: 10.1103/PhysRevC.91.025502. arXiv: 1411.1476 [hep-ph].

[33] J. Kim et al. "Towards a determination of the nucleon EDM from the quark chromo-EDM operator with the gradient flow". In: *PoS* LATTICE2018 (2019), p. 260. DOI: 10.22323/1.334.0260. arXiv: 1810.10301 [hep-lat].

[34] J. Aebischer, A. J. Buras, and J. Kumar. SMEFT ATLAS: The Landscape Beyond the Standard Model. July 2025. arXiv: 2507.05926 [hep-ph].

[35] M. Creutz. "Standard model and the lattice". In: *Phys. Rev. D* 109.3 (2024), p. 034514. DOI: 10.1103/PhysRevD.109.034514. arXiv: 2310.00061 [hep-lat].

[36] J. Artz et al. "Results and techniques for higher order calculations within the gradient-flow formalism". In: *JHEP* 06 (2019). [Erratum: *JHEP* 10, 032 (2019)], p. 121. DOI: 10.1007/JHEP06(2019)121. arXiv: 1905.00882 [hep-lat].

[37] F. Lange. "Applications of the perturbative gradient flow at higher orders in quantum chromodynamics". PhD thesis. Rheinisch-Westfälische Technische Hochschule (RWTH) Aachen, RWTH Aachen U., 2021. DOI: 10.18154/RWTH-2021-07652.

[38] N. Brambilla et al. "QCD static force in gradient flow". In: *JHEP* 01 (2022), p. 184. DOI: 10.1007/JHEP01(2022)184. arXiv: 2111.07811 [hep-ph].

[39] M. Boers. "Nonminimal gradient flows in QCD-like theories". In: *JHEP* 01 (2021), p. 204. DOI: 10.1007/JHEP01(2021)204. arXiv: 2011.05316 [hep-th].

[40] J. Rongen. "Scalar QED and QCD in the Gradient-Flow Formalism". MA thesis. Rheinisch-Westfälische Technische Hochschule (RWTH) Aachen, RWTH Aachen U., 2020.

[41] J. C. Collins. Renormalization: An Introduction to Renormalization, the Renormalization Group and the Operator-Product Expansion. Cambridge Monographs on Mathematical Physics. Cambridge University Press, 1984.

[42] R. Harlander, unbuplished.

[43] V. A. Smirnov. "Applied asymptotic expansions in momenta and masses". In: *Springer Tracts Mod. Phys.* 177 (2002), pp. 1–262.

[44] S. Gorishny and S. Larin. "Coefficient functions of asymptotic operator expansions in the minimal subtraction scheme". In: *Nuclear Physics B* 283 (1987), pp. 452–476. ISSN: 0550-3213. DOI: https://doi.org/10.1016/0550-3213(87)90283-5. URL: https://www.sciencedirect.com/science/article/pii/0550321387902835.

[45] S. Gorishny, S. Larin, and F. Tkachov. "The algorithm for OPE coefficient functions in the MS scheme". In: *Physics Letters B* 124.3 (1983), pp. 217–220. ISSN: 0370-2693. DOI: https://doi.org/10.1016/0370-2693(83)91439-9. URL: https://www.sciencedirect.com/science/article/pii/0370269383914399.

[46] R. V. Harlander, F. Lange, and T. Neumann. "Hadronic vacuum polarization using gradient flow". In: *JHEP* 08 (2020), p. 109. DOI: 10.1007/JHEP08(2020)109. arXiv: 2007.01057 [hep-lat].

[47] J. Borgulat et al. "Short-flow-time expansion of quark bilinears through next-to-next-to-leading order QCD". In: *JHEP* 05 (2024), p. 179. DOI: 10.1007/JHEP05(2024)179. arXiv: 2311.16799 [hep-lat].

[48] R. V. Harlander et al. "ftint: Calculating gradient-flow integrals with pySecDec". In: *Comput. Phys. Commun.* 306 (2025), p. 109384. DOI: 10.1016/j.cpc.2024.109384. arXiv: 2407.16529 [hep-ph].

[49] F. Lange. "The Perturbative Gradient Flow at Higher Orders". MA thesis. Rheinisch-Westfälische Technische Hochschule (RWTH) Aachen, RWTH Aachen U., 2017.

[50] W. R. Inc. Mathematica, Version 13.0.1. Champaign, IL, 2024. URL: https://www.wolfram.com/mathematica.

[51] H. Werthenbach. "Gradient flow integrals with masses". MA thesis. Rheinisch-Westfälische Technische Hochschule (RWTH) Aachen, RWTH Aachen U., 2024.

[52] S. Laporta. "High-precision calculation of multiloop Feynman integrals by difference equations". In: *Int. J. Mod. Phys. A* 15 (2000), pp. 5087–5159. DOI: 10.1142/S0217751X00002159. arXiv: hep-ph/0102033.

[53] P. Maierhöfer, J. Usovitsch, and P. Uwer. "Kira—A Feynman integral reduction program". In: *Comput. Phys. Commun.* 230 (2018), pp. 99–112. DOI: 10.1016/j.cpc.2018.04.012. arXiv: 1705.05610 [hep-ph].

[54] P. Maierhöfer and J. Usovitsch. "Kira 1.2 Release Notes". In: (Dec. 2018). arXiv: 1812.01491 [hep-ph].

[55] J. Klappert et al. "Integral reduction with Kira 2.0 and finite field methods". In: *Comput. Phys. Commun.* 266 (2021), p. 108024. DOI: 10.1016/j.cpc.2021.108024. arXiv: 2008.06494 [hep-ph].

[56] J. Klappert and F. Lange. "Reconstructing rational functions with FireFly". In: *Comput. Phys. Commun.* 247 (2020), p. 106951. DOI: 10.1016/j.cpc.2019.106951. arXiv: 1904.00009 [cs.SC].

[57] J. Klappert, S. Y. Klein, and F. Lange. "Interpolation of dense and sparse rational functions and other improvements in FireFly". In: *Comput. Phys. Commun.* 264 (2021), p. 107968. DOI: 10.1016/j.cpc.2021.107968. arXiv: 2004.01463 [cs.MS].

[58] T. Huber and D. Maître. "HypExp, a Mathematica package for expanding hypergeometric functions around integer-valued parameters". In: *Comput. Phys. Commun.* 175 (2006), pp. 122–144. DOI: 10.1016/j.cpc.2006.01.007. arXiv: hep-ph/0507094.

[59] T. Huber and D. Maître. "HypExp 2, Expanding hypergeometric functions about half-integer parameters". In: *Comput. Phys. Commun.* 178 (2008), pp. 755–776. DOI: 10.1016/j.cpc.2007.12.008. arXiv: 0708.2443 [hep-ph].

[60] A. V. Smirnov and A. V. Petukhov. "The Number of Master Integrals is Finite". In: *Lett. Math. Phys.* 97 (2011), pp. 37–44. DOI: 10.1007/s11005-010-0450-0. arXiv: 1004.4199 [hep-th].

[61] R. N. Lee and A. A. Pomeransky. "Critical points and number of master integrals". In: *JHEP* 11 (2013), p. 165. DOI: 10.1007/JHEP11(2013)165. arXiv: 1308.6676 [hep-ph].

[62] T. Bitoun et al. "The number of master integrals as Euler characteristic". In: *PoS* LL2018 (2018), p. 065. DOI: 10.22323/1.303.0065. arXiv: 1809.03399 [hep-th].

[63] G. Heinrich et al. "Numerical scattering amplitudes with pySecDec". In: *Comput. Phys. Commun.* 295 (2024), p. 108956. DOI: 10.1016/j.cpc.2023.108956. arXiv: 2305.19768 [hep-ph].

[64] S. Borowka et al. "pySecDec: A toolbox for the numerical evaluation of multi-scale integrals". In: *Comput. Phys. Commun.* 222 (2018), pp. 313–326. DOI: 10.1016/j.cpc.2017.09.015. arXiv: 1703.09692 [hep-ph].

[65] S. Borowka et al. "A GPU compatible quasi-Monte Carlo integrator interfaced to pySecDec". In: *Comput. Phys. Commun.* 240 (2019), pp. 120–137. DOI: 10.1016/j.cpc.2019.02.015. arXiv: 1811.11720 [physics.comp-ph].

[66] T. Binoth and G. Heinrich. "An automatized algorithm to compute infrared divergent multi-loop integrals". In: *Nucl. Phys. B* 585 (2000), pp. 741–759. DOI: 10.1016/S0550-3213(00)00429-6. arXiv: hep-ph/0004013.

[67] T. Binoth and G. Heinrich. "Numerical evaluation of multi-loop integrals by sector decomposition". In: *Nucl. Phys. B* 680 (2004), pp. 375–388. DOI: 10.1016/j.nuclphysb.2003.12.023. arXiv: hep-ph/0305234.

[68] G. Heinrich. "Sector Decomposition". In: *Int. J. Mod. Phys. A* 23 (2008), pp. 1457–1486. DOI: 10.1142/S0217751X08040263. arXiv: 0803.4177 [hep-ph].

[69] E. Panzer. "On hyperlogarithms and Feynman integrals with divergences and many scales". In: *JHEP* 03 (2014), p. 071. DOI: 10.1007/JHEP03(2014)071. arXiv: 1401.4361 [hep-th].

[70] J. C. Collins. "Structure of Counterterms in Dimensional Regularization". In: *Nucl. Phys. B* 80 (1974), pp. 341–348. DOI: 10.1016/0550-3213(74)90521-5.

[71] S. D. Joglekar and B. W. Lee. "General Theory of Renormalization of Gauge Invariant Operators". In: *Annals Phys.* 97 (1976), p. 160. DOI: 10.1016/0003-4916(76)90225-6.

[72] S. D. Joglekar. "Local Operator Products in Gauge Theories. 1." In: *Annals Phys.* 108 (1977), p. 233. DOI: 10.1016/0003-4916(77)90014-8.

[73] S. D. Joglekar. "Local Operator Products in Gauge Theories. 2." In: *Annals Phys.* 109 (1977), p. 210. DOI: 10.1016/0003-4916(77)90170-1.

[74] H. Makino and H. Suzuki. "Lattice energy–momentum tensor from the Yang–Mills gradient flow—inclusion of fermion fields". In: *PTEP* 2014 (2014). [Erratum: *PTEP* 2015, 079202 (2015)], 063B02. DOI: 10.1093/ptep/ptu070. arXiv: 1403.4772 [hep-lat].

[75] J. Artz. "Automatic approach to the perturbative gradient flow". MA thesis. Rheinisch-Westfälische Technische Hochschule (RWTH) Aachen, RWTH Aachen U., 2017.

[76] P. Nogueira. "Automatic Feynman Graph Generation". In: *J. Comput. Phys.* 105 (1993), pp. 279–289. DOI: 10.1006/jcph.1993.1074.

[77] P. Nogueira. "Abusing qgraf". In: *Nuclear Instruments and Methods in Physics Research Section A: Accelerators, Spectrometers, Detectors and Associated Equipment* 559.1 (2006). Proceedings of the X International Workshop on Advanced Computing and Analysis Techniques in Physics Research, pp. 220–223. ISSN: 0168-9002. DOI: https://doi.org/10.1016/j.nima.2005.11.151. URL: https://www.sciencedirect.com/science/article/pii/S0168900205022734.

[78] M. Gerlach, F. Herren, and M. Lang. "tapir: A tool for topologies, amplitudes, partial fraction decomposition and input for reductions". In: *Comput. Phys. Commun.* 282 (2023), p. 108544. DOI: 10.1016/j.cpc.2022.108544. arXiv: 2201.05618 [hep-ph].

[79] T. Seidensticker. "Automatic application of successive asymptotic expansions of Feynman diagrams". In: *6th International Workshop on New Computing Techniques in Physics Research: Software Engineering, Artificial Intelligence Neural Nets, Genetic Algorithms, Symbolic Algebra, Automatic Calculation*. May 1999. arXiv: hep-ph/9905298.

[80] R. Harlander, T. Seidensticker, and M. Steinhauser. "Complete corrections of Order alpha alpha-s to the decay of the Z boson into bottom quarks". In: *Phys. Lett. B* 426 (1998), pp. 125–132. DOI: 10.1016/S0370-2693(98)00220-2. arXiv: hep-ph/9712228.

[81] J. A. M. Vermaseren. "New features of FORM". In: (Oct. 2000). arXiv: math-ph/0010025.

[82] J. Kuipers et al. "FORM version 4.0". In: *Comput. Phys. Commun.* 184 (2013), pp. 1453–1467. DOI: 10.1016/j.cpc.2012.12.028. arXiv: 1203.6543 [cs.SC].

[83] J. T. Kohnen. "Small-flow-time expansion of quark bilinears at next-to-next-to-leading order QCD". MA thesis. Rheinisch-Westfälische Technische Hochschule (RWTH) Aachen, RWTH Aachen U., 2023.

[84] R. Harlander, unbuplished.

[85] A. D. Sakharov. "Violation of CP Invariance, C asymmetry, and baryon asymmetry of the universe". In: *Pisma Zh. Eksp. Teor. Fiz.* 5 (1967), pp. 32–35. DOI: 10.1070/PU1991v034n05ABEH002497.

[86] M. B. Gavela et al. "Standard model CP violation and baryon asymmetry". In: *Mod. Phys. Lett. A* 9 (1994), pp. 795–810. DOI: 10.1142/S0217732394000629. arXiv: hep-ph/9312215.

[87] A. Shindler. "Flavor-diagonal CP violation: the electric dipole moment". In: *Eur. Phys. J. A* 57.4 (2021), p. 128. DOI: 10.1140/epja/s10050-021-00421-y.

[88] I. S. Altarev et al. "A New Upper Limit on the Electric Dipole Moment of the Neutron". In: *Phys. Lett. B* 102 (1981), pp. 13–16. DOI: 10.1016/0370-2693(81)90202-1.

[89] K. Smith et al. "A search for the electric dipole moment of the neutron". In: *Physics Letters B* 234.1 (1990), pp. 191–196. ISSN: 0370-2693. DOI: https://doi.org/10.1016/0370-2693(90)92027-G. URL: https://www.sciencedirect.com/science/article/pii/037026939092027G.

[90] C. Abel et al. "Measurement of the Permanent Electric Dipole Moment of the Neutron". In: *Phys. Rev. Lett.* 124.8 (2020), p. 081803. DOI: 10.1103/PhysRevLett.124.081803. arXiv: 2001.11966 [hep-ex].

[91] J. M. Pendlebury et al. "Revised experimental upper limit on the electric dipole moment of the neutron". In: *Phys. Rev. D* 92.9 (2015), p. 092003. DOI: 10.1103/PhysRevD.92.092003. arXiv: 1509.04411 [hep-ex].

[92] J. de Vries et al. "The Effective Chiral Lagrangian From Dimension-Six Parity and Time-Reversal Violation". In: *Annals Phys.* 338 (2013), pp. 50–96. DOI: 10.1016/j.aop.2013.05.022. arXiv: 1212.0990 [hep-ph].

[93] T. Chupp et al. "Electric dipole moments of atoms, molecules, nuclei, and particles". In: *Rev. Mod. Phys.* 91.1 (2019), p. 015001. DOI: 10.1103/RevModPhys.91.015001. arXiv: 1710.02504 [physics.atom-ph].

[94] V. Cirigliano and M. J. Ramsey-Musolf. "Low Energy Probes of Physics Beyond the Standard Model". In: *Prog. Part. Nucl. Phys.* 71 (2013), pp. 2–20. DOI: 10.1016/j.ppnp.2013.03.002. arXiv: 1304.0017 [hep-ph].

[95] S. Syritsyn, T. Izubuchi, and H. Ohki. "Calculation of Nucleon Electric Dipole Moments Induced by Quark Chromo-Electric Dipole Moments and the QCD θ-term". In: *PoS* Confinement2018 (2019), p. 194. DOI: 10.22323/1.336.0194. arXiv: 1901.05455 [hep-lat].

[96] M. Abramczyk et al. "Lattice calculation of electric dipole moments and form factors of the nucleon". In: *Phys. Rev. D* 96.1 (2017), p. 014501. DOI: 10.1103/PhysRevD.96.014501. arXiv: 1701.07792 [hep-lat].

[97] M. D. Rizik, C. J. Monahan, and A. Shindler. "Short flow-time coefficients of CP-violating operators". In: *Phys. Rev. D* 102.3 (2020), p. 034509. DOI: 10.1103/PhysRevD.102.034509. arXiv: 2005.04199 [hep-lat].

[98] R. Harlander et al. "Two-loop matching of the chromo-magnetic dipole operator with the gradient flow". In: *PoS* LATTICE2022 (2023), p. 313. DOI: 10.22323/1.430.0313. arXiv: 2212.09824 [hep-lat].

[99] Ò. L. Crosas et al. "One-loop matching of the CP-odd three-gluon operator to the gradient flow". In: *Phys. Lett. B* 847 (2023), p. 138301. DOI: 10.1016/j.physletb.2023.138301. arXiv: 2308.16221 [hep-lat].

[100] V. P. Spiridonov. "Anomalous Dimension of $G^2_{\mu\nu}$ and β Function". Report. No. IYaI-P-0378 (1984).

[101] V. P. Spiridonov and K. G. Chetyrkin. "Nonleading mass corrections and renormalization of the operators $m\bar{\psi}\psi$ and $G^2_{\mu\nu}$". In: *Sov. J. Nucl. Phys.* 47 (1988), pp. 522–527.

[102] K. G. Chetyrkin and J. H. Kühn. "Quartic mass corrections to R_{had}". In: *Nucl. Phys. B* 432 (1994), pp. 337–350. DOI: 10.1016/0550-3213(94)90605-X. arXiv: hep-ph/9406299.

[103] P. A. Baikov and K. G. Chetyrkin. "QCD vacuum energy in 5 loops". In: *PoS* RADCOR2017 (2018). Ed. by A. Hoang and C. Schneider, p. 025. DOI: 10.22323/1.290.0025.

[104] M. Gorbahn, U. Haisch, and M. Misiak. "Three-loop mixing of dipole operators". In: *Phys. Rev. Lett.* 95 (2005), p. 102004. DOI: 10.1103/PhysRevLett.95.102004. arXiv: hep-ph/0504194.

[105] L. Naterop and P. Stoffer. "Renormalization-group equations of the LEFT at two loops: dimension-five effects". In: *JHEP* 06 (2025), p. 007. DOI: 10.1007/JHEP06(2025)007. arXiv: 2412.13251 [hep-ph].

[106] J. Brod and E. Stamou. "Electric dipole moment constraints on CP-violating heavy-quark Yukawas at next-to-leading order". In: *JHEP* 07 (2021), p. 080. DOI: 10.1007/JHEP07(2021)080. arXiv: 1810.12303 [hep-ph].

[107] K. Fujikawa. "Path Integral Measure for Gauge Invariant Fermion Theories". In: *Phys. Rev. Lett.* 42 (1979), pp. 1195–1198. DOI: 10.1103/PhysRevLett.42.1195.

[108] J. S. Bell and R. Jackiw. "A PCAC puzzle: $\pi^0 \to \gamma\gamma$ in the σ model". In: *Nuovo Cim. A* 60 (1969), pp. 47–61. DOI: 10.1007/BF02823296.

[109] S. L. Adler. "Axial vector vertex in spinor electrodynamics". In: *Phys. Rev.* 177 (1969), pp. 2426–2438. DOI: 10.1103/PhysRev.177.2426.

[110] S. L. Adler and W. A. Bardeen. "Absence of higher order corrections in the anomalous axial vector divergence equation". In: *Phys. Rev.* 182 (1969), pp. 1517–1536. DOI: 10.1103/PhysRev.182.1517.

[111] H. B. Nielsen and M. Ninomiya. "Absence of Neutrinos on a Lattice. 1. Proof by Homotopy Theory". In: *Nucl. Phys. B* 185 (1981). Ed. by J. Julve and M. Ramón-Medrano. [Erratum: Nucl.Phys.B 195, 541 (1982)], p. 20. DOI: 10.1016/0550-3213(82)90011-6.

[112] H. B. Nielsen and M. Ninomiya. "Absence of Neutrinos on a Lattice. 2. Intuitive Topological Proof". In: *Nucl. Phys. B* 193 (1981), pp. 173–194. DOI: 10.1016/0550-3213(81)90524-1.

[113] H. B. Nielsen and M. Ninomiya. "No Go Theorem for Regularizing Chiral Fermions". In: *Phys. Lett. B* 105 (1981), pp. 219–223. DOI: 10.1016/0370-2693(81)91026-1.

[114] K. Hieda and H. Suzuki. "Small flow-time representation of fermion bilinear operators". In: *Mod. Phys. Lett. A* 31.38 (2016), p. 1650214. DOI: 10.1142/S0217732316502143X. arXiv: 1606.04193 [hep-lat].

[115] W. Siegel. "Supersymmetric Dimensional Regularization via Dimensional Reduction". In: *Phys. Lett. B* 84 (1979), pp. 193–196. DOI: 10.1016/0370-2693(79)90282-X.

[116] G. 't Hooft and M. J. G. Veltman. "Regularization and Renormalization of Gauge Fields". In: *Nucl. Phys. B* 44 (1972), pp. 189–213. DOI: 10.1016/0550-3213(72)90279-9.

[117] S. A. Larin. "The Renormalization of the axial anomaly in dimensional regularization". In: *Phys. Lett. B* 303 (1993), pp. 113–118. DOI: 10.1016/0370-2693(93)90053-K. arXiv: hep-ph/9302240.

[118] D. A. Akyeampong and R. Delbourgo. "Dimensional regularization, abnormal amplitudes and anomalies". In: *Nuovo Cim. A* 17 (1973), pp. 578–586. DOI: 10.1007/BF02786835.

[119] P. Breitenlohner, D. Maison, and K. S. Stelle. "Anomalous Dimensions and the Adler-bardeen Theorem in Supersymmetric Yang-Mills Theories". In: *Phys. Lett. B* 134 (1984), pp. 63–66. DOI: 10.1016/0370-2693(84)90985-7.

[120] M. Lüscher. "Renormalization and continuum limit of the gradient flow in non-Abelian gauge theories". Talk given at *Workshop on Chiral Dynamics with Wilson Fermions*, Trento, 24–28 October 2011.

[121] P. A. Baikov, K. G. Chetyrkin, and J. H. Kühn. "Five-Loop Running of the QCD Coupling Constant". In: *Phys. Rev. Lett.* 118.8 (2017), p. 082002. DOI: 10.1103/PhysRevLett.118.082002. arXiv: 1606.08659 [hep-ph].

[122] S. A. Larin and J. A. M. Vermaseren. "The α_s^3 corrections to the Bjorken sum rule for polarized electroproduction and to the Gross-Llewellyn Smith sum rule". In: *Phys. Lett. B* 259 (1991), pp. 345–352. DOI: 10.1016/0370-2693(91)90839-I.

[123] L. Chen and M. Czakon. "Renormalization of the axial current operator in dimensional regularization at four-loop in QCD". In: *JHEP* 01 (2022), p. 187. DOI: 10.1007/JHEP01(2022)187. arXiv: 2112.03795 [hep-ph].

[124] J. Bühler and P. Stoffer. "One-loop matching of CP-odd four-quark operators to the gradient-flow scheme". In: *JHEP* 08 (2023), p. 194. DOI: 10.1007/JHEP08(2023)194. arXiv: 2304.00985 [hep-lat].

[125] B. Henning, X. Lu, and H. Murayama. "How to use the Standard Model effective field theory". In: *JHEP* 01 (2016), p. 023. DOI: 10.1007/JHEP01(2016)023. arXiv: 1412.1837 [hep-ph].

[126] G. Isidori, F. Wilsch, and D. Wyler. "The standard model effective field theory at work". In: *Rev. Mod. Phys.* 96.1 (2024), p. 015006. DOI: 10.1103/RevModPhys.96.015006. arXiv: 2303.16922 [hep-ph].

[127] J. de Vries et al. "Two- and three-loop anomalous dimensions of Weinberg's dimension-six CP-odd gluonic operator". In: *Phys. Rev. D* 102.1 (2020), p. 016010. DOI: 10.1103/PhysRevD.102.016010. arXiv: 1907.04923 [hep-ph].

[128] Z. Bern, J. Parra-Martinez, and E. Sawyer. "Nonrenormalization and Operator Mixing via On-Shell Methods". In: *Phys. Rev. Lett.* 124.5 (2020), p. 051601. DOI: 10.1103/PhysRevLett.124.051601. arXiv: 1910.05831 [hep-ph].

[129] R. Alonso, E. E. Jenkins, and A. V. Manohar. "Holomorphy without Supersymmetry in the Standard Model Effective Field Theory". In: *Phys. Lett. B* 739 (2014), pp. 95–98. DOI: 10.1016/j.physletb.2014.10.045. arXiv: 1409.0868 [hep-ph].

[130] W. Dekens and P. Stoffer. "Low-energy effective field theory below the electroweak scale: matching at one loop". In: *JHEP* 10 (2019). [Erratum: JHEP 11, 148 (2022)], p. 197. DOI: 10.1007/JHEP10(2019)197. arXiv: 1908.05295 [hep-ph].

[131] F. Maltoni, G. Ventura, and E. Vryonidou. "Impact of SMEFT renormalisation group running on Higgs production at the LHC". In: *JHEP* 12 (2024), p. 183. DOI: 10.1007/JHEP12(2024)183. arXiv: 2406.06670 [hep-ph].

[132] J. Aebischer, A. J. Buras, and J. Kumar. "NLO QCD renormalization group evolution for nonleptonic ΔF=2 transitions in the SMEFT". In: *Phys. Rev. D* 106.3 (2022), p. 035003. DOI: 10.1103/PhysRevD.106.035003. arXiv: 2203.11224 [hep-ph].

[133] Z. Bern, J. Parra-Martinez, and E. Sawyer. "Structure of two-loop SMEFT anomalous dimensions via on-shell methods". In: *JHEP* 10 (2020), p. 211. DOI: 10.1007/JHEP10(2020)211. arXiv: 2005.12917 [hep-ph].

[134] Z. Bern et al. "One loop n point gauge theory amplitudes, unitarity and collinear limits". In: *Nucl. Phys. B* 425 (1994), pp. 217–260. DOI: 10.1016/0550-3213(94)90179-1. arXiv: hep-ph/9403226.

[135] C. F. Berger et al. "An Automated Implementation of On-Shell Methods for One-Loop Amplitudes". In: *Phys. Rev. D* 78 (2008), p. 036003. DOI: 10.1103/PhysRevD.78.036003. arXiv: 0803.4180 [hep-ph].

[136] S. Caron-Huot and M. Wilhelm. "Renormalization group coefficients and the S-matrix". In: *JHEP* 12 (2016), p. 010. DOI: 10.1007/JHEP12(2016)010. arXiv: 1607.06448 [hep-th].

[137] K. G. Chetyrkin and F. V. Tkachov. "Infrared R operation and ultraviolet counterterms in the MS scheme". In: *Phys. Lett. B* 114 (1982), pp. 340–344. DOI: 10.1016/0370-2693(82)90358-6.

[138] K. G. Chetyrkin. "Combinatorics of R-, R^{-1}-, and R*-operations and asymptotic expansions of feynman integrals in the limit of large momenta and masses". In: (Jan. 2017). arXiv: 1701.08627 [hep-th].

[139] K. G. Chetyrkin and V. A. Smirnov. "R* Operation corrected". In: *Phys. Lett. B* 144 (1984). Ed. by A. N. Tavkhelidze et al., pp. 419–424. DOI: 10.1016/0370-2693(84)91291-7.

[140] F. Herzog and B. Ruijl. "The R*-operation for Feynman graphs with generic numerators". In: *JHEP* 05 (2017), p. 037. DOI: 10.1007/JHEP05(2017)037. arXiv: 1703.03776 [hep-th].

[141] G. 't Hooft. "The Background Field Method in Gauge Field Theories". In: *12th Annual Winter School of Theoretical Physics*. 1975.

[142] L. F. Abbott. "Introduction to the Background Field Method". In: *Acta Phys. Polon. B* 13 (1982), p. 33.

[143] E. E. Jenkins, A. V. Manohar, and M. Trott. "Renormalization Group Evolution of the Standard Model Dimension Six Operators I: Formalism and lambda Dependence". In: *JHEP* 10 (2013), p. 087. DOI: 10.1007/JHEP10(2013)087. arXiv: 1308.2627 [hep-ph].

[144] E. E. Jenkins, A. V. Manohar, and M. Trott. "Renormalization Group Evolution of the Standard Model Dimension Six Operators II: Yukawa Dependence". In: *JHEP* 01 (2014), p. 035. DOI: 10.1007/JHEP01(2014)035. arXiv: 1310.4838 [hep-ph].

[145] R. Alonso et al. "Renormalization Group Evolution of the Standard Model Dimension Six Operators III: Gauge Coupling Dependence and Phenomenology". In: *JHEP* 04 (2014), p. 159. DOI: 10.1007/JHEP04(2014)159. arXiv: 1312.2014 [hep-ph].

[146] J. Borgulat et al. "Two-loop gradient-flow renormalization of scalar QCD". In: *SciPost Phys. Core* 8 (2025), p. 032. DOI: 10.21468/SciPostPhysCore.8.1.032. arXiv: 2501.07150 [hep-ph].

[147] C. Monahan and K. Orginos. "Locally smeared operator product expansions in scalar field theory". In: *Phys. Rev. D* 91.7 (2015), p. 074513. DOI: 10.1103/PhysRevD.91.074513. arXiv: 1501.05348 [hep-lat].

[148] L. Del Debbio et al. "Renormalisation of the energy-momentum tensor in three-dimensional scalar SU(N) theories using the Wilson flow". In: *Phys. Rev. D* 103.11 (2021), p. 114501. DOI: 10.1103/PhysRevD.103.114501. arXiv: 2009.14767 [hep-lat].

[149] C. Q. Geng and R. E. Marshak. "Uniqueness of Quark and Lepton Representations in the Standard Model From the Anomalies Viewpoint". In: *Phys. Rev. D* 39 (1989), p. 693. DOI: 10.1103/PhysRevD.39.693.

[150] N. Lohitsiri and D. Tong. "Hypercharge Quantisation and Fermat's Last Theorem". In: *SciPost Phys.* 8.1 (2020), p. 009. DOI: 10.21468/SciPostPhys.8.1.009. arXiv: 1907.00514 [hep-th].

[151] L. N. Mihaila, J. Salomon, and M. Steinhauser. "Gauge Coupling Beta Functions in the Standard Model to Three Loops". In: *Phys. Rev. Lett.* 108 (2012), p. 151602. DOI: 10.1103/PhysRevLett.108.151602. arXiv: 1201.5868 [hep-ph].

[152] M.-x. Luo and Y. Xiao. "Two loop renormalization group equations in the standard model". In: *Phys. Rev. Lett.* 90 (2003), p. 011601. DOI: 10.1103/PhysRevLett.90.011601. arXiv: hep-ph/0207271.

[153] R. Harlander, S. Klein, and M. Lipp. "FeynGame". In: *Computer Physics Communications* 256 (2020), p. 107465. ISSN: 0010-4655. DOI: https://doi.org/10.1016/j.cpc.2020.107465. URL: https://www.sciencedirect.com/science/article/pii/S0010465520302186.

[154] L. Bündgen et al. "FeynGame 3.0". In: *Comput. Phys. Commun.* 314 (2025), p. 109662. DOI: 10.1016/j.cpc.2025.109662. arXiv: 2501.04651 [hep-ph].

[155] R. Harlander, S. Y. Klein, and M. C. Schaaf. "FeynGame-2.1 – Feynman diagrams made easy". In: *PoS* EPS-HEP2023 (2024), p. 657. DOI: 10.22323/1.449.0657. arXiv: 2401.12778 [hep-ph].